U.PORTO

FEUP FACULDADE DE ENGENHARIA
UNIVERSIDADE DO PORTO

Hybrid Friction Stir Bonding

Luís Miguel Campos de Sousa

A dissertation submitted in partial fulfilment of the requirements for the degree of
Master in Mechanical Engineering – Manufacturing, Product Development and Automotive Engineering

Supervisor: Pedro M.G.P.Moreira (INEGI)

Co-Supervisor: Daniel F. O. Braga (INEGI)

Co-Supervisor: Professor Lucas da Silva (FEUP- DEMec)

September 2015

Abstract

Weight reduction is the current trend in structural design, especially in the transportation industry where customers are pushing for more lightweight and efficient designs. The use of new, lighter materials is key to achieve this goal, and to integrate these materials new joining processes are required.

Replacing conventional steel alloys with lighter materials, such as aluminum alloys, has been pursued in the design of metallic structures. It is therefore necessary to increase the number of assembly techniques available to lead to improved attributes regarding actual joining processes.

Friction stir welding combined with adhesive bonding is an innovative technique where it is expected that the drawbacks of each process can be reduced by the other. Since it is a recent technique, there are still improvements that are needed to achieve a higher maturity of the process.

To design an adequate friction stir weld bonded structure it is required to combine the two techniques and vary its parameters in order to find the most suited combination. This thesis will focus on testing aluminum adhesive, welded and hybrid joints under tensile and fatigue tests as well as distortions, microhardness and micrographs of the joints that were subject to welding.

It was observed that adhesive joints are the strongest for the chosen geometry, but when comparing the hybrid and welded only joints, there was a significant improvement that almost equals the adhesive joint. It was found out that the manufactured joints were over dimensioned and a reduction of the bond's overlap length might lead to a hybrid joint that surpasses both adhesive and welded joints.

Resumo

A redução de peso em design estrutural é uma tendência cada vez mais prevalente, especialmente na indústria dos transportes, onde o cliente exige redução de peso e designs mais eficientes. O uso de novos materiais é a solução para alcançar este objetivo, no entanto esta solução passa pelo uso de novos processos de ligação de materiais.

Substituir as convencionais ligas de aço por materiais mais leves, como é o caso de ligas de alumínio, é um dos objetivos no design de estruturas metálicas. Desta forma, é necessário aumentar o número de processos que permitam a ligação deste tipo de materiais, melhorando as suas características quando comparados com os atuais processos de ligação.

Soldadura por fricção linear combinada com adesivos é uma técnica inovadora onde é esperado que as desvantagens de um dos processos sejam reduzidas pelas vantagens do outro e vice-versa. Uma vez que é ainda uma técnica recente, existem melhoramentos que precisam de ser feitos de forma a obter um processo "maduro" e estável.

Para arquitetar uma estrutura onde esteja presente a técnica de soldadura por fricção linear em conjunto com adesivos, é necessário variar os parâmetros de ambos os processos de forma a encontrar a solução mais eficiente. Esta tese vai se focar em testar juntas soldadas, adesivas e híbridas a testes de tração e fadiga, mas também leitura de distorções, micro durezas e micrografias das juntas que foram sujeitas a soldadura.

Foi observado que as juntas adesivas são as mais fortes e resistentes para a geometria escolhida, no entanto, quando se compara as juntas hibridas com as apenas soldadas, existe um melhoramento significativo que quase iguala as juntas adesivas. Durante a realização do projeto foi descoberto que as juntas produzidas tinham um comprimento de sobreposição muito elevado e com uma redução deste comprimento talvez seja possível produzir uma junta hibrida que seja superior a ambas juntas adesivas e soldadas.

Acknowledgments

I would like to thank Dr. Pedro Moreira and Prof. Lucas da Silva for allowing me to have this project and support me during its development.

To my co-adviser Eng. Daniel Braga, my sincere gratitude for all the hours spent helping me and guiding me through this thesis and for being one of the most influent people throughout its development. Without him I would not be able to perform all the required tasks.

A sincere thank you to the staff from LET laboratory, FEUP Adhesives Group and LOME for all the support, where the names Eng. Shayan Eslami, Eng. Ricardo Carbas, Eng. Miguel Figueiredo and Eng. José Teixeira cannot be ignored.

I want to acknowledge my colleagues Daniel Rosendo and Diogo Gonçalves for their collaboration during this work.

I would also like to acknowledge the master thesis student Manuel Miranda from the metallurgic department, who supported me in obtaining some relevant data for this thesis

Finally, and most important, my family that supported me economically and emotionally during this work where it would otherwise have been impossible to accomplish this important stage of my life.

Contents

List of figures

List of tables

List of acronyms

AA	Aluminum Alloy
AB	Adhesive Bonding
CCW	Counter Clock Wise
cp-W	Commercially Pure Tungsten
DCB	Double Cantilever Beam
DOE	Design of Experiments
DZ	Damage Zone
EA	Energy Absorption
ENF	End-Notched Flexure
FEM	Finite Element Method
FEUP	Faculdade de Engenharia da Universidade do Porto
FS	Friction Stir
FSSW	Friction Stir Spot Welding
FSW	Friction stir Welding
HAZ	Heat Affect Zone
IMC	Intermetallic
LOME	Laboratório de Óptica e Mecânica Experimental
LWB – PE	Laser Weldbonding with weld direction parallel to the loading force
LWB – PA	Laser Weldbonding with weld direction perpendicular to the loading force
Mg	Magnesium
NZ	Nugget Zone
PAA	Phosphoric Acid Anodization
pcBN	Polycrystalline Cubic Boron Nitride
rpm	Rotation per minute
SLJ	Single Lap Joint
TAST	Thick Adherent Shear Test
TMAZ	Thermally Mechanical Affected Zone
TWI	The Welding Institute of UK
URS	Ultimate Remote Stress
WT	Working Tim

List of symbols

t_p	Adherent thickness in Weld-Bonded Joint
T_A	Adhesive thickness Weld-Bonded Joint
δ	Displacement
u	Displacement in bolt adhesive
aeq	Equivalent crack length
G_{IC}	Fracture toughness in mode I
G_{IIC}	Fracture toughness in mode II
b	Joint width in Weld-Bonded
P	Load force in Weld-Bonded Joint
R	Minimum stress divided by maximum stress
N_r	Number of cycles in fatigue test prediction formula
L_0	Overlap Weld-Bonded Joint
L_T	Overlap Length in Weld-Bonded Joint
τ	Shear Stress
G	Shear Modulus
σ	Stress
W	Watts
E	Young's Modulus

Chapter 1 – Introduction

1.1. Motivation

Joining solid materials plays a critical role in most "engineering industries" (e.g. aeronautic or transportation) and due to this fact there is a search for new techniques or improvement of the ones that already exist. Friction stir weldbonding is another attempt to improve two distinct processes by uniting them in a single process, as already has been done for other processes like laser weldonding or bolts/rivets with adhesive. Even if no improvements are achieved by combining these two techniques it is important to explore and see what outcomes this combination might bring.

Furthermore, this dissertation allows to study and learn about two distinct processes that are increasingly present in the industries related to engineering.

Since this is a completely new process, there are some challenges associated; is it possible to improve these two distinct processes? Can it be applied to the industry? How? For this purpose a set of parameters will be studied including a deep research of the hybrid joints, e.g. microhardness, micrographs, tensile tests and others in order to find out what are the outcomes.

1.2. Objectives

The objectives of the present thesis is to design and investigate joints manufactured by two distinct bonding processes and the combination of both, allowing to analyze hybrid joints behavior under tensile and fatigue tests. The main concern is the production of high strength joints with reduced weights and manufacturing costs. FSW and adhesive joints were manufactured in order to serve as a benchmark for the hybrid joints.

1.3. Research Methodology

The methodology defined to achieve the objectives previously explained, is described in this section. Tasks were carried out to accomplish the objectives:

1) Research of similar works. Improve previously work in order to increase the strength of hybrid joints;

2) Evaluate adhesive properties;

3) Manufacture of welded, adhesive and hybrid joints with the different parameters and geometries;

4) Quasi-static tensile tests followed by carefully choosing the joints with best tensile curves to advance to the fatigue tests in order to study the influence of adhesive and welding. Load – displacement curves were verified and failure modes investigated;

5) Micro hardness profiles and micro/macrostructure observation were performed of the transversal area affected by FSW;

6) The manufactured joints' plate surfaces were analyzed by measuring the temperature of the upper plates during FSW and measuring the distortions of the lower plates generated after FSW;

7) Organization and comparison of the results from the different configurations as well discussion of the different analyses performed.

1.4. Thesis Overview

The dissertation is divided in five chapters including the first one that is the introduction.

Chapter 2: Summarized review of friction stir welding, adhesive bonding processes as well as other hybrid joints such as weldbonding, rivet-adhesive, bolt-adhesive, laser adhesive and friction stir spot welding with adhesive. A detailed description of friction stir welding process parameters and properties is included as well with application of the both welding and adhesive techniques.

Chapter 3: Specimen manufacturing process, geometries and configurations are described. Static and fatigue test procedures are detailed and the testing settings are defined. Also, includes distortion and microhardness measurements and micrograph settings. All the performed experimental work will be explained including the temperature readings with a thermographic camera and thermocouples.

Chapter 4: Results and discussion of all the tests and analyses performed, such as: static and fatigue tests, microhardness profiles, distortions measurement and micrographs. Also the temperature readings of the results obtained using the thermographic camera are discussed.

Chapter 5: Final remarks with the most important conclusions presented, describing the different results obtained in the experimental work. Future work suggestions are made for future researchers in this project to improve hybrid friction stir weld bonded joints.

Chapter 2 – Literature Review

2.1. Friction Stir Welding (FSW)

Friction stir welding (FSW), was developed at The Welding Institute (TWI) of UK in 1991 [1]. FSW is an efficient and versatile solid-state (or semi-solid) joining process (melting point not achieved during welding) [2], which allows aluminum and other metallic alloys to be joined that until now were very difficult to weld with conventional techniques due to the poor solidification microstructure and porosity in the fusion zone [2]. Some aluminum alloys (AA) are even nonweldable due to the high chance of a hot cracking formation [3]. FSW may help reduce these drawbacks associated to other conventional methods, in addition to having the advantage of the low material waste and the lack of radiation and harmful gas emissions that are normally associated to fusion welding process, resulting in an environment friendly process.

Besides the possibility of FSW being used in metallic materials like copper and magnesium alloys, zinc, titanium and even steel, it is mostly used on aluminum alloys regarding the industrial application [3]. It is difficult to measure how much FSW is applied in the industrial environment, but figure 1 shows a graph with the number of licenses sold by TWI since 1995-2009 where it is possible to see that there has been an increase licenses sold over the years [3].
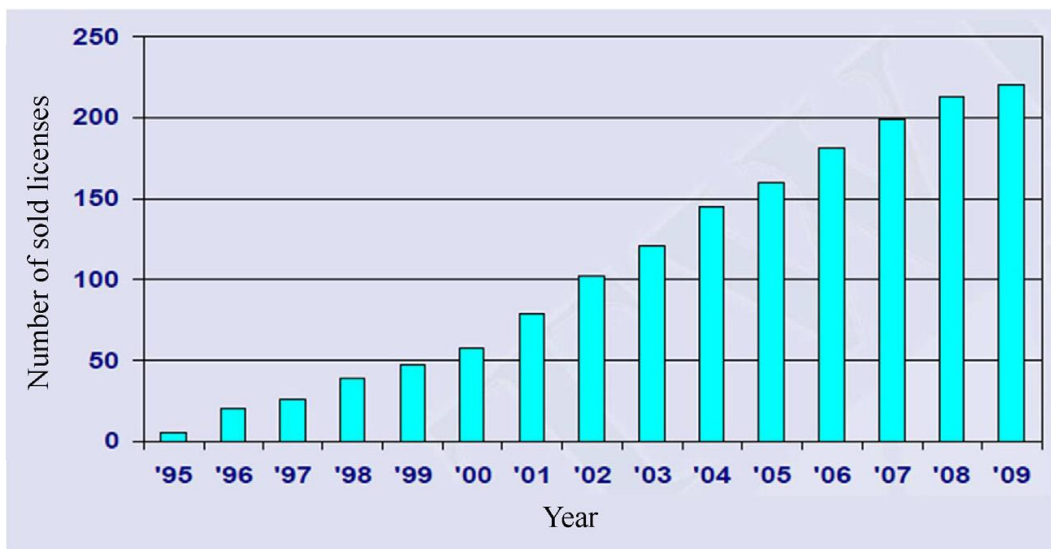
Figure 1 – Number of FSW licenses sold between years 1995 and 2009 [3].

The FSW concept is remarkably simple, it uses a rotating tool equipped with a pin/probe and shoulder, which is pressed onto the edges of the work pieces that are to be joined, generating a heat that allows the material to suffer plastic deformation and then to translate the tool along the welding line, creating a weld seam. This tool, pin plus shoulder, has two main functions that are heating the work piece and create a material flow that will result in a joint [1, 3]. In figure 2, it is possible to see the previously explained schematic.
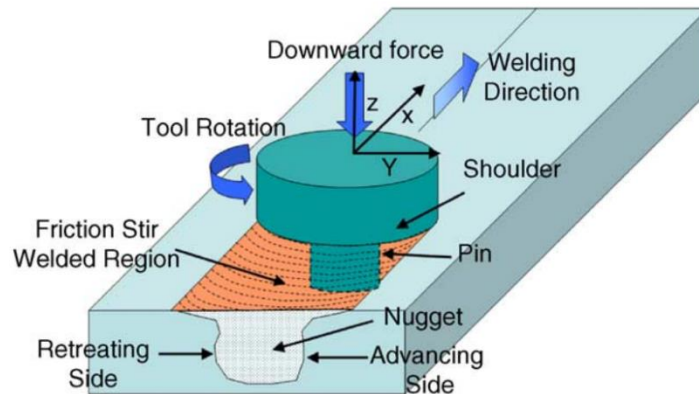
Figure 2 - Schematic drawing of friction stir welding[4].

2.1.1. Process Parameters

FSW gathers some variables that may influence the quality of the joint. Within this topic 4 relevant parameters of this technique will be stated.

The process parameters may be divided as proposed in [4]:

- Tool Design
- Clamp Design
- Materials Properties
- Machine Parameters

2.1.1.1. Tool Design

The design of the tool is considered the most important aspect of the process since it is the one that most influences the development of the process [4]. The tool may be divided in shoulder and pin, the first responsible mainly for generating heat while the pin creates material flow. The heating is very important in order to soften the material, allowing to the pin create the flow. Another function of the tool is to keep the material flow controlled and to not cause uplift [5].
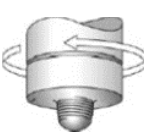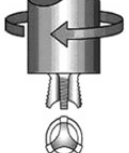
Initially the tool is rotating and when the pin gets in contact with the material it starts "drilling" it, generating heat to allow the formation of the material flow, even though the heat generated this way is insufficient to perform the FSW process. Once the pin gets the sufficient depth to let the shoulder get in contact with the work piece, most of the heat required for the process is generated due to the friction between shoulder and work piece. This heat will allow the transport of the material from the front of the tool to the trailing edge where it is forged into a joint. The relative size of the pin and shoulder is important [1, 4, 5].

In the literature where the influence of the tool in the process is reported, no single geometry is pointed out as the best of all for every kind of material and joint configuration, but there are 3 geometries that must be mentioned regarding the pin - the conventional threaded pin, the triflute pin and Whorl tool. For example the triflute pin and Whorl tool aim to join 25-40 mm thick plates of the AA 6082-T6 by single sided welding, and up to 75 mm thick plates by double side welding [1].

R.S. Mishra and Ma [4], suggested that the triflute pin increases the ratio between the volume of material that is swept and static volume of the pin, improving the flow of material. Compared to the conventional pin, the triflute pin has a 100 % increase in welding speed, 20 % reduction in axial force and a reduction in the upper plate thinning by a factor of more than 4, being this comparison performed on a lap welds. But K. Krasnowski et al. [3] in a recent paper, working on AA 6082 alloy, stated that the performance of the conventional threaded pin and the triflute are very similar when regarding the tensile test results on lap welds.

Besides these geometries, depending on the type of the welding application, other tools might provide better results. Table 1 presents some examples of these tools regarding the application, the scheme and the possibility of rotary reversal [6].

Table 1 – A selection of the tools design at TWI [5].

Tool	Cylindrical	WhorlTM	MX trifluteTM	Flared trifluteTM	A-skewTM	Re-stirTM
Scheme						
Tool pin shape	Cylindrical with threads	Tapered with threads	Threaded, tapered with three flutes	Tri-flute with flute ends flared out	Inclined cylindrical with threads	Tapered with threads
Rotary reversal	No	No	No	No	No	Yes
Application	Butt welding; fails in lap welding	Butt welding with lower welding torque	Butt welding with further lower welding torque	Lap welding with lower thinning of upper plate	Lap welding with lower thinning of upper plate	When minimum asymmetry in weld property is desired

2.1.1.2. Materials

The physical, mechanical and chemical properties of the material to be welded are important in order for the operator to regulate the welding parameters according to those properties. For example, for a material with a low melting point, it is important to control the rotation and welding speed in order to avoid overheating since this technic requires the material to not melt.

FSW [4] was originally developed for welding aluminum and can perform welds with good quality to a thickness range of 1.2 to 75mm. Besides aluminum, FSW can be associated to magnesium alloys, zinc, lead, copper and even steel. There have also been developments in the use of FSW on polymers and amorphous matrix composites [7] and other materials with higher melting points, such as steels[8].

2.1.1.3. Tool Materials

Depending on the materials that are to be joined, the tool material must be carefully selected in order to guarantee lower costs (tool wear) and higher weld joint quality. R.Rai et al. [5], exposed 3 major materials for FSW tools: steel, polycrystalline cubic boron nitride (pcBN) and commercially pure tungsten (cp-W) tools. Steel tools are mainly used to join AA and also for joining dissimilar materials, for example Al-Mg (Magnesium) in both lap and butt configurations, the pcbn and cp-W tools are important candidates for FSW of high strength materials. Pcbn shows much smaller wear when compared to others tools regarding high strength, hardness and high temperature stability, but the low fracture toughness and high cost associated with these materials requires attention. Finally the cp-W tools, although not as hard and wear resistant, are more affordable options and have been used to weld steels and Ti alloys in a limited scale.

Regarding the durability of the tool, Kallee et al.[1] states that it is possible to weld up to 1000 meters in 5 millimeter thick aluminum extrusions without changing the tool, in this case due to the application of FSW in AA, a steel tool would be used.

2.1.1.4. Machine Parameters

There are three major parameters that have to be pointed out: the welding speed (along the work piece), the tool rotation speed and the axial force applied on the tool, this last one being a versatile option since the tool's position relative to the material to be welded can be controlled instead of the force. The rotation speed in conjunction with the advancing speed of the tool has direct influence on the heat produced and the welding speed on the joint quality [3, 4, 9].

2.1.1.5. Clamp Design

The clamp system is important in order to restrain the workpiece to be worked on. It has to allow the tool to fully contact the workpiece and to be able to move along it in order to produce a weld with good properties without failed zones due to the loss of force.

V.Richter-Trummer et al. [10] found out that, when using FSW in a butt joint, there is an influence on the residual stresses, distortions and properties of the joint with the variation of the clamping force. The conclusions of this work were that clamping forces in the order of 2500 N may lead to better joint properties. Concerning the distortions and residual stresses, higher clamping forces lead to lower distortions but higher residual stresses, being necessary to find out an equilibrium between these two properties. A moderate but higher clamping force should lead to better results regarding the two properties.

Another parameter referred on some papers is the tool tilt angle [11, 12], as the pin angle increases the temperature around the weld line is higher, due to the increment of friction which has the decisive effect on generating heat during the FSW process [12]. This conclusion is a result of an experiment using 5, 15 and 25 degrees.

2.1.2. FSW Joint Properties

FSW involves flow of material during the process, and that implies several different areas with different behaviors, modifications at the micro-structure due to the temperature and recrystallization of the material [4]. It can therefore be classified by five working zones, starting with preheating, initial deformation, extrusion, forging and post heat/cool down zone that are presented in figure 3 [4].

Mishra, R.S. and Z. Ma [4], stated and explained these five zones, starting with the preheated zone, it is formed due to the friction between the tool and work piece that generates heat. With the rotation of the tool, more specifically the pin inside the material, it leads to a critical temperature and critical flow stress, creating the deformed zone.

In the extrusion zone, the materials flow around the pin from the front to the back. The forging zone is formed when the material that was in front of the tool is forced to flow to the cavity that the tool left on its rear. The shoulder acts like a support to keep the flow of material controlled. Then, the post heat zone that is behind the forging zone, where the material cools down and is forced to fully solidify. There are many factors that can influence the flow of material and the tool geometry is one of the major ones, so it is important to know what kind of design to choose according to the material to be joined and joint configuration.
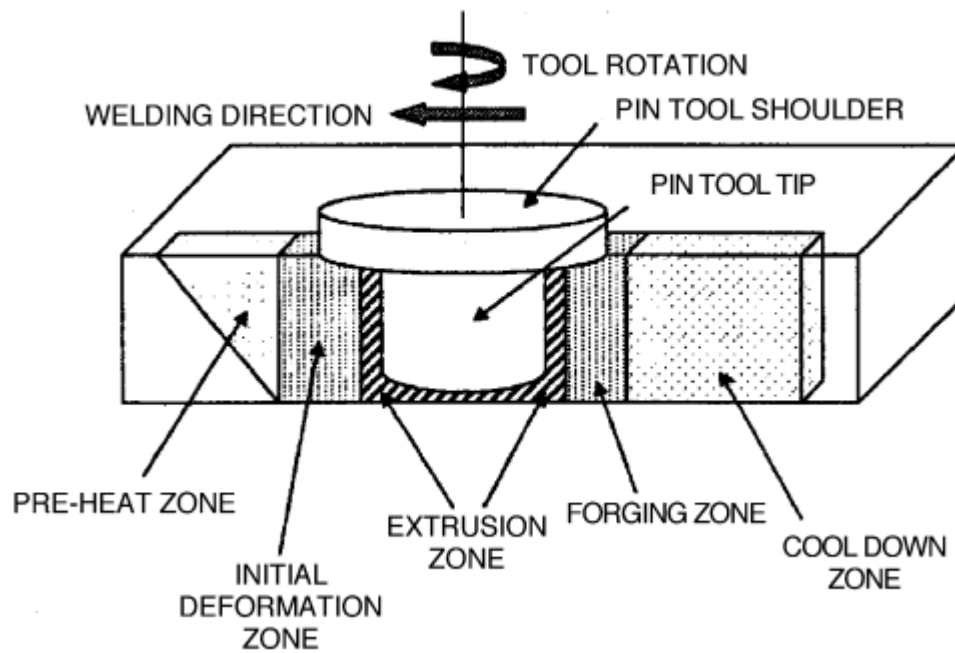
Figure 3- Schematic drawing of the FSW joint zones [4].

2.1.3. Applications

There are currently many applications for FSW in industrial environment since it is a process that can successfully weld aluminum and similar materials with low melting point and high electrical/thermal conductivity, and still present good weld quality. Regarding the automotive industry, there is continuous competition and an increased improvement of vehicle performance while maintaining safety of passengers. For this effect reducing the weight of the vehicles is key [13]. Aluminum is one of the materials that can guarantee enough strength while also being lightweight, due to this fact the transportation industry is increasingly looking for good solutions to be able to apply this material. In general all aluminum components in a car can be succefully welded by FSW, examples are: bumper beams, drive shafts, intake manifolds, rear axles, stiffening frames, wheel rims, etc. Motorcycle and bicycle frames are other potential fields to apply FSW. The application of FSW in large vehicles is even more interesting, it can be used on tail lifts for lorries, mobile cranes, armor plated vehicles, fuel tankers, caravans and buses [13]. A car with most of it components produced using FSW is presented in figure 4.
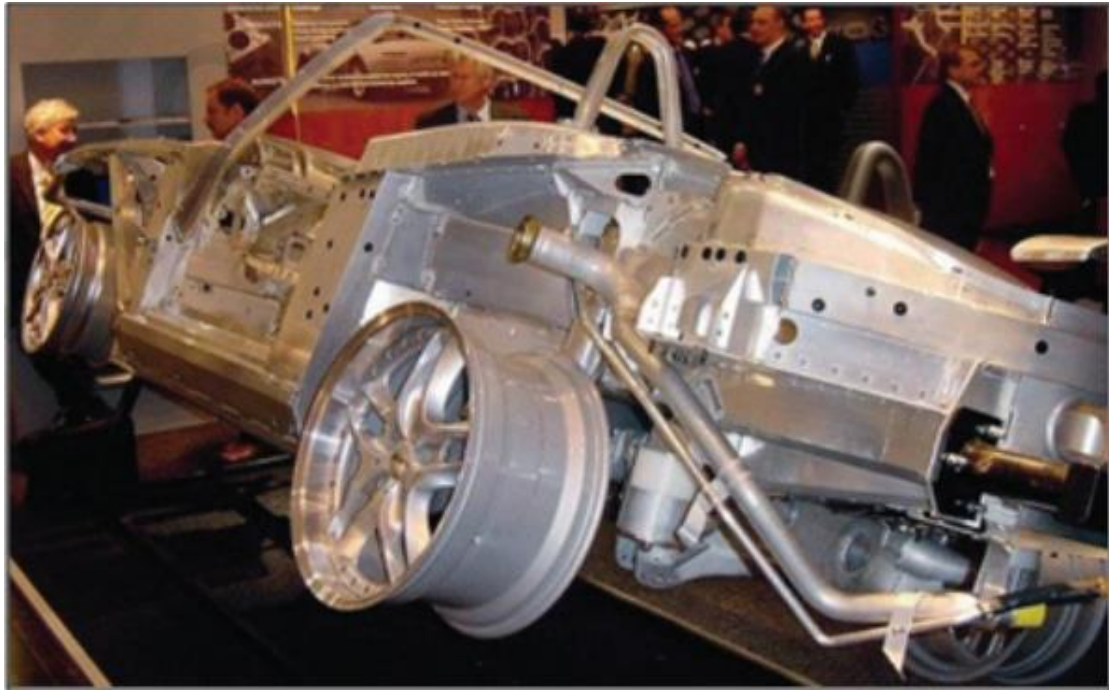
Figure 4 - A car featuring countless application areas for FSW [13].

Honda [2] was the first company to make a mass production of components for automotive industry using FSW to weld dissimilar materials. To accomplish this, a robot was used with the ability to friction stir weld, as shown in figure 5.
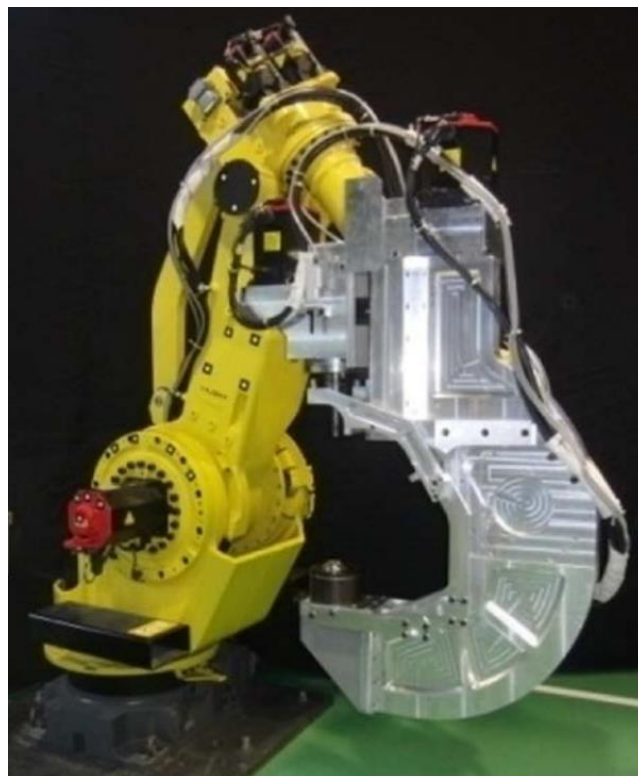
Figure 5- Fanuc M-700 with C-type FSW gun [2].

Some of possible joints configurations are highlighted in figure 6.
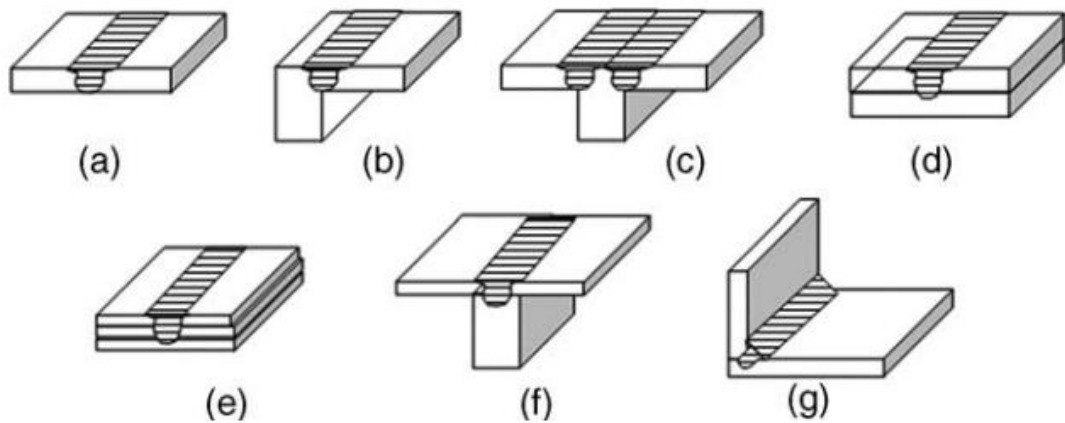
Figure 6 - Joints configurations for FSW: (a) square butt, (b) edge butt, (c) T butt joint, (d) lap joint, (e) multiple lap joint, (f) T lap joint, and (g) fillet joint. [4].

Automotive industry is one of the major industries that uses FSW. Other industrial applications of this technique may be found in aerospace and aviation industries since demand for lightweight is extremely necessary. It can therefore be considered for wings, fuselages, empennages, cryogenic fuel tanks for space vehicles, military and scientific rockets, aircraft fuel tanks, and also repair faulty MIG welds [13]. Figure 7 shows a space shuttle that used a large external fuel tank that was successfully joined using FSW.

Figure 7 - Space shuttle and the external fuel tank [13].

There are countless applications for FSW, besides the previously mentioned, such as the railway, shipbuilding, heat and piping, electrical and construction industries which directly work with FSW [1, 13, 14]. The possibility of welding plastics with FSW is also important, being another advantage of the process [7, 13].

Table 2 highlights some relevant benefits. A specific example of the benefit that this technique presents was divulgated by Honda [2], where engineers of this company achieved a 25 % (6Kg) of weight reduction in an automotive component that until then used bolts to join its parts.

Table 2 - Benefits of FSW [4]

Metallurgical benefits	Environmental benefits	Energy benefits
Solid phase process	No shielding gas required	Improved materials use (e.g. joining different thickness) allows reduction of weight
Low distortion of work piece	No surface cleaning required	Only 2.5 % of the energy needed for a laser weld
Good dimensional stability and repeatability	Eliminate solvents required for degreasing	Decreased fuel consumption in aircraft (jet airliner), automotive and ship applications
No loss of alloying elements	Consumable materials saving, such as rugs, wire or any other gases	50 % electrical consumption when compared with MIG[2]
Excellent metallurgical properties on joint area		
Fine microstructure		
Absence of cracking		
Replace multiple parts joined by fasteners		

2.2. Adhesive Bonding (AB)

Adhesive bonding (AB) is a technology with much longer history than FSW and is a known joining process for solid materials that has been proven to be efficient. In a gross way, it consists in joining materials using an adhesive, in liquid or semi-liquid form, between the two work pieces, with following solidification, resulting in a strong joint [15].

From the point of view of engineering the most relevant are the structural adhesives that are able to resist considerable forces and are responsible for the resistance and rigidity of the structure (more or less 7 MPa shear strength) [16].
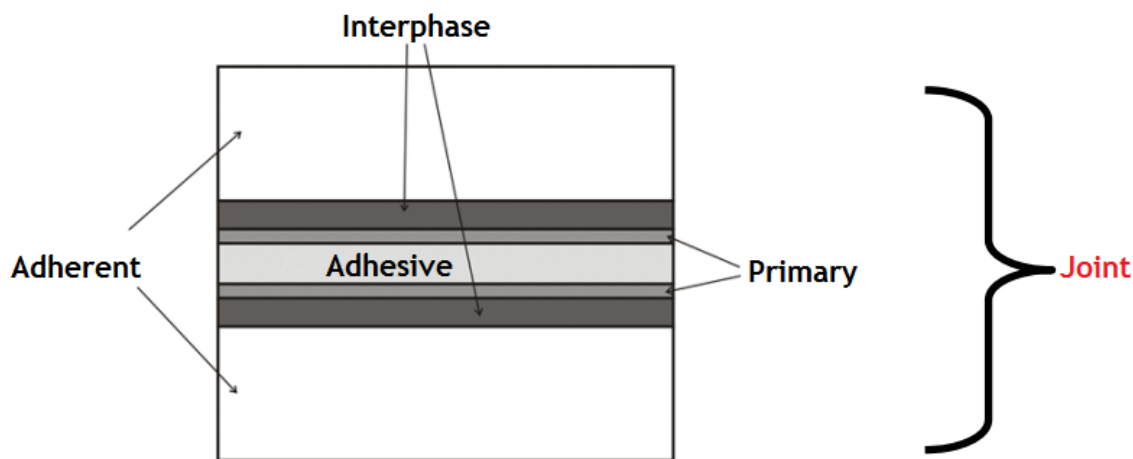
Figure 8 – Schematic Adhesive Bonding [16].

The adherent represents the materials to be joined, the interphase is the region of contact between the adhesive and the material. The primary is a product that sometimes is applied to improve the adhesion of the adhesive to the material. Figure 8 presents the different materials in a process of AB.

There are several advantages using this process, like the uniform distribution of stress that improves the resistance to fatigue and the capacity of damping vibrations. Both of these advantages are very good for mixing with FSW, or is expected to. Others benefits are the ability to join different materials, the possibility of automation, the non-need of holes, screws and marks of welding and the reduction of weight that is very important. Like any other process, it has disadvantages like low resistance to low and high temperatures, short working and shelf life, low resistance to peeling strength and the necessity of preparations of surfaces [15].

2.2.1. Failures on Adhesive Bonding

In the AB process it three kinds of possible failures must be considered that are illustrated in figure 9.
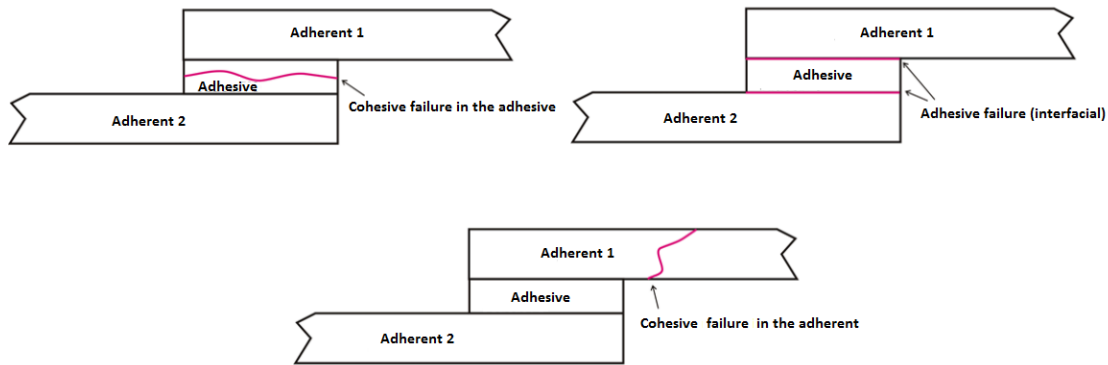
Figure 9 – Failures in Adhesive Bonding, a) Cohesive failure; b) Adhesive failure; c) Cohesive failure in the adherent [16].

Cohesive failure in the adhesive is the one that every operator is looking for, since the rupture actually happens on the adhesive like it is expect to. In figure 9 a) it is possible to see that the failure happens across the adhesive structure. Figure 9 b) shows an adhesive failure (interfacial), this shouldn't happen if the process was correctly done, and the main cause for this situation is a bad preparation of the surfaces that hold the adhesive, causing failure on the bonding surface. And the last one is cohesive failure in the adherent, and the cause is that the joint has greater resistance than the adherent itself, and in this case a lower resistance adhesive or a stronger material should be used that can handle the stress better than the adhesive [15].

2.2.2. Applications

AB has been used for many centuries and along the last seventy years this technique has been developed significantly, leading to a considerable use in different industrial fields [17]. For example in aerospace industry, the Boeing 787 and the AirBus A350 contain more than 50 % bonded structures. Also, the adhesives for the automotive industry grow significantly every year, and the reasons for the global increasing of adhesive use are related to the easy application, high corrosion resistance, crack retardance and good damping characteristics [17].

Specifying on the transportation industry, figure 10 and figure 11 show some of the applications like adhesive badges for bond the logotype of the vehicle brand, floor coverings laying in flexible buses and aircraft floors [18].

Figure 10 - Logotype Cayenne S bonded with adhesive [18].

Figure 11 - Floor of Bus bonded with adhesive [18].

AB, like previously mentioned, is a multi-application process, so there are numerous applications for it, for example, recently FEUP has been working with bosch in application of adhesive in a gas boiler to bond the cover glass of the front panel. With the development of this process, a considerable amount of studies are being performed in order to obtain the best possible joint for a specific application that can be subjected to loads, impact or even fatigue loads.

Another research that is very interesting is the smart adhesive joints that in sum are joints in which the adhesive can self-heal with the presence of cracks. M.D.Banea et al. [19], have been studying this new technology and it is a promising technique where the research is in an initial stage but, with the successful application of it, might lead to application of the adhesive in other fields that until now used other joining process have been used.

2.3. Hybrid Adhesive Joints

The use of hybrid adhesive bonded joints is present in the transportation industry as is in others, since this joining technology allows the reduction of weight and therefore a lower cost associated to joining of solid materials. There are still a number of disadvantages associated to this type of joints but tests are being performed in order to obtain the best configurations of hybrid adhesive joints. The adhesive allows the joint to resist harsh environments, to increase the life of the joint regarding fatigue life and also a uniform distribution of stress, however adhesive bonds are known for the stress concentration at the edges of the overlap, and this leads to a premature failure [20].

The combination of these techniques can lead to a higher static and fatigue strength, stiffness and durability. The possibility to perform the other process while the adhesive is curing is another advantage, since both techniques can be performed without having a substantial additional time.

Along this chapter the following hybrid joints will be presented: Weld-bonded, rivet-adhesive, bolt-adhesive, laser-adhesive and friction stir spot welding-adhesive.

2.3.1. Weld – Bonded

Weldbonding is a hybrid process, schematized in figure 12, which combines the spot weld resistance and the AB. The process consists in applying the adhesive (paste) and then the spot weld through the adhesive. The force of the electrode is used to displace the adhesive in order to make the electrical contact between the plates and perform the weld. Also, heat cured adhesives are used to allow their cure while the weld is made. Normally the adhesives are cured in temperatures up to 180 ℃ for 30 minutes, since the weld process generates a located heating, the damage on the adhesive is low [20].

This hybrid process was developed in the Soviet Union with the same procedure that was described above but instead of using an adhesive with a consistent viscosity, one with low viscosity was used since the adhesive was applied after doing the spot weld [20].

When compared with conventional mechanical holding processes this technique offers [20]:

- Better fatigue strength;
- Better corrosion resistance;
- Non-existence of sealing operations;
- Lower manufacturing costs;
- Appropriate for automation;
- Less noise (no need for riveting);

The main objective is to get the advantages of each process, for example the adhesive is known for having a low peel stress resistance and with the weld points this disadvantage can be reduced. Also, the adhesive has an excellent strength in shear, uniform distribution of loads, softening of stress concentrations, good fatigue resistance and energy absorption, therefore it can improve the joint made by weld spotting [21].
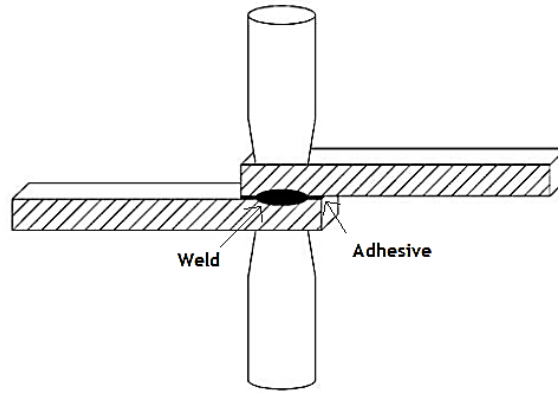
Figure 12 – Schematic of spot weldbonding process [22].

2.3.1.1. MIG weld + Adhesive

MIG spot weldbonding technology includes 3 steps: applying the adhesive, drilling through the adhesive and MIG spot weld [21].

Liu and Ren [21], tested this process on single lap joints (SLJ's), with substrates of Mg alloy AZ31 and AA 6061, and obtained the following results regarding shear and peeling stress of the joint:

Table 3 - Mechanical property of the joints [21]

	Tensile shear/kN	T-peel/N
MIG spot welding	1.7	340
Adhesive bonding	6.0	200
MIG spot weld bonding	5.3	345
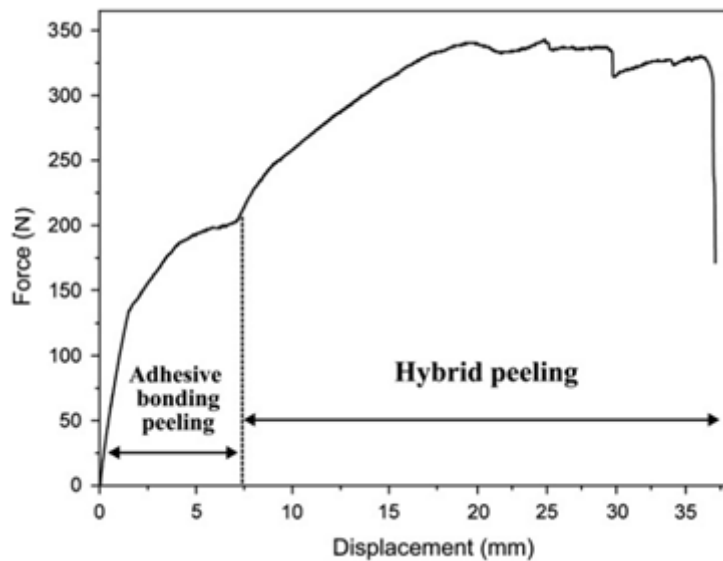
Figure 13 - Force–displacement curve of MIG spot weld bonded joint in peel test [21].

On table 3, is possible to verify that the tensile shear test using MIG spot weld bonding is 5.3 kN, which is an improvement of about 3 times the results of MIG spot weld only. The adhesive granted a great shear stress failure, but the low peeling stress is still a problem when using it. As it can be seen in figure 13 and table 3, the AB provides a peel stress failure of 200-210 N, and with hybrid process it can resist up to 345 N, that is very close to what the original MIG spot weld can actually resist. It can be concluded that the joining of these two processes improves when compared to one alone, creating a joint with good properties.

2.3.1.2. WeldBonding: Dissimilar Thickness Joints and Materials

Regarding the contributions of the hybrid process when working with dissimilar thickness joints, S.M. Darwish [23], shows that it is beneficial to add an adhesive layer to the spot weld process because it not only improves the strengthening but also helps the balance of the stresses on this type of joints. It is therefore recommended to use weldbonding instead of only spot welding to join dissimilar thickness joints.

S.M. Darwish [24] also investigated the contribution of the adhesives on welds of dissimilar materials and the results were very similar to the welding of bonded dissimilar thickness joints. Steel–aluminum and brass–steel SLJ's were tested, and a uniform distribution of the stresses was verified when the adhesive is present. In brass-steel joints, a high stress concentration on the weaker part of the joint is verified (material with the low melting point), in others words, in brass. With the introduction of the adhesive, both weak and strong parts are loaded with same level of stresses [24].

The conclusion is that once again the use of the adhesive results not only in strengthening but also balances the stresses and avoids stress concentrations. Both of the studies were performed in single lap joints.

The main advantage of weldbonding is the increase of energy absorption, stiffness and strength. The adherent thickness is an important parameter to welded and weld-bonded joints, on the other side, it is not important for bonded joints, influencing the peel stress. There is an improvement of the ageing and high temperature reaction of the weld-bonded joints when compared with just bonded joints [25].

In a study, Campilho et al. [25] tested three conditions, welding immediately after bonding and assembly (0 % of the Working Time), at 50 % of the WT and at 100 % of the WT. Since the welding parameters directly influence the resistance of the joint and how the adhesive will behave, some parameters were varied - squeezing time, upslope, welding time and welding current, being the sets defined: set 1– 3/5/30/40, set 2– 3/5/35/45 and set 3– 3/5/43/53, respectively.
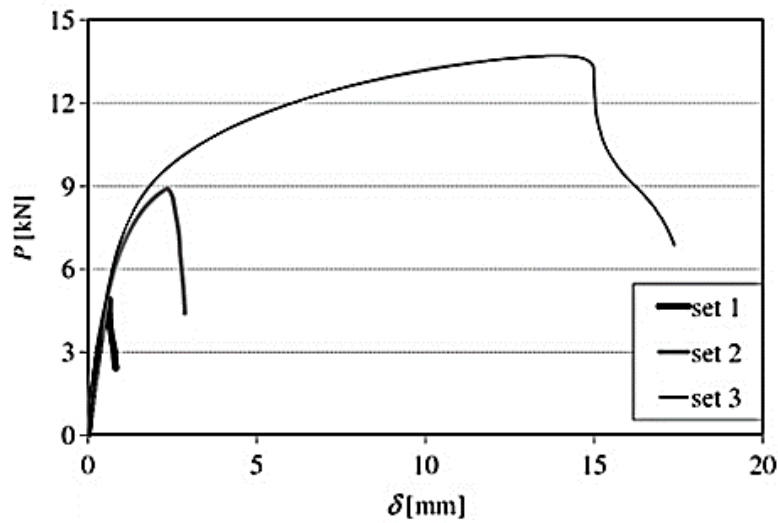
Figure 14- P- δ curve, from numerical simulation for weld-bonded sets [25].

As it is possible to verify in figure 14, where is represented the numerical simulation for weld-bonded sets, the welding parameters do have an influence on the joint properties. Set 1 showed a brittle shear fracture of the welding nugget, on set 2 a fracture after plasticization is shown at the weld-nugget of the adherents starting at $\delta \approx 0.65$ mm, and on set 3 an adherent failure near the weld-nugget. Even though set 3 had a better strength joint, the adhesive degradation was expected (visible burning at the overlap periphery) due to the high amount of current and welding time [25].
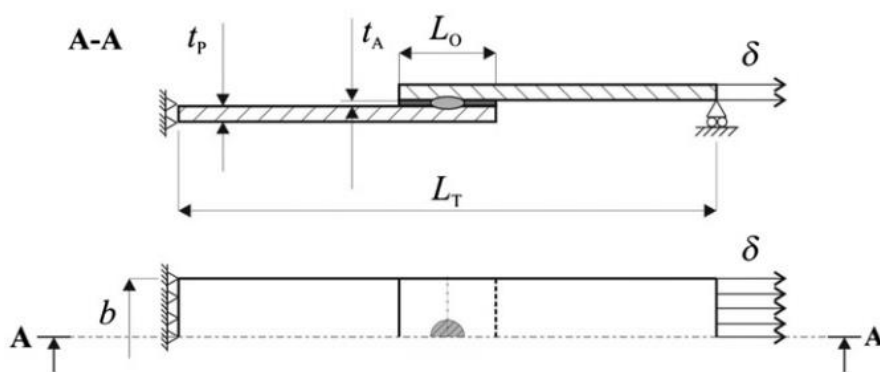
Figure 15- Representation of weldbonding process indicating L_0 and T_A.

Campilho et al. found out in [25] that when using set 2, around 1-2 mm of the adhesives was carbonized around the weld nugget, but they were not as influenced with higher overlaps. Table 4 shows the results of the study.

Table 4 – Improvement of weldbonding in comparative with only bonded or welded joints.

L0 (mm)	Bonded	Welded
15	24 % improvement	-
30	6.4 % improvement	22 % improvement
45	3.3 % improvement	46 % improvement
60	1.8 % improvement	58 % improvement

It was concluded, considering figure 15, that for stronger adherents an increase of loading values for bigger values of L_0 is expected, because it prevents adherent plasticization. The Young's modulus value (of the adhesive) directly influences the load value, as the adhesive has small values of this property, the joint allows the weld-nugget to support the majority of the loads. The increase of the T_A also reduces the stresses at the periphery of the weld-nugget and at the overlap edges, which provides higher values of P (load), while bigger values of E on the adherents reduce the peel and shear stress, increasing the strength of hybrid joints.

2.3.2. Rivet – Adhesive

Hybrid rivet- adhesive, schematized in figure 16, is a process that involves using rivets plus adhesive bonding in order to join solid materials. In the industry three manufacturing techniques can be defined [20]:

- Flow-in: the rivet is set and then the adhesive, with low viscosity, flows between the plates already with the rivets;
- Rivet - through uncured adhesive: The adhesive is placed and then before it fully cures one or more rivets are placed to hold the sheets;
- Rivet – through cured adhesive: similar to the second but the rivet is only placed when the adhesive is fully cured (this technique is not used in the industry);

This hybrid process represents a 40 % reduction of time and a 30 % reduction of the costs when compared to the arc weld, representing this way a powerful rival to one of the most common welding processes [20].

The advantages of these hybrid joints already has been mentioned, but if the adhesive and the rivet are well chosen, it is possible to obtain the advantages of each technique [26]:

- More stiffness(adhesive) and high ductility (rivet);
- Static strength (rivet) and resistance to fatigue (flexible adhesive);
- Mechanical strength (rivet) and resistance to corrosion (sealing adhesive);

T.Sadowski et al.[27], estimated that this hybrid process, even when compared with the strong bond of adhesive joints, leads to a 35 % improvement of the energy absorption (EA) with the use of rivets, when applied to double lap joints (DLJ).
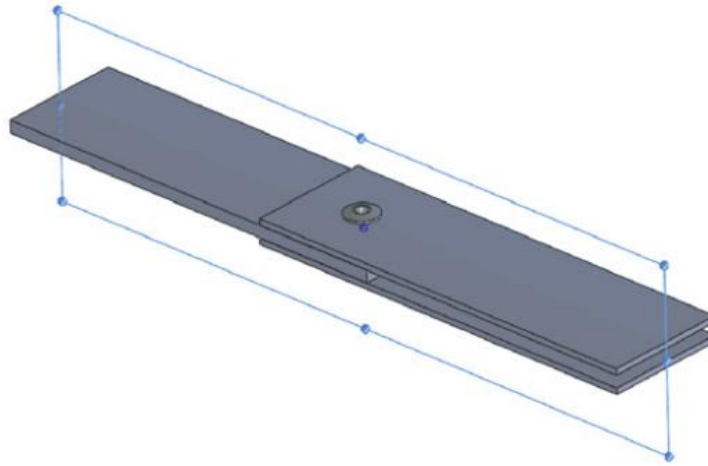
Figure 16- Scheme of Rivet + Adhesive DLJ [27].

Table 5 - EA of different joint configurations.

Type of joint	Energy absorption (EA) in [J]
Simple riveted joint	7
Simple adhesive joint	122
Hybrid joint	165

There is a synergic effect when joining these 2 processes since there is actually a 35 % improvement of EA when compared with the higher EA of one process only (simple adhesive joint). This fact is shown in table 5.

In this study it was also concluded that the use of rivets on a DLJ improves static strength and stiffness of the joint, therefore these conditions leads to a higher reliability and durability of structural joining of different parts such as in: automotive, nautical, aerospace, (...).

2.3.2.1. Rivet – Adhesive: More than one rivet

Sadowski et al. [28], performed an experiment where the proper adhesive was previously chosen, and the proper amount and configuration of rivets for sheets that were desired to be joined (DLJ). The number of rivets chosen, from 1 to 9, was 5, schematized in figure 17, since the increase of number of rivets also weakens the aluminum plates.
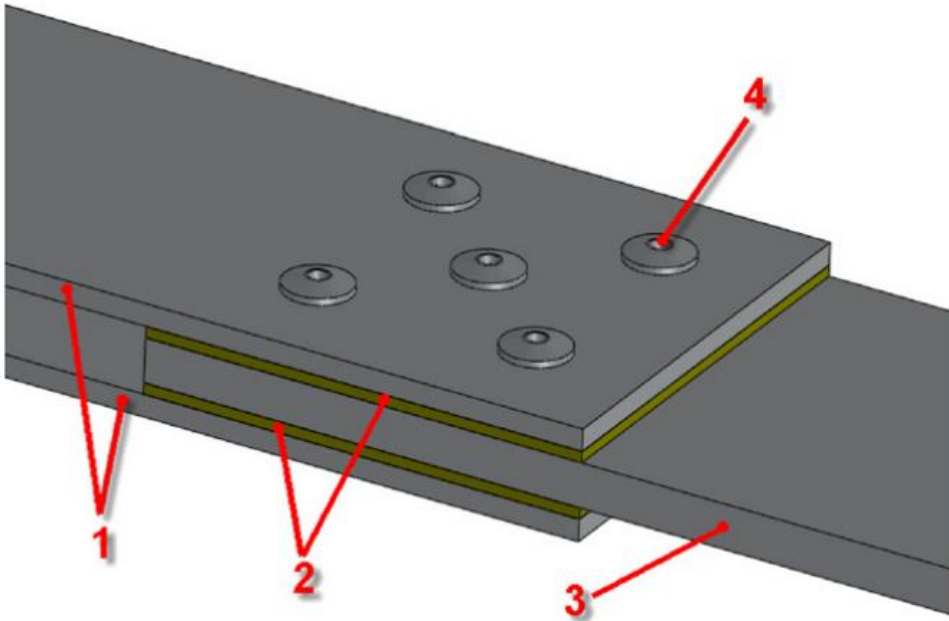
Figure 17 – Hybrid joint; 1, 3- Aluminum plates; 2 - Adhesive layer; 4 – Rivet [28].

The results of the tensile tests had shown that the hybrid joint is the best solution since its maximum load is about 11 % higher than an adhesive bonded joint and 130 % higher that a joint with 5 rivets only. The reinforcement of five rivets leads to a 64 % higher EA when compared with an adhesive bonded joint. This EA of the hybrid joint is equal to the sum of the EA of each technique alone [28].

The study also made numerical predictions using the software ABAQUS® and the results of the experimental and the numerical tests are in figure 18.
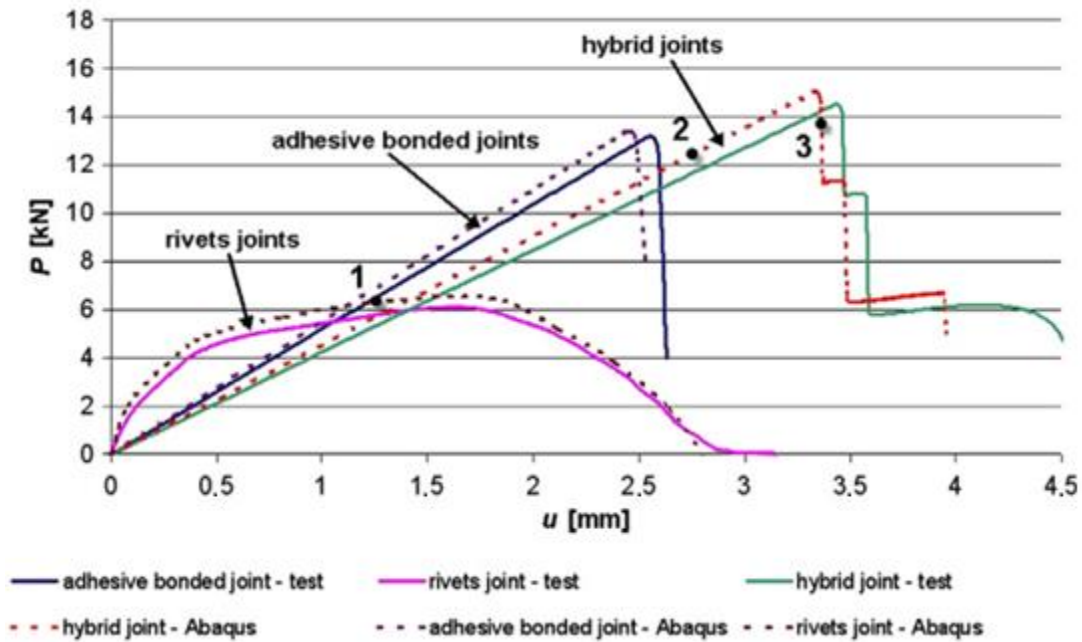
Figure 18 - Experimental and numerical comparison of the force–displacement tests results for the adhesive bonded joint, the five – rivet joints and the hybrid adhesive–rivet joints [28].

Figure 18 shows that hybrid joints have a synergic effect and improve the resistance to the tensile test. The numerical test showed very similar results. The assessment of the graph shows that the rivet joints only are stiffer at the beginning due to the high compressive stress introduced on the joint. Point 1 represents the failure of this rivet joint only, while point 2 represents damage initiation of the hybrid joint.

The stress in the adhesive layer is maximum in its central part, between the holes for rivets, leading to 60 % of the maximum stress at these spots. The maximum of the Huber–von Mises stress is localized in the riveted regions like in the case of the strip with a hole, which is subjected to uniaxial tension. These concentrations can create crack initiators, which can emanate from the edge of the hole.

2.3.2.2. Rivet – Adhesive: Layout of the rivets

The same authors of the previously study also tested the influence of the layout of rivets in a hybrid adhesive joint. With 3 rivets it was vary the configurations like is presented in Figure 19
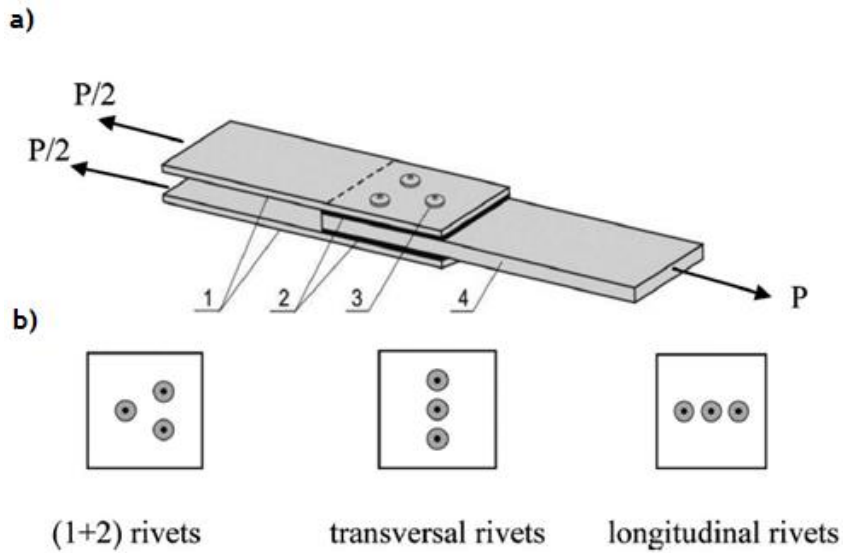
Figure 19- a) Schematic picture of the hybrid joint with its geometry: 1 – two aluminum laps 40 x 130 x 2 mm; 2 – two adhesive layers 40 x 40 x 0.1 – 0.2 mm, 3 – rivets d = 3.2 mm, 4 – aluminum plate 40 x110 x 4 mm, b) Different geometry of rivet layout in rivets joints and hybrid adhesive bonded/riveted joints for three rivets [29].

The results of EA from hybrid, AB and rivets only joints, when subjected to a force like is represented in figure 19, are in table 6:

Table 6 - Energy absorption in all types of joints (R, A, H) according to experimental and numerical researches [29].

Type of joint			Energy absorption [10^{-3}]		
			Before max shearing force	After max shearing force	Total
Hybrid longitudinal		Experiment	2.312	5.762	8.074
		Abaqus	4.630	2.266	6.896
Hybrid transversal		Experiment	3.500	3.700	7.200
		Abaqus	4.420	2.890	7.310
Hybrid 1 +2		Experiment	4.940	6.030	10.970
		Abaqus	8.324	4.140	12.464
Adhesive		Experiment	4.040	0.390	4.430
		Abaqus	4.290	0.284	4.574
Rivets	Logintudinal	Experiment	2.570	2.040	4.610
		Abaqus	3.440	3.196	6.636
	Transversal	Experiment	3.320	2.410	5.730
		Abaqus	3.450	3.720	7.170
	1+2	Experiment	3.290	2.160	5.450
		Abaqus	3.750	3.500	7.250

As it is possible to see, numerical work was performed during this study [29] and the results are relatively close to the experiment. The hybrid configuration 1+2 rivets showed better results of energy absorption, 1.7 times higher than adhesive and 1.4 higher than rivet only, and is therefore the best solution. It showed a displacement of 1.6 mm before failure, and the rest of the cases had the failure at 1.1-1.2 mm accordingly the authors. The tensile strength of the hybrid joint is about 3 % higher than the adhesive bonded joint and about 112 % higher than the rivet joint only.

2.3.3. Bolt – Adhesive

The hybrid process bolt-adhesive, represented in figure 20, has been tested in order to improve the properties of the joints of these two distinct processes and showed some promising results. The concept is similar to the rivet-adhesive technology but instead of rivets, bolts are used.

The motivation for using these hybrid joints can be summarized in some points [20, 30]:

- Structures that can eventually get in contact with fire, the bolts can hold them together when the adhesive would fail;
- Easily predicted long time performance, since the adhesive is combining with a proven technique;
- In the case of the joint being subjected to different loading directions, the adhesive will hold the shear stress and the bolts the transversal stresses;
- Continuous instead of discrete load transfer distribution along the overlap;
- Decrease of load transferred by fasteners;
- Possibility to reduce the mass of structures.

The use of hybrid joints carries some disadvantages as well. These joints are not benefic to structures that are subject to higher temperatures where a stiffer joint is required, since the adhesive will lose properties and lose its stiffness. Another problem is the cost, since 2 operations are being performed, it will surely be more expensive than only one. Another disadvantage is an interruption of electrical contact between the materials due to the use of adhesive [20].
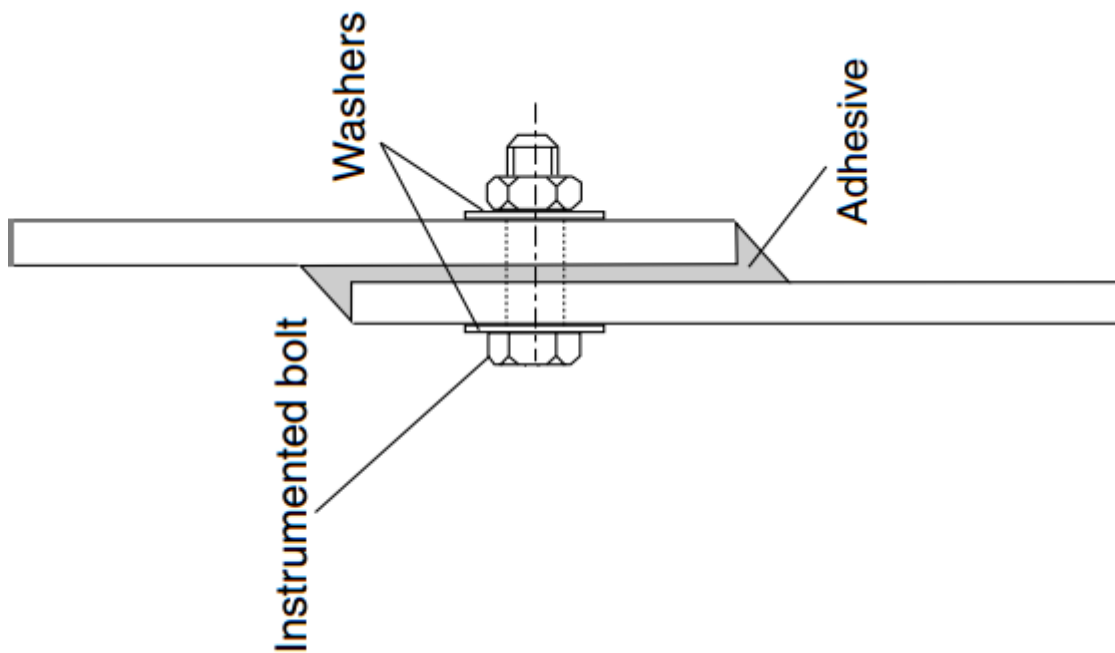
Figure 20 – Schematic of a Bolted- Bonded hybrid joint [31].

Kelly [31] has performed experimental and numerical studies on hybrid bolted-bonded joints. One of the scopes was to test different adhesives combined with bolts and see how they interact. The conclusion was that with stiff adhesive, the bolts have minor influence on the load transfers, but on more flexible adhesives, the bolts had a more important role on the loading transfers. The results of the study were:

- The load transferred by the bolt increases with an increase of adherent thickness;
- The load transferred by the bolt increases with an increase of adhesive thickness;
- The load transferred by the bolt decreases with an increase of overlap length;
- The load transferred by the bolt decreases with an increase of pitch distance;
- The load transferred by the bolt decreases with an increase of adhesive modulus.

In all existing designs of hybrid joints, bolts do not participate in supporting loads until the adhesive is almost failing, until then is the adhesive that carry the loads.

2.3.3.1. Bolt – Adhesive: Improvements with use attachments

Sun et al. [32] performed a study to characterize the hybrid joints and based on other papers, it was found out that the use of attachments would improve the resistance of the joint.

The experimental tests used composites as adherents but the results are interesting. Two kinds of attachment were used, an L-shaped and a stepped attachment, both represented in figure 21.

Joint with L-shaped attachment

Joint with stepped attachment

Figure 21 - Scheme of the joints with the attachments with one bolt only [32].

Besides these configurations, conventional hybrid joints were tested (without attachments), bonded and bolted.
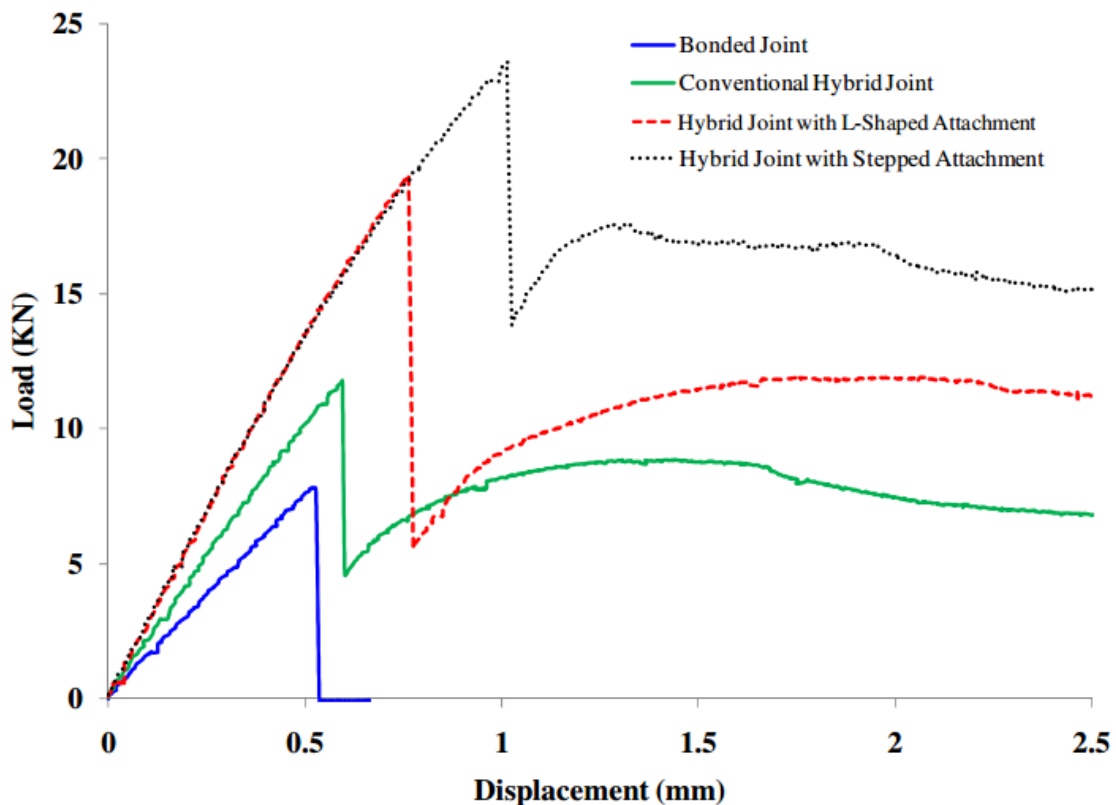
Figure 22 – Load-displacement curves for all joints tested [32].

Four configurations were tested and figure 22 shows the results. It was found that hybrid joints with stepped attachments show the best results, but the L-shaped ones also showed better resistance to the loading force when compared to conventional hybrid and bonded joints. Enhancements in the joint strength were verified of about 75 % and 115 % for the L-shaped and stepped attachments, respectively, over the conventional hybrid joint.

Finite elements analysis demonstrated that hybrid joints with stepped attachments had the lowest peel stress among the other joints.

2.3.3.2. Bolt – Adhesive: Influence of torque tightening

Kelly [31] also performed a series of experiments with the objective of studying the effect of the torque tightening on the bolts, with the configurations of simple double lap and hybrid double lap joints, in order to obtain the fatigue behavior.

The configuration of the hybrid joint is shown in figure 23.
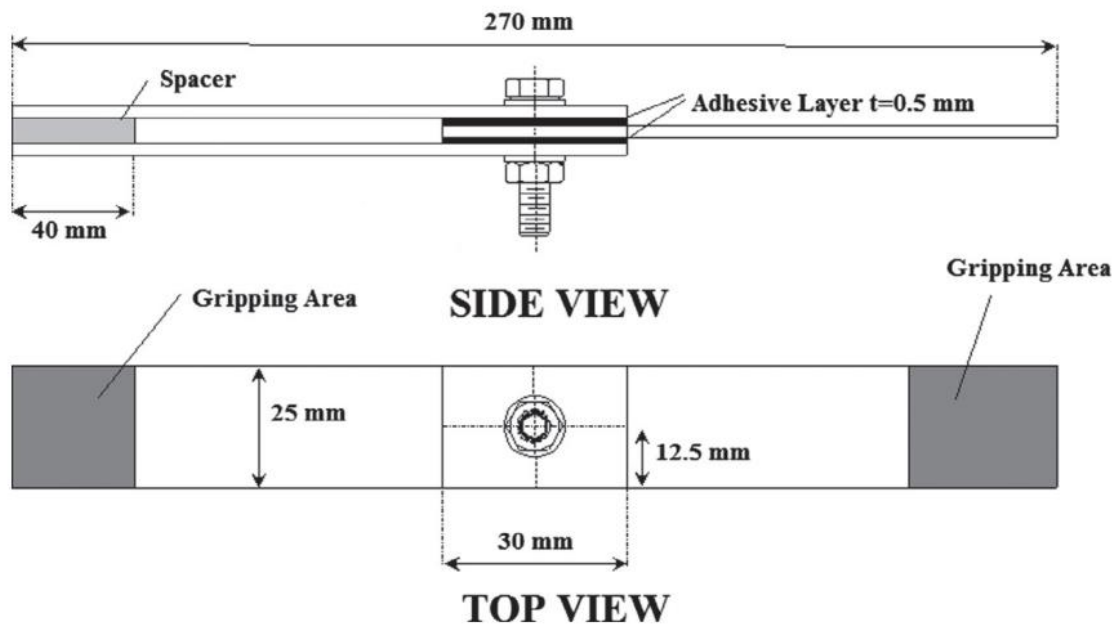
Figure 23 – Hybrid joint scheme for the study [31].
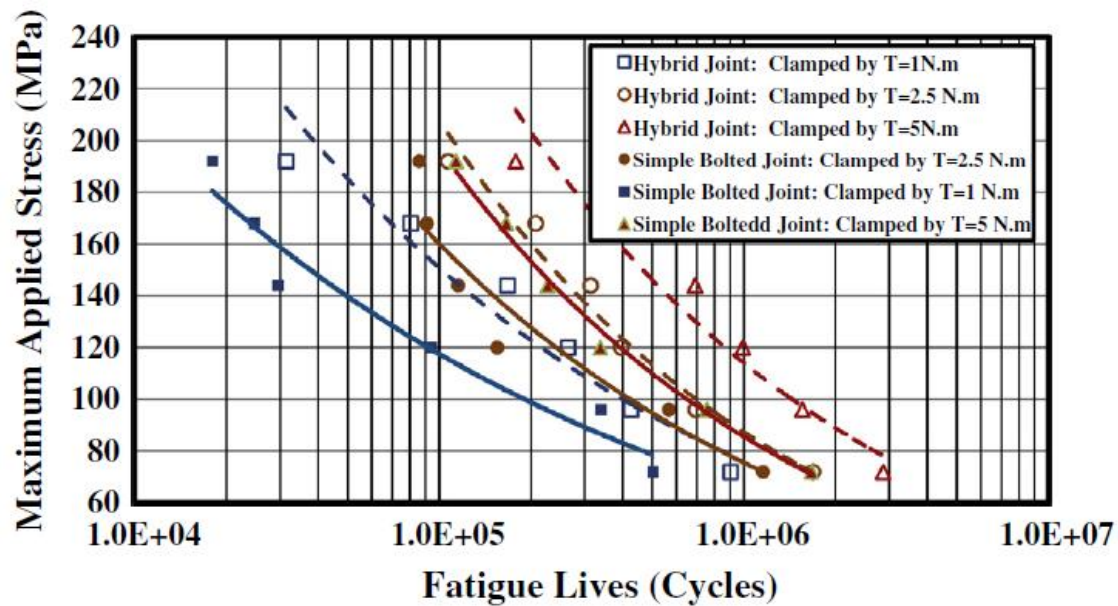
Figure 24 - S–N curve obtained from experimental fatigue tests for both kinds of the joints [31].

Figure 24 shows that increasing the tightening torque leads to a significant enhancement in the fatigue strength. As the clamping force value increases, the maximum tensile stress value at the edge of the hole is lower due to the higher clamping force value, which has a significant effect in reducing the maximum stress at the edge of the hole and at the same time developing friction force on contact surfaces. In addition, on the hybrid joints, the stress concentration around the hole is reduced significantly since a portion of the total load is transmitted by the adhesive layer.

Finally, the comparison of the obtained results from the experimental tests confirms that the hybrid joints have better fatigue performance than simple joints for all levels of the tightening torque. In addition, it should be noted that, in the hybrid joints, direct metallic contact between the plates does not occur (due to the adhesive layer presence), therefore, the possible fretting fatigue (that causes an early fatigue crack initiation) is eliminated [31].

In sum, the conclusions when comparing simple bolted joints and hybrid bolted joints, were that increasing the tightening torque or clamping force on the joint leads to an enhancement of the fatigue strength of double lap bolted joints and hybrid joints do have better resistance to fatigue than simple bolted joints.

2.3.4. Laser Weldbonding

The technique that combines laser plus adhesive for joining solid materials, represented in figure 25, is known as laser weld bonding (LWB) and it is a hybrid welding process. Initially the adhesive is applied between the two sheets to be joined and then it is welded using a laser beam. With the advances on the adhesives field every day, engineers started supporting known welding techniques with the use of it, and the results are interesting [33].

As already thoroughly discussed and shown, adhesives have a lot of advantages like good fatigue properties and the ability to join dissimilar metals. This hybrid process is mainly associated to join Mg and AA, but is expected to be very successful to join others dissimilar materials. One of the problems that are expected when combining such techniques is how the adhesive will react to the welding and vice versa.
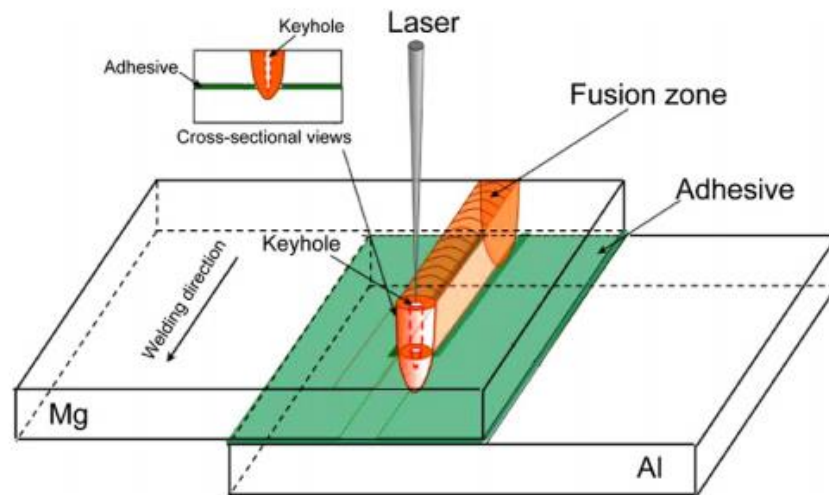
Figure 25- Schematic of LWB [33].

Wang, H. and L. Liu [33] verified that the adhesive decomposes due to the thermal effect caused by the beam power. In the fusion zone the adhesive decomposes and is released from the welding pool, subsequently the one close to the weld seam is also thermally affected. This decomposed area of wrecked adhesive varies with different welding parameters, and it is mainly influenced by pulse laser beam power and adhesive thickness.

2.3.4.1. Laser-Adhesive: Power beam vs Impaired Adhesive

In figure 26 and figure 27, it is possible to visualize that a higher power of the laser beam leads to an increased width of impaired adhesive.
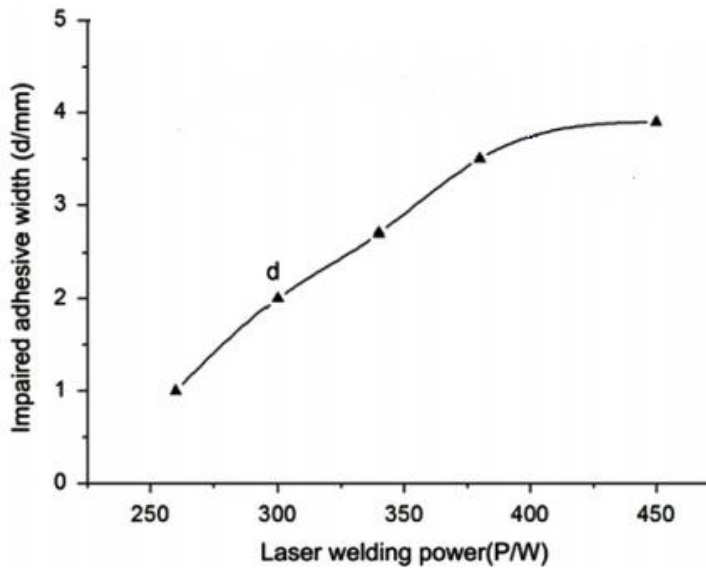
Figure 26– Impaired adhesive width at different laser welding beam powers [33].
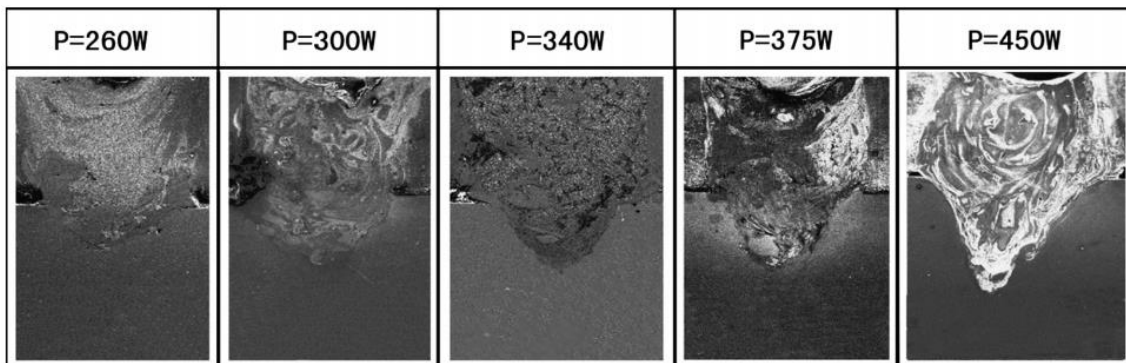
Figure 27 – Impaired adhesive areas at different laser welding beam powers [33].

Due to the porosity formation, the thicker the adhesive applied for LWB, the harder it is to control the welding parameters. It was concluded [33] that the thinner the adhesive layer is at the welding zone, the better it is to control its decomposition. The solution is to use a metallic interlay that will maintain the adhesive, close to the welding zone, thinner than 0.1 mm. The use of adhesive reduces the intermetallic content of the fusion zone, which improves the properties of the joint. The tensile shear load increases with a higher thickness of adhesive (up to 0.2 mm), therefore the interlayer is used to improve the LWB for dissimilar metal joints.

2.3.4.2. Laser – Adhesive: Direction of welding

The laser weld technique can also be varied according to the direction of the beam. Therefore LWB can be evaluated as LWB – PA (weld direction parallel to the loading force) in figure 29 and LWB – PE (weld direction perpendicular to loading force) in figure 28. In a study performed by Liu, L., D. Ren, and Y. Li [34], these configurations were tested.
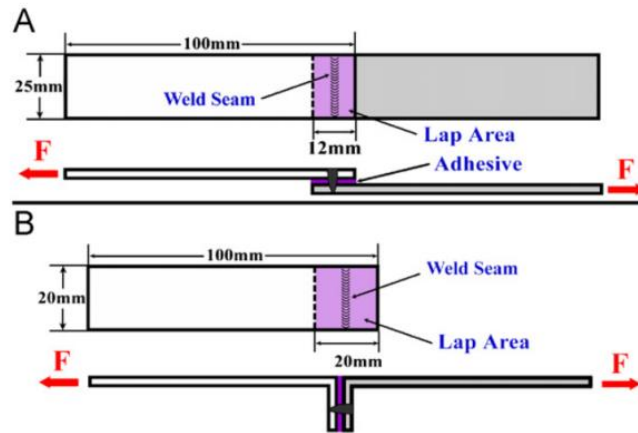
Figure 28 – LWB-PE [34].
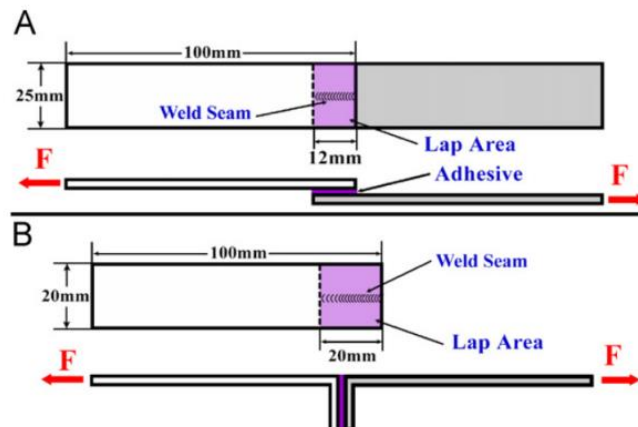
Figure 29 - LWB-PA [34].

2.3.4.2.1. LWB – PE

The most common configuration of laser welding is PE, and the results are displayed in table 7 and figure 30.

Table 7 – Tensile shear failure loads of different joints (PE) (kN) [34].

	1	2	3	Average
Laser welding - PE	3.2	3	2.9	3
Adhesive Bonding	6.5	6.7	6.7	6.6
Laser weld bonding - PE	7.1	7.3	7.8	7.4
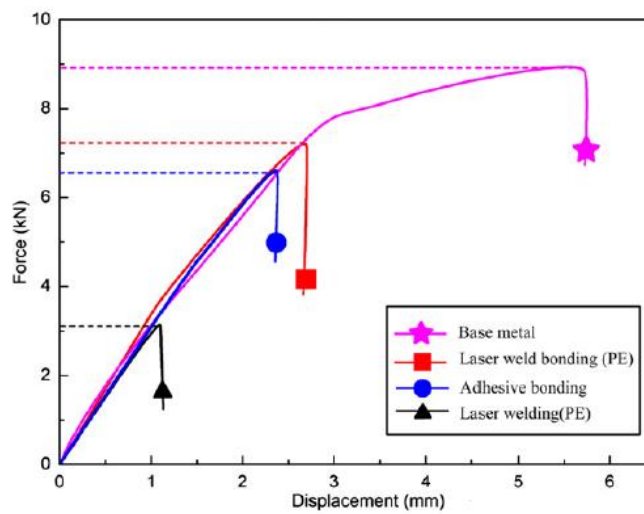
Figure 30- Tensile shear test results of the different processes [34].

Analyzing table 7, it is possible to see that there is a synergic effect on laser weld bonding, since it is the one that got better results of maximum force before failure. Results in figure 30 show that LWB can get 85 % of the force failure of the base metal, which is a good result compared to one of the processes alone.

Tests to see the peeling resistance of the joints were also performed and their results are presented in figure 31.
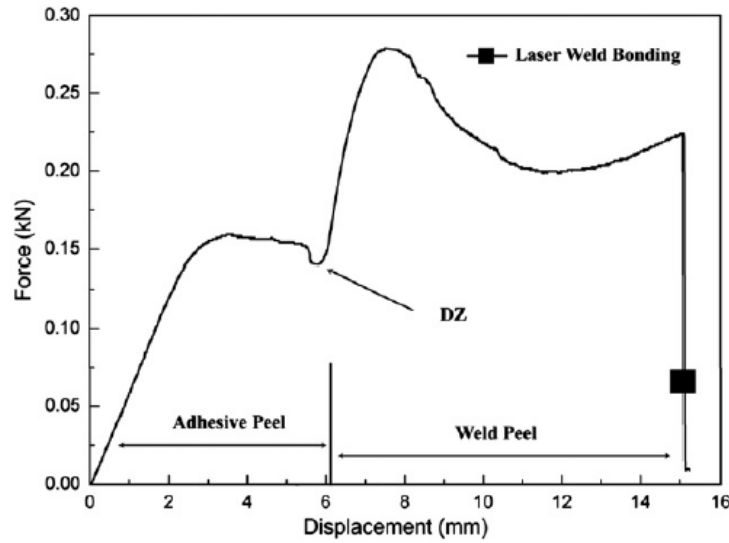
Figure 31 – Peel tests results of LWB– PE [34].

In figure 31 it is possible to see that at 6 mm displacement there is a drop of force, which is identified as DZ. DZ means damage zone and it happens because the laser beam thermally damages the adhesive around the weld and that is why a drop of force can be seen when the adhesive peel ends. Since the peeling resistance of LWB is equal to laser welding only, it can be concluded that there was not an improvement of the maximum peel stress with or without the adhesive.

2.3.4.2.2. LWB – PA

Liu, L., D. Ren, and Y. Li [34], also performed tests on parallel laser weldbonding and the results of the tensile tests are displayed in table 8 and figure 32.

Table 8 – Tensile failure loads of different joints (PA) (kN).

	1	2	3	Average
Laser welding - PA	1.5	1.4	1.5	1.5
Adhesive Bonding	6.5	6.7	6.7	6.6
Laser weld bonding - PA	7.7	8.2	8.5	8.1
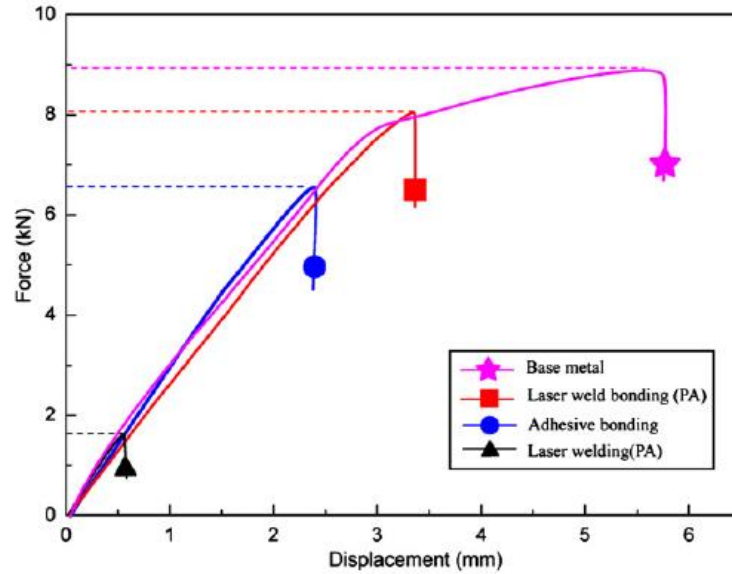
Figure 32 - Tensile test results of the different processes [34].

The tensile failure of LWB-PA was of about 8.1 kN, which is not only better than the non-hybrid processes but also better than LWB-PE. This is because this configuration allows to the laser weld to hold the peeling stresses that are concentrated at the edges of the overlap.

Regarding the peel stress there was an improvement when compared with AB and laser weld only.

With this study it can be concluded:

- LWB (in the two configurations) shows better tensile shear loads than AB and laser weld only;
- LWB-PA shows better tensile results, with a higher strength and EA than LWB-PE;
- LWB-PE shows no synergic effect regarding T-peel stresses, on the other hand, LWB-PA shows improvement and synergic effect;

The LWB-PA had proven itself the most benefic technique of both processes, but more operations are required to perform it, but this disadvantage can be eliminated with the use of a welding robot.

2.3.5. Hybrid FSSW + AB

Due to the lack of literature concerning FSW plus AB joints this section includes some information about a derivate of this process, known as friction stir spot welding.

Friction stir spot welding (FSSW) is a novel solid state process that has recently received considerable attention from various industries including automotive sectors due to the many advantages over resistance spot welding. It is similar to friction stir welding, but there is no transversal speed since it only welds specific points defined by the operator.

Chowdhury et al. [35], performed some experiments to combine FSSW with adhesive, and figure 33 shows the load-displacement curves of the combination of these two distinct processes and the materials chosen to join were Al and Mg sheets. As it is possible to see in figure 33, three configurations were tested: FSSW Al/Mg, FSSW Mg/Al with adhesive and FSSW Al/Mg with adhesive, this last configuration meaning that the top plate is aluminum and the bottom plate is magnesium. The tests were performed on SLJ's.
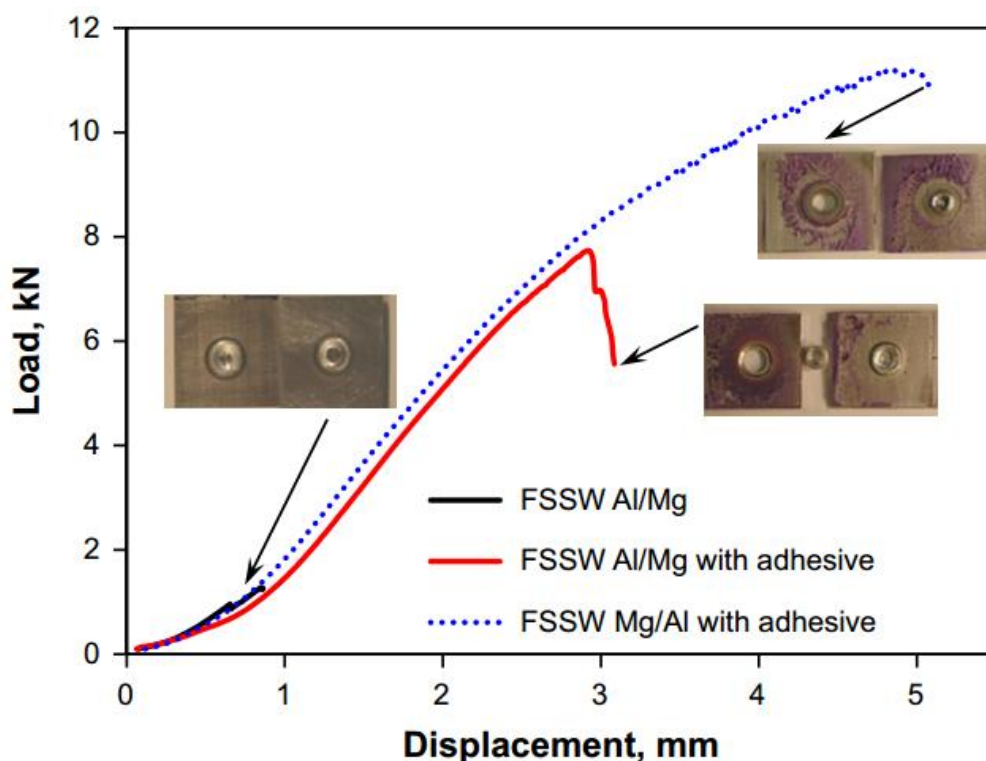
Figure 33 – Lap shear properties of the dissimilar Al/Mg weld, Al/Mg adhesive weld, and Mg/Al adhesive weld tested at a crosshead speed of 10 mm/min [35].

Analyzing the graphic it is possible to verify that the best configuration is Mg/Al weld with the use of adhesive. But the welded Al/Mg with adhesive also showed improvement over FSSW Al/Mg only.

The considerably lower maximum lap shear load in the Al/Mg dissimilar weld was attributed to the formation of the brittle intermetallic (IMC) layer at the interface. Therefore decreasing the extent of IMC formation at the interface and load concentrations by using an adhesive in the Mg/Al joint resulted in a higher lap shear load. Both hybrid joints showed higher failure energy, Mg/Al → 26.5 J and Al/Mg → 9.5 J, when compared to the dissimilar Al/Mg weld

→ 0.34 J. Since lap shear tensile and failure energy tests are directly correlated to impact tests, it is expected that the hybrid joints have similarly better results in those tests [35].

Regarding the fatigue life, tests were also performed in order to find out if any improvements were obtained by joining these two processes in one. The results are shown in figure 34.
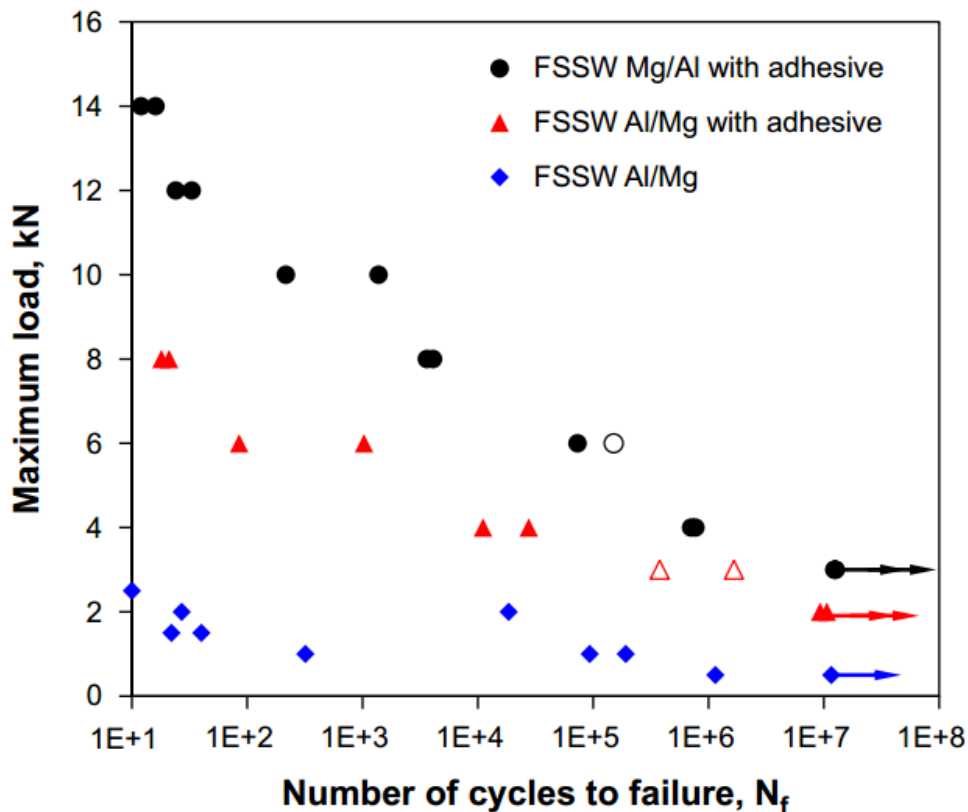
Figure 34 - S–N curves of the dissimilar Al/Mg weld, Al/Mg adhesive weld and Mg/Al adhesive weld tested at R = 0.2, 50 Hz and room temperature, where solid symbols indicates the nugget pull-out failure and empty symbols indicates the failure perpendicular to the loading direction [35].

As it is possible to interpret, the Mg/Al adhesive weld was once again the configuration that achieved the best results in general. The Al/MG dissimilar weld fatigue life was much shorter than the hybrid joints, especially with loads above 1 kN. The main reason for this difference was the use of the adhesive layer that eliminated stress concentration surrounding the weld nugget which may lessen the formation of IMC layer at the interface and lead to a uniform distribution of stresses along the overlap.

From this work [35], the conclusions were that the hybrid joints Al/Mg and Mg/Al in comparison to the Al/Mg FSSW only, showed that the extent of forming the IMC compounds decreased in the dissimilar adhesive joints and also a much higher hardness with values in-between HV 90 and 125 was observed in the stir zone of Al/Mg and Mg/Al adhesive welds due to the presence of IMC compound layer.

Both Mg/Al and Al/Mg adhesive welds had significantly higher lap shear strength and failure energy than the Al/Mg dissimilar weld without adhesive. The failure energy of the Mg/Al adhesive weld was further higher than that of the Al/Mg adhesive weld.

Concerning the fatigue life of the Mg/Al adhesive weld was generally higher than that of the Al/Mg adhesive weld, both the Mg/Al and Al/Mg adhesive welds had a much longer fatigue life than the dissimilar weld without adhesive especially at higher cyclic load levels. Two distinct failure modes were observed to be dependent on the cyclic load level in the dissimilar adhesive welds. At higher cyclic loads nugget pull-out failure occurred in both the Mg/Al and Al/Mg adhesive welds where fatigue crack propagated circumferentially around the nugget, while at lower cyclic loads fatigue failure in the Al/Mg adhesive weld occurred in the bottom Mg sheet due to the stress concentration of the keyhole leading to crack initiation and then propagation at right angles to the loading direction.

2.4. FSW + AB (Friction Stir Welding with Adhesive Bonding)

Joining AA and other similar materials is a complex process due to the low melting points and poor joint properties associated with them. A revolutionary technique that can achieve a joint with good properties was the friction stir welding process. However the low resistance to loads that create shear stresses and affect the fatigue life is a problem. With addition of adhesive an improvement of the fatigue life of the joint is expected due to vibration damping, and it will also will work as a sealant of the joint (solving/helping the corrosion associated to FSW).

From the literature review it was possible to conclude that it is becoming increasingly interesting to combine known joining processes with AB. As such, hybrid joints were presented: weld-bonded, rivets and bolts with adhesive, laser weldbonding and even FSSW with adhesive. As already stated, there is no research about combining FSW with adhesive until now.

All of the researched hybrid joints for the literature review were improved relative to one of their processes alone except FSSW with adhesive, for which the hybrid joints were not compared with adhesive joints.

Chapter 3 - Experimental Work

The experimental work required the manufacture of different joints in order to assess the effect of the different parameters employed as well as to compare the three different technologies used, where the only welded and adhesive joints were a benchmark to the study of the hybrid friction stir weldbonded joints.

3.1.Material Properties

The substrates used on this project were made from AA6082 aluminum alloy with T6 treatment. The chemical and mechanical properties of the aluminum alloy are presented in table 9 and table 10, respectively.

Table 9 – Chemical composition of Aluminum Alloy 6082-T6 (% of total mass) [36].

Manganese (Mn)	Iron (Fe)	Magnesium (Mg)	Silicon (Si)	Copper (Cu)	Zinc (Zn)	Titanium (Ti)	Chromium (Cr)	Others (Total)	Aluminum (Al)
0 - 1.00	0.0 - 0.50	0.60 - 1.20	0.70 - 1.30	0.0 - 0.10	0.0 - 0.20	0.0 - 0.10	0.0 - 0.2	0.0 - 0.1	Balance

Table 10 – Mechanical properties of Aluminum Alloy 6082-T6 [36].

Material	Young's modulus [GPa]	Yield strength [MPa]	Ultimate tensile strength [MPa]	Elongation [%]
AA6082-T6	70	>260	>310	7

Regarding FSW, there are fixed and variable parameters that were chosen from a combination of trial and error and previous experience within the work group at LOME and IST (Instituto Superior Técnico) on FS welded joint manufacture. The fixed parameters are presented in table 11, and table 15 contain the experimental matrix of the manufactured joints within the focus of this thesis. The tool used for welding was a patented modular concept composed by a body, shoulder and probe/pin, and is shown in figure 35. The fixed parameters were chosen due to the previous experience within the workgroup and some articles researched [37, 38]. Although the values for the fixed parameters are not exactly the same as the articles, in this project some values were changed due to the necessity to avoid degradation of the adhesive.

Figure 35 - Tool used to weld.

Table 11 - Fixed FSW parameters.

FSW parameter	Vertical force
Rotation direction	CCW
Plunge speed	0.1 mm/s
Dwell time	5 s
Tilt angle	0º
Welding speed	200 mm/min
Rotational speed	1000 rpm
Pin length	2.8 mm
Pin diameter	5 mm
Shoulder diameter	16 mm

3.1.1. Adhesive Properties Characterization

Along this section the mechanical characterization of the Araldite 420 A\B adhesive will be presented and in addition to the performed tests it is included some previous work performed within the work group in order to contextualize and fully characterize the adhesive used.

The adhesive container is shown in figure 36. Some of the most important properties are:

- Very high shear and peel strength;
- Extremely tough and resilient;
- Good moisture resistance;
- High ductility;
- Chemical stability;

Araldite 420 A\B is a two component epoxy adhesive, thermosetting cured at room temperature that leads to a strong and tough bond. It supports up to 70 ºC, keeping the high shear strength and good peel strength.

The mechanical properties of this adhesive are presented in table 12.

Table 12 – Mechanical properties of Araldite 420 A\B [39].

Adhesive	Young's modulus [GPa]	Yield strength [MPa]	Maximum strain [mm/mm]
Araldite 420 A\B	1.85	29.25	0.22

Figure 36 – The adhesive araldite 420 A/B.

The adhesive cures at room temperature, with the possibility of being speed up with increased temperature. It presents good resistance and durability, with a service temperature of around -40 to 100 ℃. It is used on transportation industry and others.

3.1.1.1. Bulk Tensile

Bulk specimens (represented in figure 37) were previously tested under tensile loads in order to determine the mechanical properties of the adhesive Araldite 420 A\B, such as yield and ultimate strength and also to estimate the Young's modulus. The specimen geometry was based on the British Standards Institution BS 2782 standard method 320C.
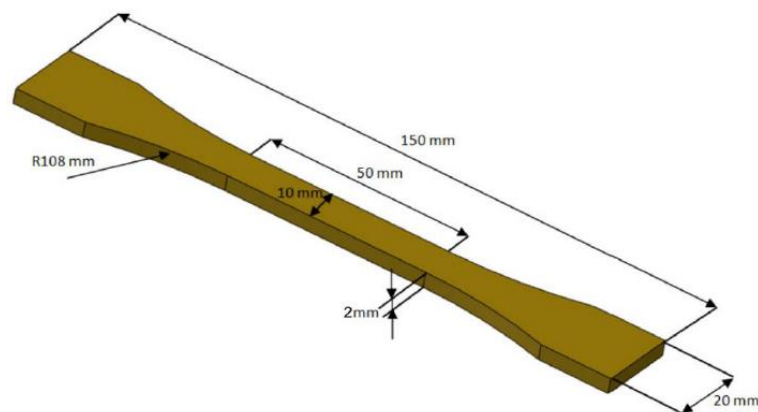
Figure 37 – Bulk Specimen geometry.

From the tensile test of the bulk specimen at 1mm/min, figure 38 shows the stress/displacement curve of the adhesive araldite 420 A\B with: no post cure, post cure at 195 ℃ and post cure at 235 ℃. Since the adhesive suffers post cure when welding with the adhesive fully cured, the tests were performed in order to understand what happens to the mechanical properties of the adhesive under such temperatures, since the rotation and advancing speed of the tool during welding can create peaks of 250 ℃.
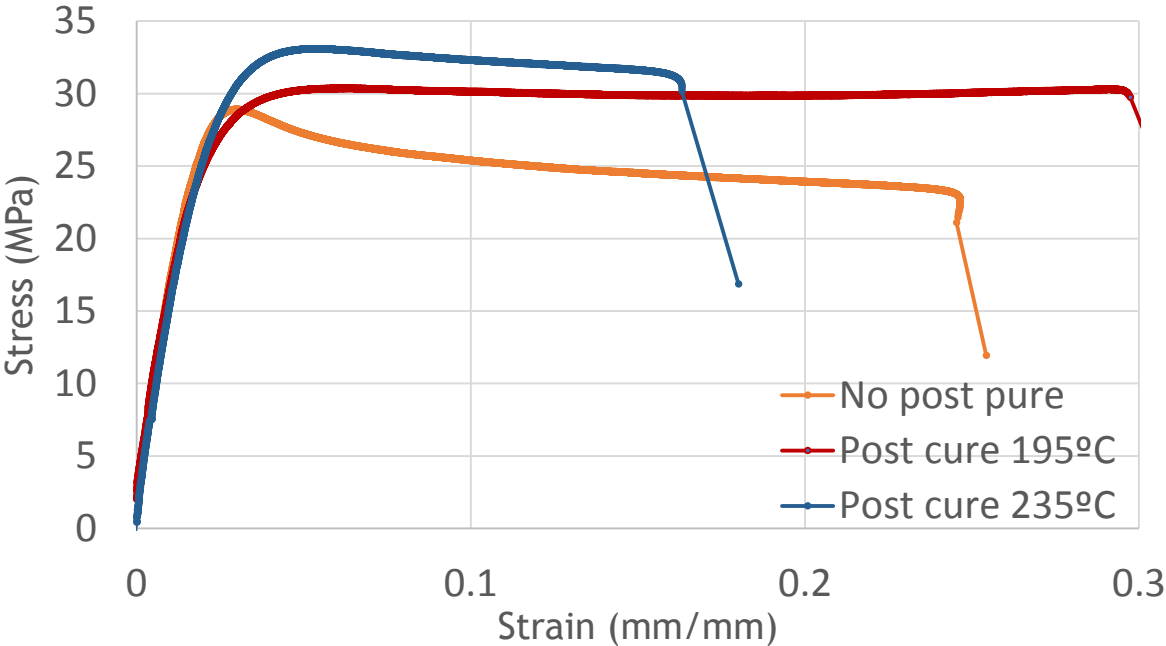
Figure 38 - Bulk tensile curves with and without post cure of the adhesive.

Figure 39 and figure 40 present the variation of Young's modulus and ultimate maximum strength of the adhesive, with and without post cure, respectively. For the calculation of these properties, 2 specimens were tested in each test, except for the results for post cure at 235 °C, in which 3 specimens were used.
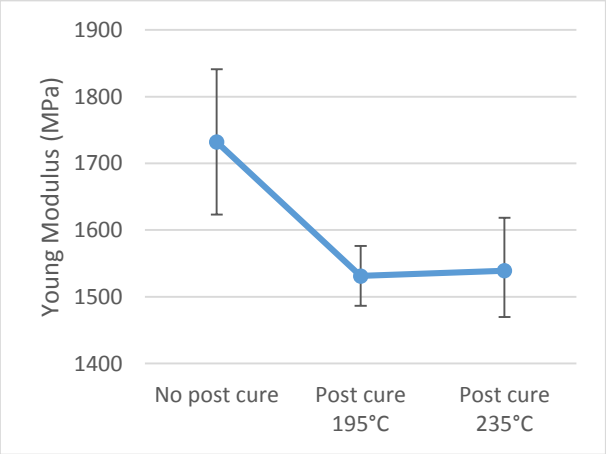
Figure 39 – Young's modulus variation with and without post cure.
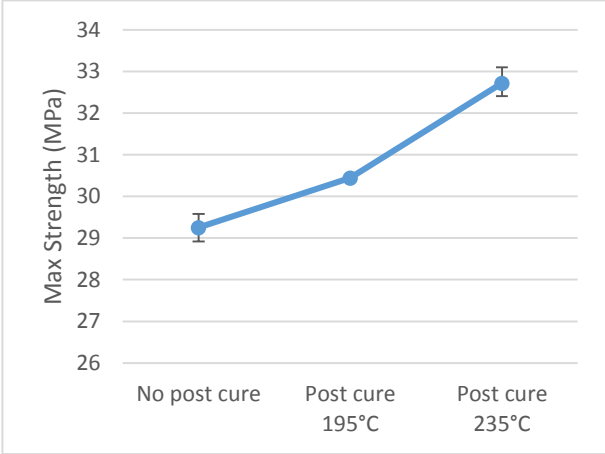
Figure 40 - Maximum ultimate strength of adhesive with and without post cure.

The results for the tensile test on the bulk specimen are presented in table 13 where it is shown the Young's modulus and maximum strength values for the adhesive with/without post cure.

Table 13 - Results for the tensile test on bulk specimens of Araldite 420 A\B.

	Young's Modulus (MPa)	Maximum Strength (MPa)
No post cure	1731	29.5
Post cure 195 ºC	1531	30.4
Post cure 235 ºC	1539	32.7

3.1.1.2. Fracture Energy

To characterize the adhesive for modelling purposes, it was necessary to determine the fracture properties of the adhesive under mode I and in mode II (tensile and shear). In order to obtain these properties double cantilever beam (DCB) specimens were used for mode I and end-notched flexure (ENF) specimens for mode II. Both tests used the compliance-based beam method (CBBM) to obtain the facture toughness. This study was also previously made within the work group including only specimens cured at room temperature for more than 8 hours. The DCB's were tested at 1 mm/min and the ENF's at 0.25 mm/min.

Figure 41 and figure 42 represents the R curves for mode I and for mode II, respectively. The value of fracture energy for mode I is around 2.5 N/mm and 12.75 N/mm for mode II.
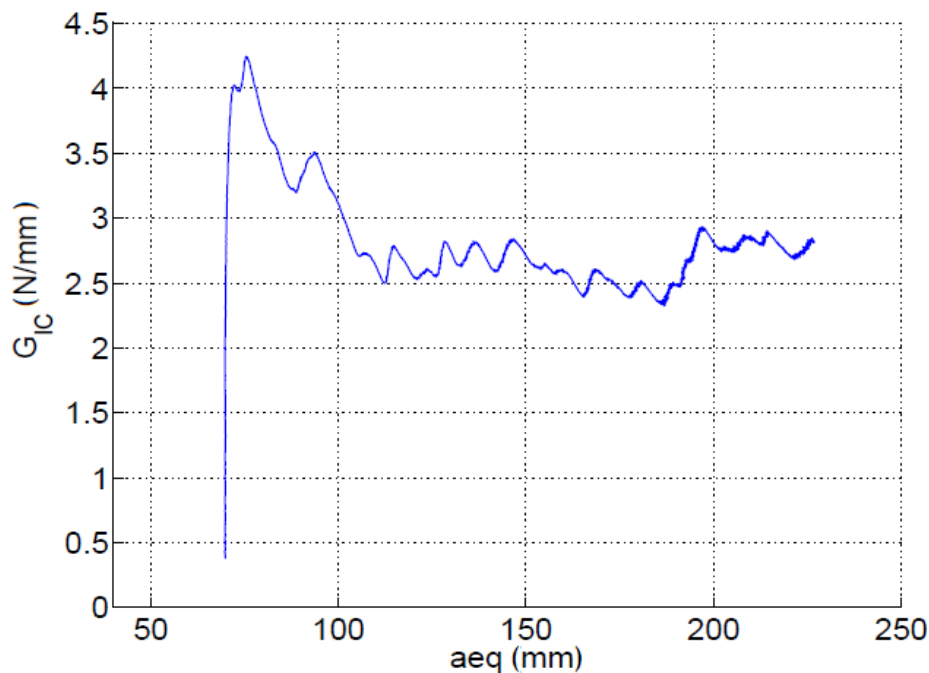
Figure 41 - R-curve for mode I of araldite 420 A\B.
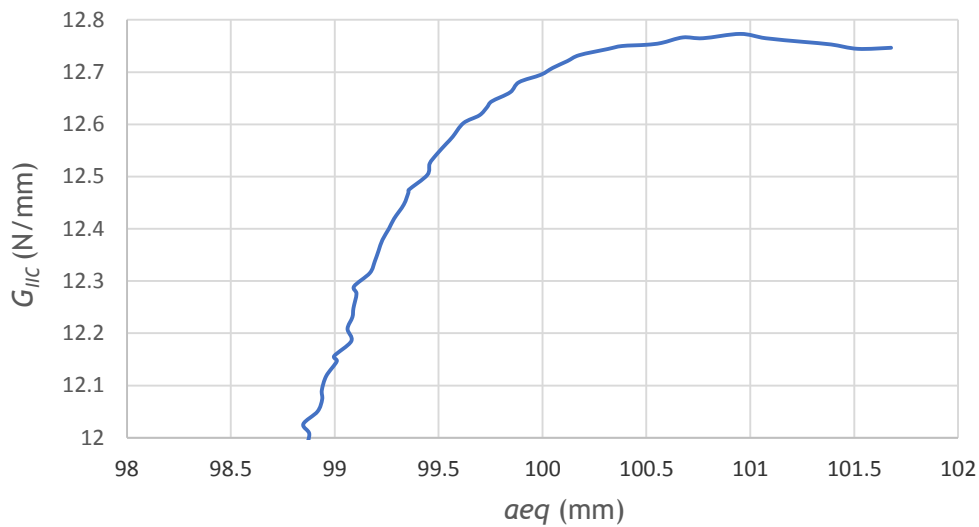
Figure 42 - R-curve ENF for mode II of araldite 420 A\B.

3.1.1.3. TAST – Thick Adherent Shear Test

In order to measure the shear properties of the adhesive, TAST (Thick Adherent Shear Test) specimens were manufactured and tested. TAST is a popular failure strength test due to the easy manufacture of the adherents and can be seen as a logical extension of the single lap shear test method, because the geometry is very similar but thick adherents are used. In order to improve the adherence of the surfaces to bond, the adherents were sandblasted and degreased with acetone before the application of the adhesive. The thickness of the adhesive was 0.8 mm.

With 0.8 mm of adhesive thickness, the objective of these TAST specimens is to reduce the peel stress and then lead to the value of shear stress of the adhesive. Since this test requires a rigorous control of the results obtained, a clip gauge was used in order to get strain/displacement as accurate as possible. Figure 43 shows a TAST specimen being tested with the clip gauge in place.
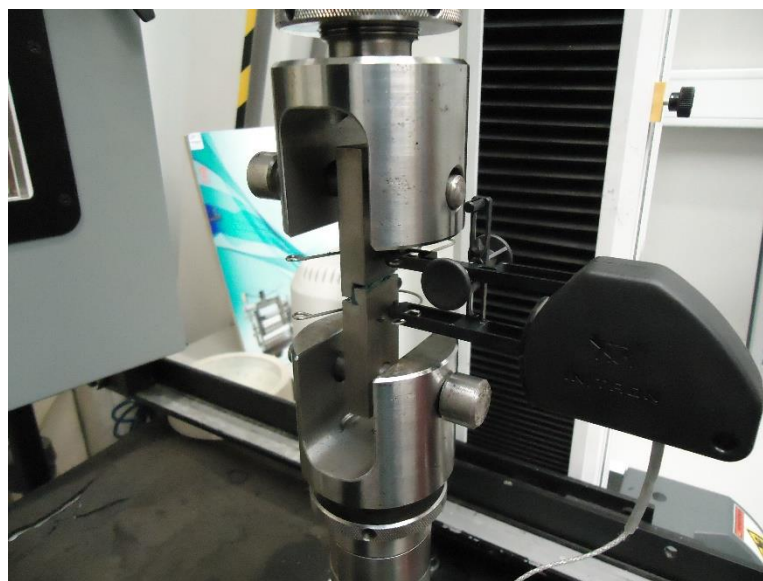
Figure 43 - TAST test with use of an extensometer.

The geometry of the TAST specimen is presented in figure 44. In order to reduce the chance of specimens bending during the tests, it was used steel adherents due to high rigidity that these presents, avoiding peeling stresses and also a possible plastic deformation of the adherents. Due to the geometry of the specimens, the bonded area can be inconveniently extended to the vertical surfaces, compromising the results of the tests. To avoid this problem spacers were placed between the vertical surfaces and removed after the curing process. A mold was used to correctly align the specimens and it was left under pressure for more than 8 hours to complete the curing process of the adhesive.
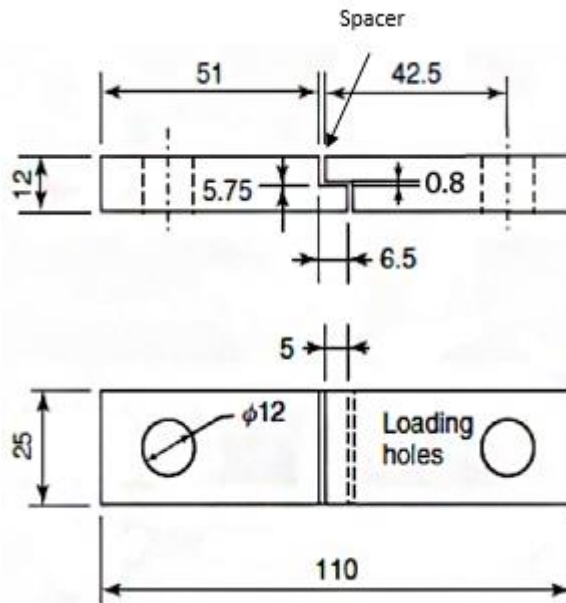
Figure 44 - TAST specimen geometry with dimensions in mm [40].

The results achieved in the TAST testing are presented in figure 45 and table 14. The tests were performed using an Instron 3367 tensile test machine, at room temperature and at a constant crosshead rate of 1 mm/min. For this test 5 specimens were used, however one of the specimens had incoherent results (the adhesive failure was premature), leaving only 4 tests to analyze.

Table 14 – TAST results.

TAST	Spec-01	Spec-02	Spec-03	Spec-04	Average	Max	Min	+	-
τ (Shear stress) (Mpa)	22.53	22.83	23.64	21.86	**22.72**	23.64	21.86	0.93	0.85
G (Shear modulus) (MPa)	2621.8	1890.8	1819.2	2337.8	**2167.4**	2621.8	1819.2	454.4	348.2
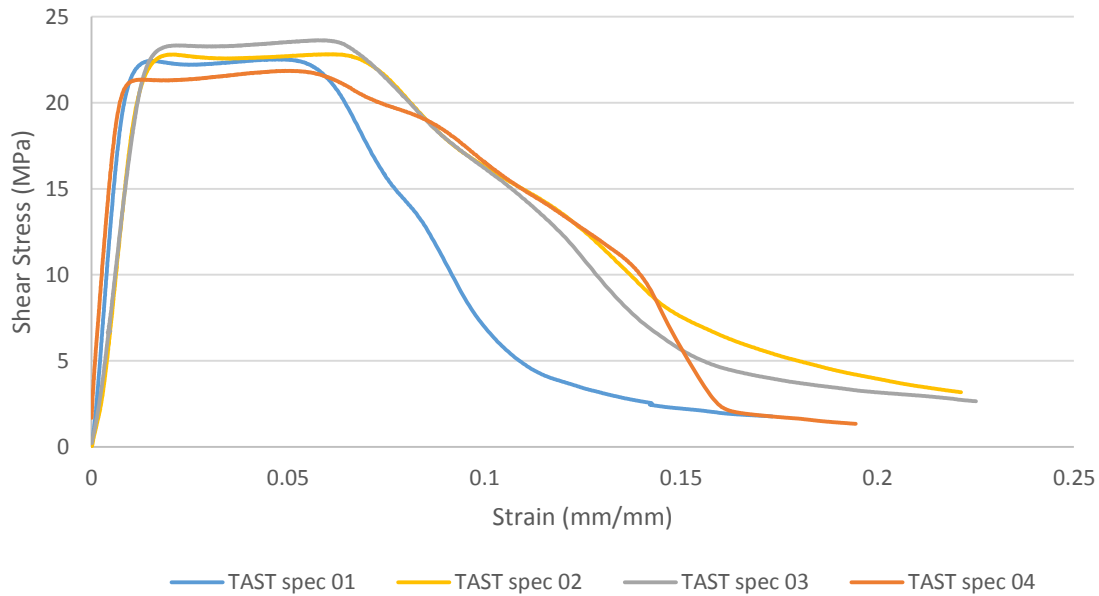
Figure 45 - Shear Stress - Strain curve of araldite 420 A\B at 1 mm/min.

3.1.2. Discussion of Adhesive Properties Characterization

The bulk tensile test allowed to obtain the different Young's modulus of Araldite 420 A\B with and without post cure. Comparing the results, it is possible to see that with post cure at 235 °C the adhesive is more ductile, with a lower Young's modulus and a higher maximum strength when compared to the no post cure configuration. Post cure does increase the Young's modulus and consequently improves the maximum strength but after 250 °C the adhesive starts to degrade.

Comparing the results of bulk tensile tests with the results obtained in the work group AdFEUP (adhesives that are used in automotive industry as well), the adhesive XNR 6852-E2 had a similar Young's modulus (1830 MPa). The adhesive Araldite 420 had a Young's modulus of 1731 MPa without post cure. Regarding the SIKA POWER 4720, this adhesive is more brittle and had 2170 MPa. However, XNR showed a higher tensile strength, 41 MPa, when compared with SIKA POWER and Araldite that had only 32 and 29.5 MPa, respectively.

Concerning the results obtained in TAST, it was possible to see that the adhesive had a shear stress of 23 MPa and a shear modulus of 2.2 GPa. However the measurements made are not reliable due to the failure mechanism that had adhesive failure as can be seen in figure 46. It can be concluded that sandblasting treatment to the steel is not suited for this adhesive. The steel cannot be anodized and for future work it should be attempted to manufacture TAST specimens of aluminum in order to anodize and increase the adherence of the adhesive, leading to more reliable results. Note that the new specimens should be redesigned to avoid plastic and elastic deformations of the adherents during the tests.
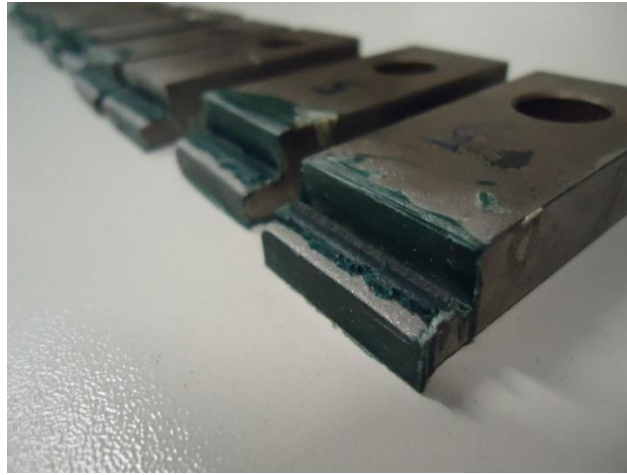
Figure 46 – Failure mode in TAST specimens for Araldite 420 A\B.

3.2. Joint manufacture

In order to test the combination of the welding process with AB, it was necessary to proceed with a rigorous and detailed manufacture process, so the measured results and conclusions are reliable and consistent.

Since the welding process is performed after bonding, the correct manufacture process for single lap joints with adhesive will be shown, and then the welding joints.

Initially it was necessary to define the dimensions of the plates to join. Normally the specimens are cut with dimensions that will be tested (20x110x2 mm), but in this case the bonded plates will have (230x110x2 mm), due to the necessary length (230 mm) to later perform the FSW. Figure 47 shows a bonded finalized specimen and the initial plate to bond. It is relevant to point out that all the specimens produced during this thesis had the plates joined in such a way that the laminate direction of the aluminum is perpendicular to the load forces applied during the tensile and fatigue tests.

Figure 47 – Comparison of the initial dimensions and final dimensions of the specimens to be tested with 230x110x2 mm for the bigger plate.

To join the plates (230x110x2 mm), 60 mm of the specimen's 110 mm length was used in the overlap, leading to a bonded area of 60 x 230 mm. Since some joints required channels of adhesive layering, presented in figure 55, in order to avoid contact between the welding seam and the adhesive. The adhesive will be placed on the grooves and the welding will be performed in the length between them. In figure 48 grooves are shown already with adhesive.
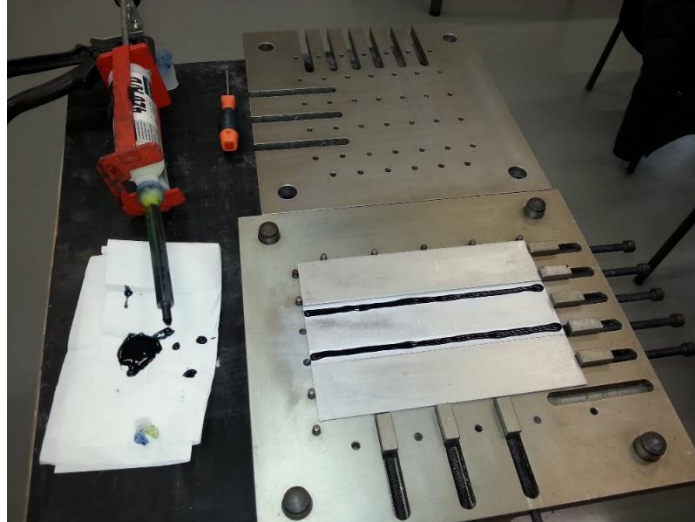
Figure 48 - Application of the adhesive that will be further compressed in order to obtain a good adhesion and a fully cured adhesive.

The groves were manufactured using an optimum bf20 machine. Figure 49 shows the process, during which channels were created by removing aluminum to be later filled with adhesive. The channels had 0.2 mm of depth and 10 mm of width.
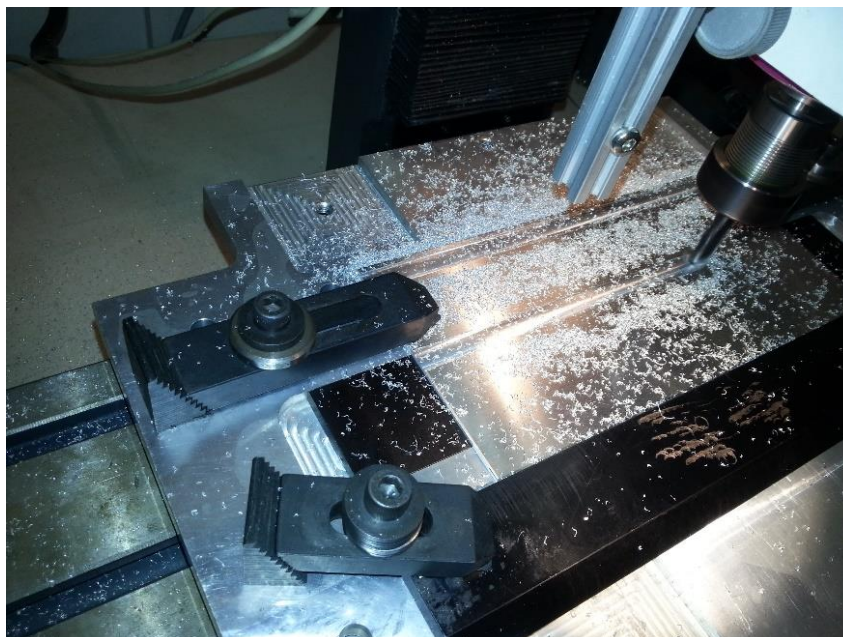
Figure 49 - Manufacture of the grooves.

The material necessary to perform bonding and FSW is:

- Aluminum plates (230x110x2 mm) with and without grooves to bond;
- Aluminum shims (230x50x2 mm) in order to correctly position the plates in the mold;
- Adhesive Araldite 420 A/B;
- Mold to correctly position and clamp the plates to bond;
- FSW welding machine;
- Correct tool (pin + shoulder) to perform FSW;

Others materials:

- Acetone to clean the surfaces to bond;
- Sandblasting machine to increase the area of bonding;
- Nozzle mixer or a centrifuge machine to correctly mix the two parts of the adhesive;
- Release agent to not allow anything else to bonded unless it is wanted to;
- Press to maintain the pressure in the bonded area and the temperature when necessary;
- Mixture gun to apply the correct percentages of each part without needing to weigh them individually;
- Material to perform adonization (phosphoric acid + water + power volt);
- Calibrated tapes to obtain the desired adhesive thickness;

3.2.1. Manufacture of Bonded Joints

The first action needed before bonding is the surface treatment of the area/plate to be joined. There are many options to make surfaces treatments, however the only options available were sand blasting or phosphoric acid anodization (PAA). Cleaning the surfaces to be bonded is very important, for which acetone was used. Since the results obtained when using sand blasting were acceptable and could provide a comparison between bonded and weldbonded joints, this was the employed surface treatment. Note that sandblasting treatment in aluminum plates of the dimensions already referred must be uniform since constant adhesion of the adhesive in the whole area is desired and should be done carefully to avoid the formation of distortions that could deform the plate if the sandblasting is not done on both sides.

Figure 50 shows the difference of the plates with or without sandblasting treatment.
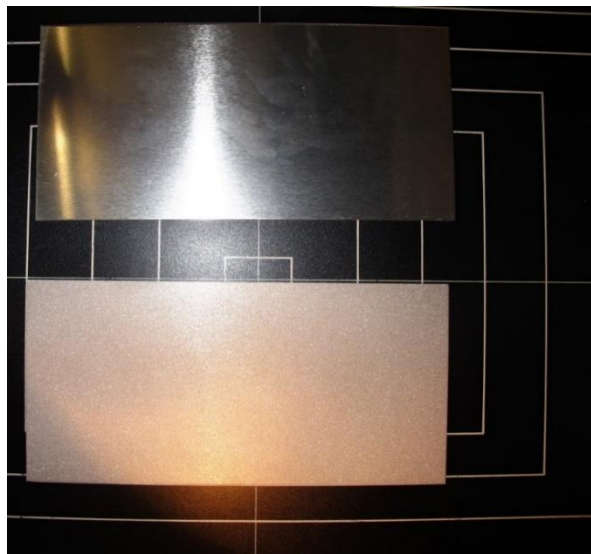
Figure 50 – Comparison of aluminum plate with and without surface treatment (sandblasting).

After a good surface treatment and preparation, the application of the release agent in all the materials that are not desired to bond is performed. The release agent must be applied to the mold, calibrated tapes and shims. After this process, the adhesive is applied and it is necessary to make sure that there is no empty spaces between the lines of adhesive applied, normally a spatula is used to disperse the adhesive along the whole area, always careful with the creation of bubbles that must be avoided.
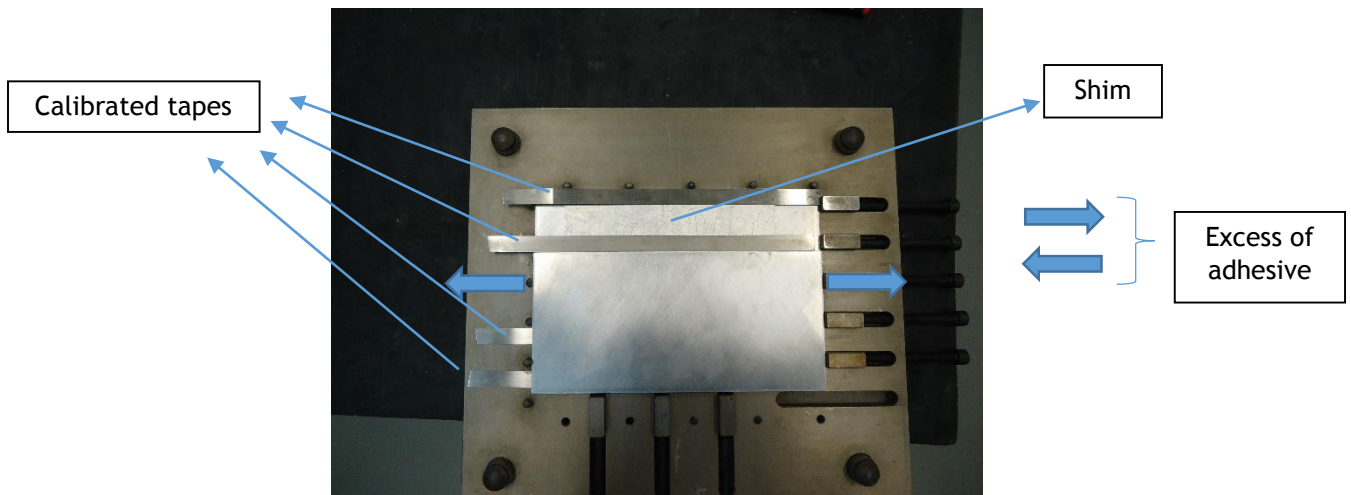
Figure 51 - Plates desired to bond with calibrated tapes

In order to guarantee the thickness of the adhesive, 0.2 mm, it requires the use of calibrated tapes, shown in figure 51, that will be placed along and between the shims and the mold, forcing the excess of adhesive to come out from the sides. These calibrated tapes had 0.2 mm of thickness and were not needed for the bonded plates with grooves, since the grooves will be filled by the adhesive. For each bonded joint there are 2 grooves.

After all this preparation, the plates are ready to join, so it is only needed to place the top of the mold and apply pressure using the press (and temperature if necessary) or weights in case of being with room temperature.

If the bonded joints are the ones that cure after the welding pressure (<30 minutes of cure) they are immediately friction stir welded then left to cure.

If the welding process is made after the cure (>8h), then it is necessary to remove the excess of adhesive in order to not interfere with the welding process. If the cure process required temperature (120 ºC during one hour), it is necessary to increase and decrease the temperature gradually, avoiding residual tensions and distortions of the aluminum plates.

3.2.2. Manufacture of FSW Joints

FSW is a solid joining process and after the plates are bonded, it is necessary to draw the path of the welding zone in order allow the operator to see if the alignment of the plates is correct and ready to be welded. Figure 52 shows the FSW being performed.

Figure 52 – FSW pin welding the bonded joint.

For FSW, those different loads were used: 320,400 and 450 kgf. All of the joints were produced in an ESAB® LEGIO™ 3UL numeric control machine, using a cylindrical threaded pin with 5 mm diameter and a 16 mm diameter shoulder.

Regarding the welded joint, it was also controlled the number of passes, that were one or two passes of welding separated by a length of 12 mm. A dwell time of 5 seconds was used, with welding rotation speed of about 100 rpm, a depth of 2.8 mm and an advancing speed of 200 mm/min.

To the correct alignment of the welding, it was necessary to position the plates with the length of 230 mm parallel to the movement that the welding tool does and the easiest way was like the figure 53 shows. Also in figure 53 it can be seen that it was used four grips and two spacers to fix the plates to the welding table, not allowing oscillations while the welding is done.
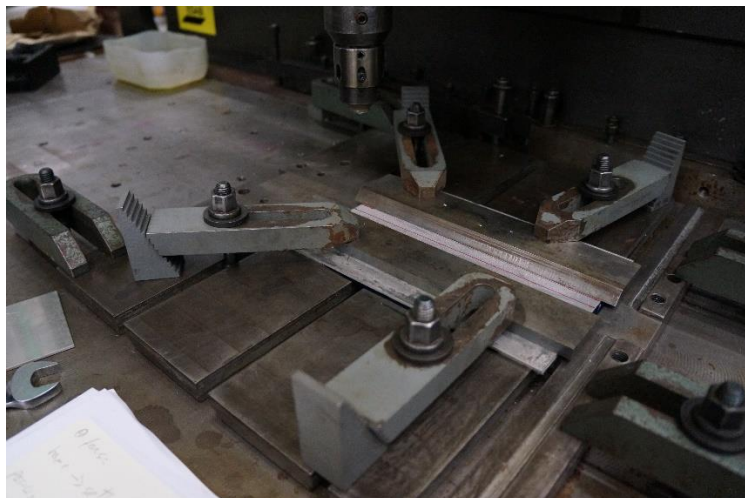
Figure 53 - Plates before welding in the welding table.

3.3. Joints Geometry and Configurations

Single lap joints were manufactured due to their simple geometry, allowing more information to be obtained regarding the combination of FSW with AB. The two hybrid joint configurations are presented in figure 54 and figure 55.

Weld seams
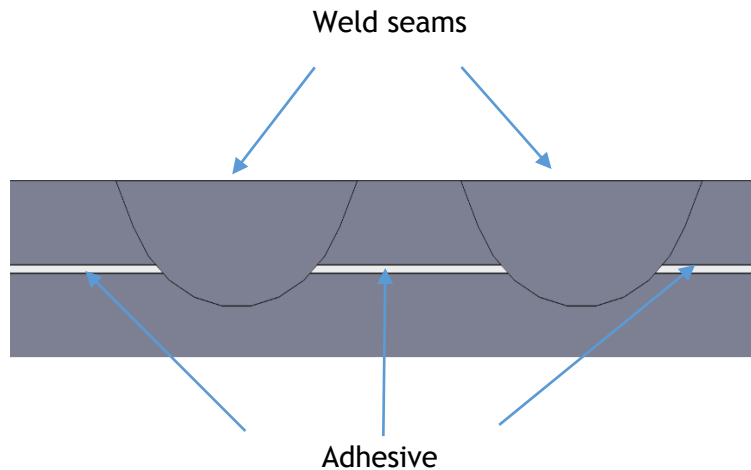
Adhesive

Figure 54 – SLJ configuration with a continuous layer of adhesive.

Weld seams
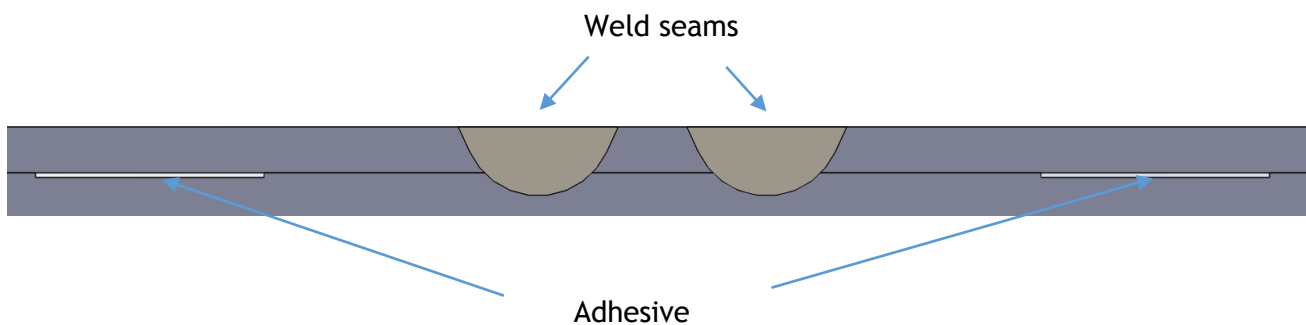
Adhesive

Figure 55 - SLJ configuration with adhesive channels.

The use of these two configurations (with adhesive channels or not) was made in order to study the effect of welding directly through the adhesive, with the pin mixing aluminum and adhesive (no channels). The channels of adhesive were 10 mm wide and 0.2 mm deep and were positioned 34 mm apart from each other. Since two passes FSW lap welding is commonly used to avoid significant property decrease due to the hook defect, it was chosen to study if the use of two passes in hybrid joints would also result in an improvement on joint strength

Beyond these studied process parameters, 3 different types of curing were employed:

- Adhesive curing for > 8 hours at room temperature and then FSW;
- Adhesive curing for 1h at 120 ºC followed by > 7 hours at room temperature and then FSW;
- Adhesive curing for < 30 minutes and then FSW.
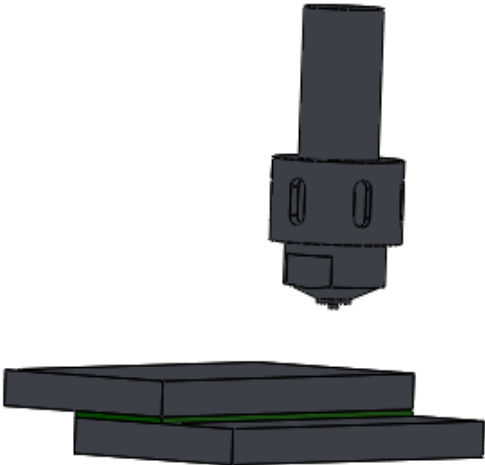
Figure 56- Schematic of SLJ plus FSW tool.

In figure 56 a schematic of the FSW process is presented showcasing the tool and a lap joint.

Figure 57 presents dimensions and a schematic of the configuration used with the front and top view of an adhesive joint. Regarding the welded joints with one and two passes, the front view geometry is shown in figure 58, the dimensions not represented in this image are represented in figure 57 since both share the same geometry.

a)

b)
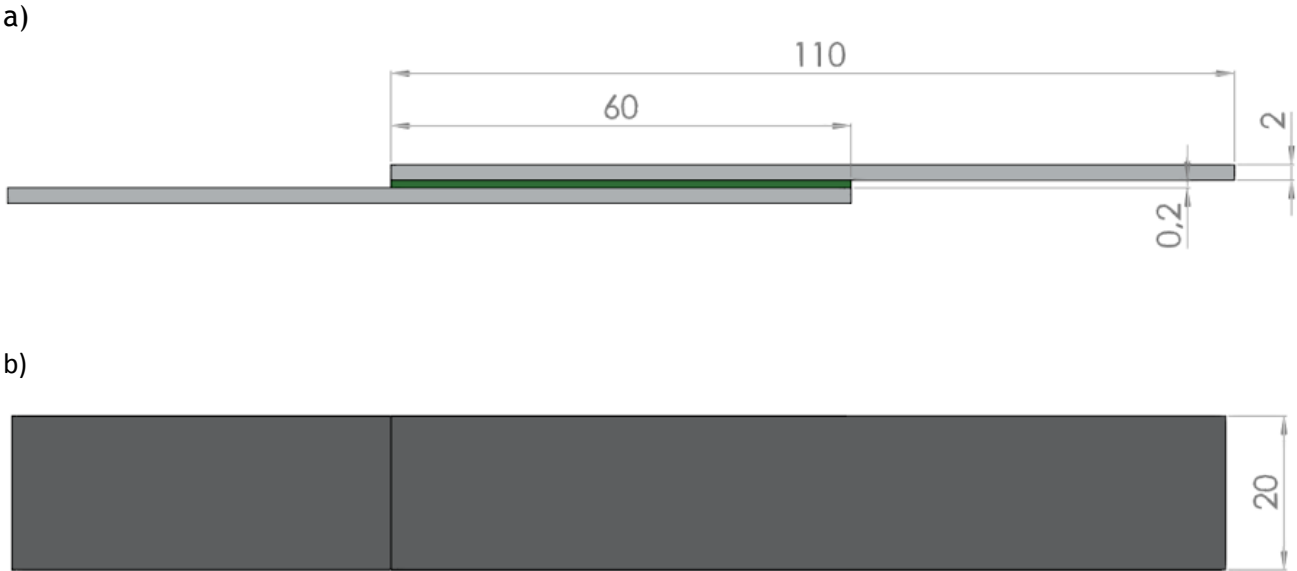
Figure 57 - Schematic of the adhesive SLJ (not to scale) with dimensions in mm: a) front view; b) top view.

a)

30 mm

10 mm

b)

25mm   25mm

10 mm
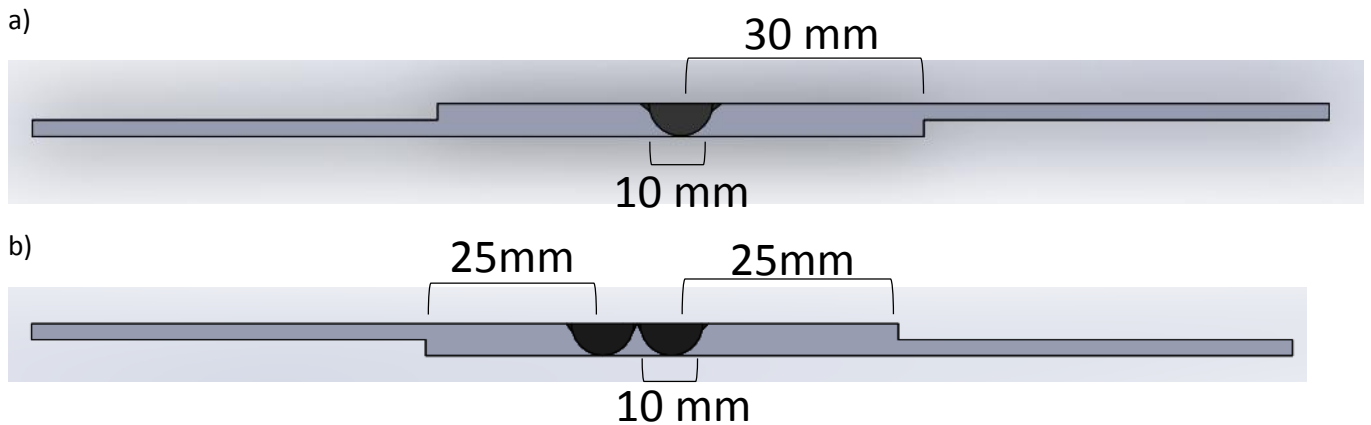
Figure 58 - Front View of welded joint with dimensions in mm: a) one pass; b) two passes.

3.4. Tests Details

The design of experiments (DOE) matrix is presented in table 15, where the configurations, curing methods and variable downward force of the welding tool are presented. All these are configurations for adhesive, welded and hybrid joints. Some references are crossed due to manufacturing errors and inability to repeat manufacturing process within the timeframe of the project.

Table 15 – DOE matrix of welded only, adhesive and hybrid joints

Ref.	Pin force (kgf)	Channels of adhesive	N° of welding passes	Curing method	Surface treatment	Adhesive
AD-A	-	-	-	Room temperature >8h	Anodization	Araldite 420 A\B
AD-SB	-	-	-	Room temperature >8h	Sandblasting	
1-FSW-1	400	-	1	-	-	-
1-FSW-2	450	-	1	-	-	-
2-FSW-1	1st 400 2nd 320	-	2	-	-	-
2-FSW-2	1st 450 2nd 400	-	2	-	-	-

Ref.(cont.)	Pin force (kgf)	Channels of adhesive	N° of welding passes	Curing method	Surface treatment	Adhesive
1-Hyb-1SB	400	Yes	1	<30 min to FSW Room temperature	Sandblasting	Araldite 420 A\B
1-Hyb-2SB	450	Yes	1	<30 min to FSW Room temperature	Sandblasting	Araldite 420 A\B
1-Hyb-3SB	400	No	1	<30 min to FSW Room temperature	Sandblasting	Araldite 420 A\B
1-Hyb-4SB	450	No	1	<30 min to FSW Room temperature	Sandblasting	Araldite 420 A\B
1-Hyb-5SB	400	Yes	1	>8 h to FSW Room temperature for >8h	Sandblasting	Araldite 420 A\B
1-Hyb-6SB	450	Yes	1	>8 h to FSW Room temperature for >8h	Sandblasting	Araldite 420 A\B
1-Hyb-7SB	400	No	1	>8 h to FSW Room temperature for >8h	Sandblasting	Araldite 420 A\B
~~1-Hyb-8SB~~	~~450~~	~~No~~	~~1~~	~~>8 h to FSW Room temperature for >8h~~	Sandblasting	~~Araldite 420 A\B~~
~~1-Hyb-9SB~~	~~400~~	~~Yes~~	~~1~~	~~>8 h to FSW 120 °c for 1 h~~	Sandblasting	~~Araldite 420 A\B~~
~~1-Hyb-10SB~~	~~450~~	~~Yes~~	~~1~~	~~>8 h to FSW 120 °C for 1 h~~	Sandblasting	~~Araldite 420 A\B~~
~~1-Hyb-11SB~~	~~400~~	~~No~~	~~1~~	~~>8 h to FSW 120 °C for 1 h~~	Sandblasting	~~Araldite 420 A\B~~
~~1-Hyb-12SB~~	~~450~~	~~No~~	~~1~~	~~>8 h to FSW 120 °C for 1 h~~	Sandblasting	~~Araldite 420 A\B~~
2-Hyb-1SB	1st 400 2nd 320	Yes	2	<30 min to FSW Room temperature	Sandblasting	Araldite 420 A\B
2-Hyb-2SB	1st 450 2nd 400	Yes	2	<30 min to FSW Room temperature	Sandblasting	Araldite 420 A\B
~~2-Hyb-3SB~~	~~1st 400 2nd 320~~	~~No~~	~~2~~	~~<30 min to FSW Room temperature~~	Sandblasting	~~Araldite 420 A\B~~
2-Hyb-4SB	1st 450 2nd 400	No	2	<30 min to FSW Room temperature	Sandblasting	Araldite 420 A\B

Ref.(cont.)	Pin force (kgf)	Channels of adhesive	Nº of welding passes	Curing method	Surface treatment	Adhesive
2-Hyb-5SB	1st 400 2nd 320	Yes	2	>8 h to FSW Room temperature for >8h	Sandblasting	Araldite 420 A\B
2-Hyb-6SB	1st 450 2nd 400	Yes	2	>8 h to FSW Room temperature for >8h	Sandblasting	Araldite 420 A\B
2-Hyb-7SB	1st 400 2nd 320	No	2	>8 h to FSW Room temperature for >8h	Sandblasting	Araldite 420 A\B
2-Hyb-8SB	1st 400 2nd 450	No	2	>8 h to FSW Room temperature for >8h	Sandblasting	Araldite 420 A\B
2-Hyb-9SB	1st 400 2nd 320	Yes	2	>8 h to FSW 120 ºC for 1 h	Sandblasting	Araldite 420 A\B
2-Hyb-10SB	1st 450 2nd 400	Yes	2	>8 h to FSW 120 ºC for 1 h	Sandblasting	Araldite 420 A\B
2-Hyb-11SB	1st 400 2nd 320	No	2	>8 h to FSW 120 ºC for 1 h	Sandblasting	Araldite 420 A\B
2-Hyb-12SB	1st 450 2nd 400	No	2	>8 h to FSW 120 ºC for 1 h	Sandblasting	Araldite 420 A\B

Due to the extensive number of joints and its references, the next diagram explains the reference numbering used in order to facilitate reading and interpretation of the experimental campaign. For example 1-Hyb-4A:

1-Hyb-4A

Number of welding passes	Type of joint	Parameters combination	Surface treatment
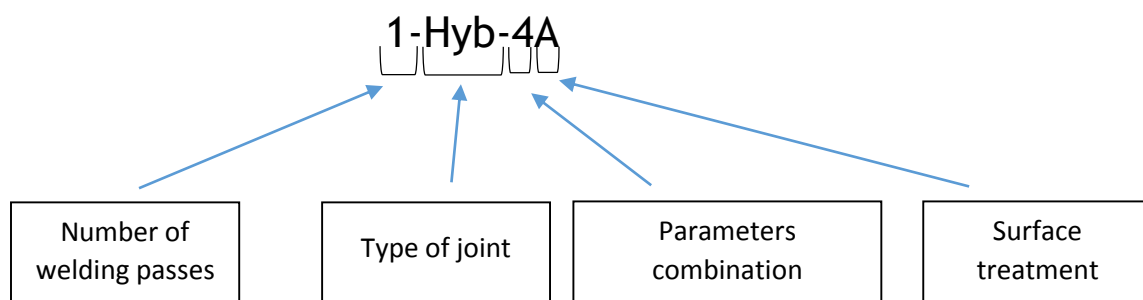
Number of welding passes: Only applies for hybrid and welded only joints.

Type of Joints: Hyb = Hybrid joint; FSW = Welded only joints; AB = Adhesive joint

Parameters combination = number corresponding to the combination of parameters employed in set joint;

Surface treatment: A = Anodized; SB = Sandblasted.

As it is possible to realize from table 15, some of the joints weren't manufactured/tested. This situation was due to two distinct situations:

- Due to the strict timeframe of this master thesis, and manufacturing and logistic time required for joint manufacturing some joints were not manufactured or tested in time. The joints that had this problem were:1-Hyb-11 to 1-Hyb-12 and 2-Hyb-10 to 2-Hyb-12;
- Failures during the FSW process due to difficult thickness control of the adhesive combined with downward force control employed in the FSW process. The joints that had this problem were: 2-Hyb-6, 2-Hyb-9 and 1-Hyb-8 to 1-Hyb-10.

Figure 59 and figure 60 represent some of the problems related to the second reason mentioned above.
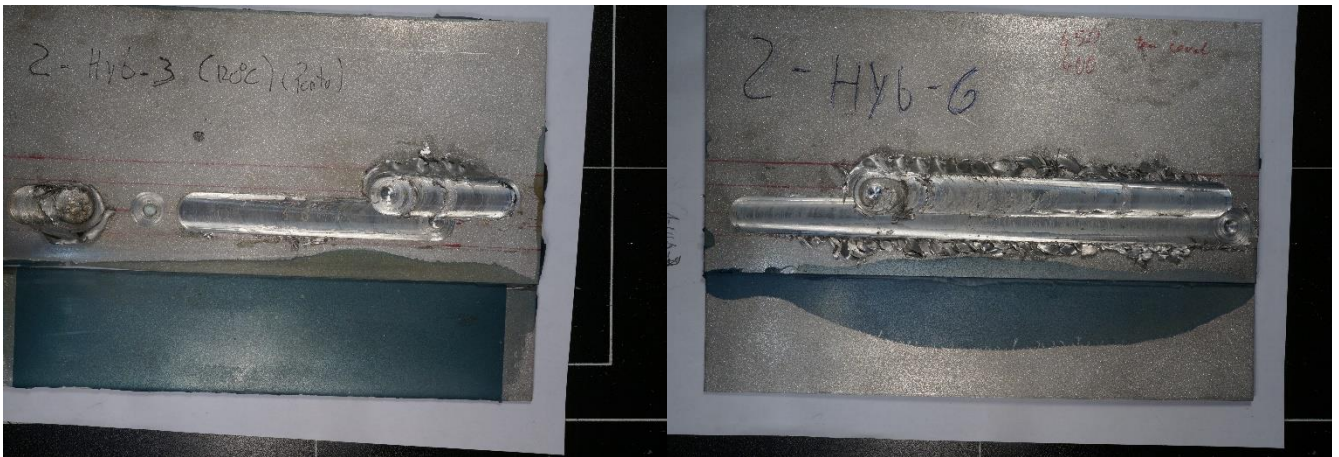
Figure 59 - Defect when welding the hybrid joint 2-Hyb-9SB.

Figure 60 - Defect when welding the hybrid joint 2-Hyb-6SB.

In figure 59 it is possible to see that the pin stopped in the middle of the welding. The machine used to perform FSW used force control and when the pin loses backing force, during the welding, due to peeling of the adhesive ahead of the tool, the machine tried to compensate the downward force, resulting in the pin suddenly plunging onto the work piece and hitting the depth safety limit.

3.5. Temperature Analysis during FSW

3.5.1. Temperature in the Weld Seam Upper Plate

Along this dissertation, a study was conducted to study the influence of the welding process in the temperature at the weld seam in the upper plate of the SLJ's. For this purpose a thermographic camera, Flir SC7000, was used that allows temperature measurement during FSW.

Figure 61 presents an image captured by the thermal camera while FSW was occurring in the specimen 1-Hyb-4A.
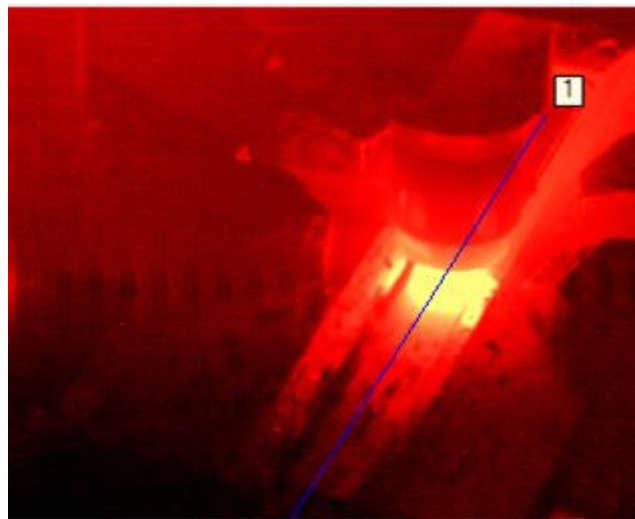
Figure 61 – Thermal camera image on specimen 1-Hyb-4A.

This information is relevant for future modeling attempts of the FSW process. Relating temperature measured with process parameters and mechanical properties also helps study the effect of these parameters in the FSW process.

3.5.2. Temperature during FSW in the Adhesive

Temperature achieved in the adhesive during FSW was previously studied. For this purpose thermocouples were embedded in a hybrid joint that had the adhesive fully cured before welding.

The used joint had the adhesive cured for more than 8 hours at room temperature and the same parameters as the specimen 2-Hyb-7SB, but the difference is that the first welding pass was performed with 400 kgf and the second with 300 kgf of downward force of the tool.

Figure 62 and the measured temperatures for the first and second welding pass are presented in figure 63 and figure 64 , respectively.
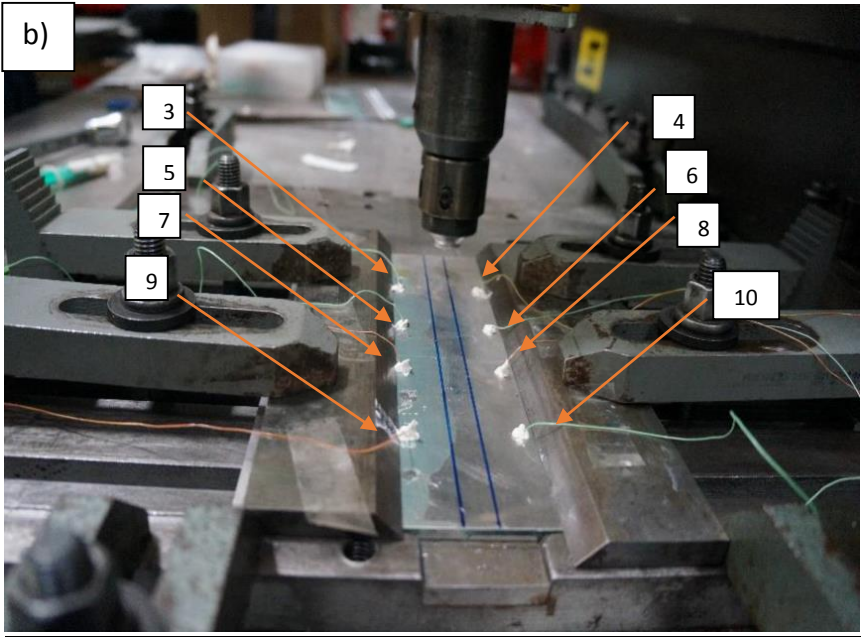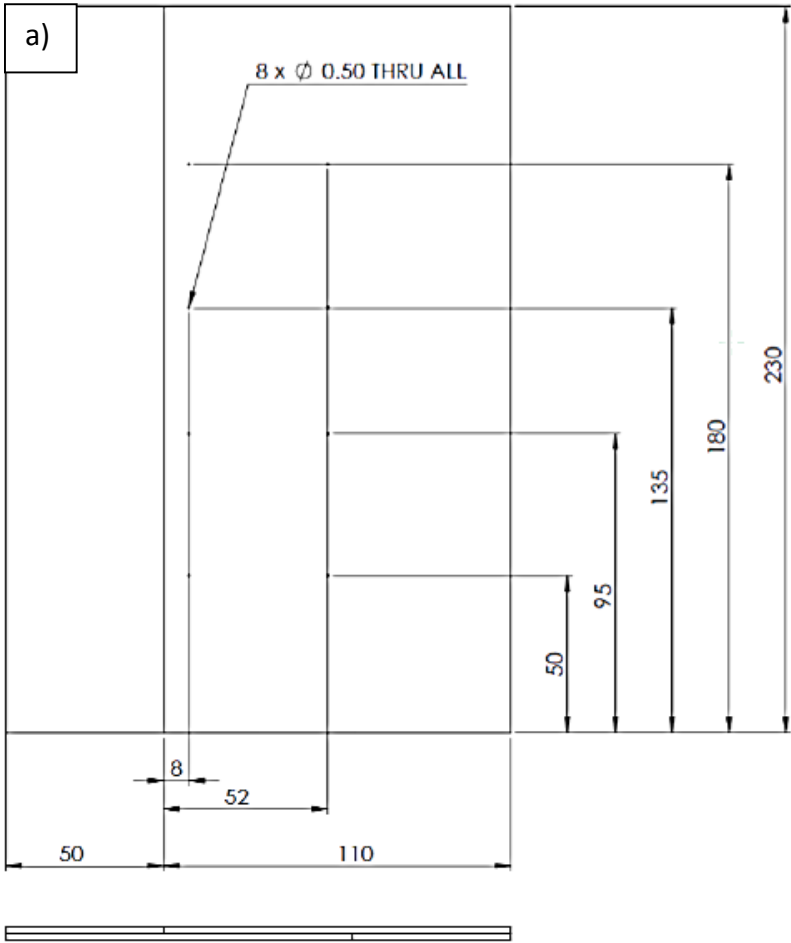
Figure 62 - Position of the thermocouples with a) Draw; b) Picture;
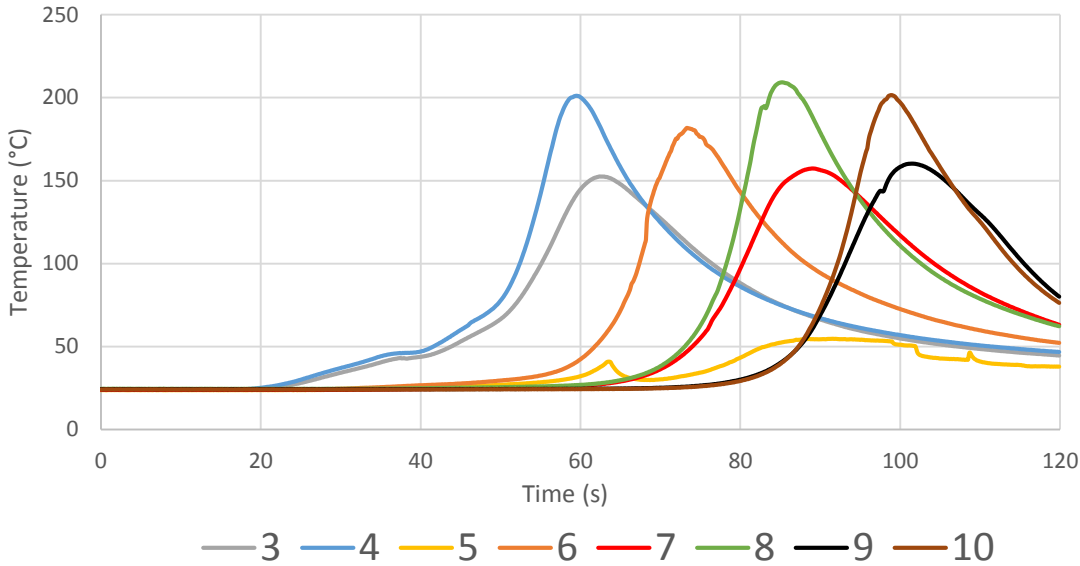
Figure 63 - Temperatures achieved in the first welding pass
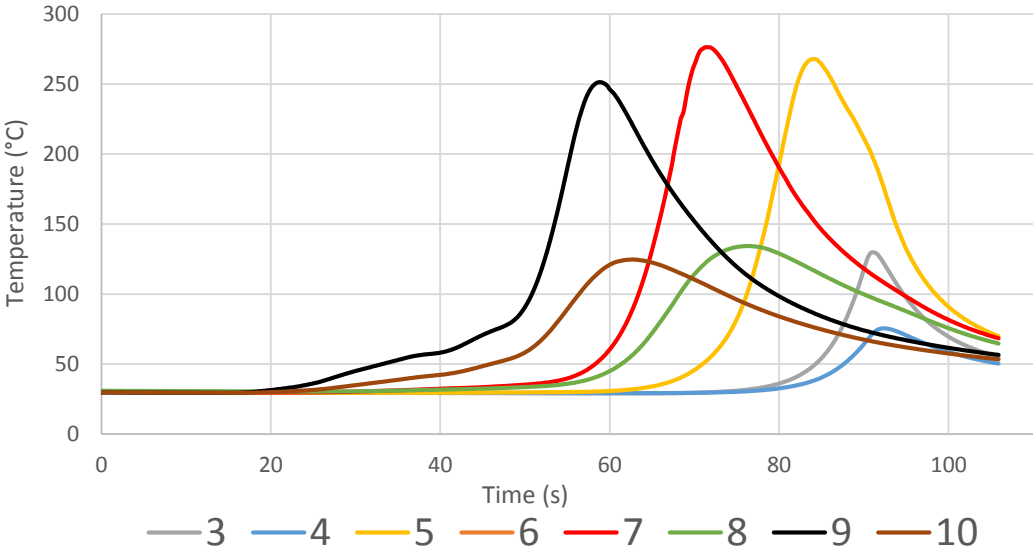
Figure 64 - Temperatures achieved in the second welding pass.

Since the thermocouples were positioned around 10 mm distance from the welding seam, plus the good conductivity of the aluminum, high temperatures were expected. Higher temperatures were achieved in the second pass (a peak of 275 °C). However, this difference might be justified by the fact that the work piece was thermally affected in the first welding pass, leading to higher temperatures in the second welding pass.

3.6.Mechanical Characterization of Welded, Adhesive and Hybrid SLJ's

3.6.1. Single Lap Shear Test

The single lap shear test is one of the most fundamental tests for the mechanical characterization of single lap joints. In order to know the strength of the joint and predict its behavior under extension loads, this test is used. The tests were made using an Instron 3367 tensile test machine (figure 65), with load capacity of 30 kN. All the tests were based on ASTM D1002-01 standard and performed with crosshead speed of 1 mm/min.

Figure 65 – Instron 3367 tensile test machine.

For each joint 3 specimens were tested in order to have reliable results. To understand the different parameters used check table 15. The average curve of results is displayed in the tensile graphs in section 4.2.1.

3.6.2. Single Lap Fatigue Test

The fatigue test technique is used for generating shear data under cyclic fatigue loading conditions, which in this situation will be applied on single lap joints that are going to be weakening until failure of the joint. In this test microscopic cracks may propagate up to a point when eventually the cracks assume a critical size leading to joint failure. The tests conducted were made using a MTS Servo hydraulic Test Systems (figure 66), with a load capacity of 250 kN.

Figure 66 – MTS Landmark Servo hydraulic Test Systems used to perform the fatigue tests.

In order to perform the fatigue test, it was necessary to define stress levels at which S-N curve points were to be taken. The R ratio used was 0.1 as described by Eq. (1):

$$R = \frac{\sigma_{min}}{\sigma_{max}} = 0.1 \ (1)$$

The σ_{max} and σ_{min} represent the values of stress that the SLJ will be submitted to during the fatigue test, with 4 cycles per second (4 Hz) until failure.

FSW joints were submitted to 50 %, 65 % and 80 % of the ultimate remote stress in static tests presented in section 4.2.1.

In order to obtain coherent results under fatigue test, ultimate remote stress (URS) will be used as σ_{max} which is calculated by Eq. (2):

$$\text{URS} = \text{Maximum loading (single lap shear test)} * \text{width} * \text{thickness (substrate)} \ (2)$$

As the formula above shows, the values of URS depend on the joint width and substrate thickness, which are in most cases constant, and also on the maximum load on the joints obtained during the single lap shear tests.

Initially, in order to prevent the sliding of the joint on the grips during the fatigue test, tabs with 35 mm of length were used for the same overlap and width, 60 mm and 20 mm, respectively, of the single lap shear test specimens. Besides this change of length of the tabs, holes with 6 mm diameter were made on each extremity of the SLJ in order to align and if necessary prevent from sliding.

A schematic of the new clamping configuration is shown in figure 67.

a)
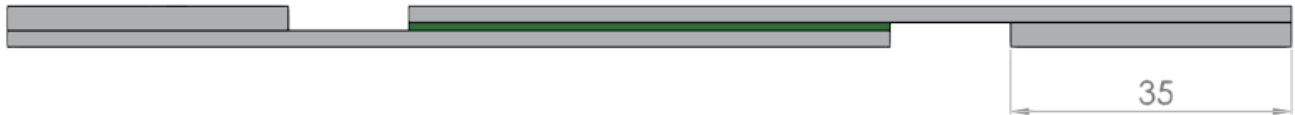
b)

Figure 67 - Schematic of the clamping configuration (not to scale) for fatigue tests with: a) front view and b) upper view.

Unfortunately the full length of the joints was too small and the overlap length was over dimensioned, causing stress concentration close to the grips and consequently the early failure of the aluminum instead of the joint as can be seen in figure 68.

Figure 68 – Failure of the aluminum on the adhesive SLJ.

The solution implemented to overcome this stress concentration was to extend the length of the tabs from 35 mm to 45 mm. Another batch of SLJ was again produced to test for fatigue, but the issue was not solved and the joints broke again close to the grips. Since it was not possible to remake all the specimens already done, it was decided to work with these values.

3.7. Other Analyses of Welded and Hybrid Joints

3.7.1. Distortion Analysis

In this section distortion of the welded only joints and hybrid joints will be studied. Tolerance control on distortions is important in most industries that use FSW and due to this fact it is necessary to control the distortions that a joining process can cause on the welded components. The goal set out in this study was to evaluate the effect of combining adhesive with FSW would generate in terms of distortion levels, as well as analyze distortion levels regarding the parameters studied. This analysis was made using DAVID-3D SCANNER which is a structured light scanning system and a MATLAB® code to interpret the data.

The system used to perform the scan of the structure is shown in figure 69. The analysis requires a camera, projector, tripod and a calibration pattern in order to obtain the points of the surface (in this particular case, the bottom surface of the bottom plate). The bottom surface of the bottom plate was used, as it avoids having to remove the surface indentation left by the contact between the shoulder and work piece, and is a smooth surface.
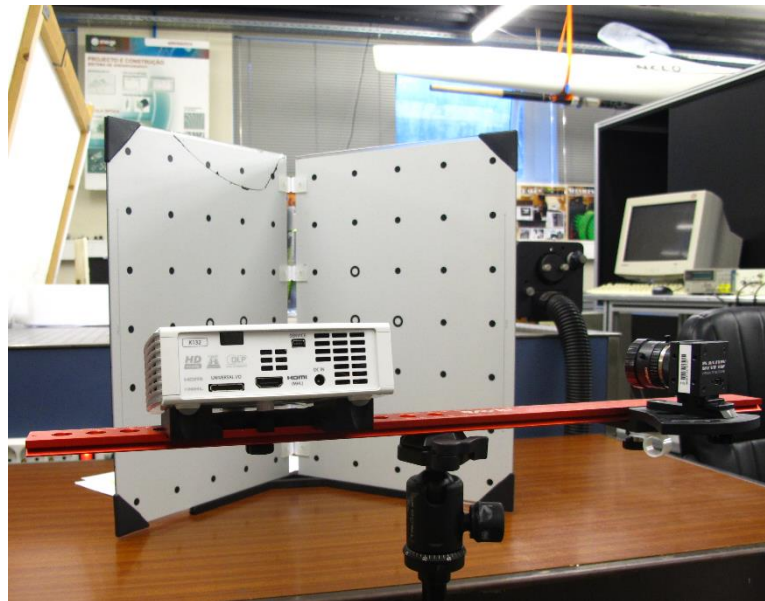
Figure 69 - Components of DAVID 3D light scanner.

Following the scan of the shape of the bottom plate (presented in figure 71) a MATLAB® code was used which interpolates the data obtained on the scanning and then calculates the centroid of the surface, the middle plane passing by the calculated centroid, and the two parallel planes that contain the furthest points from the middle plane, as shown is figure 70.
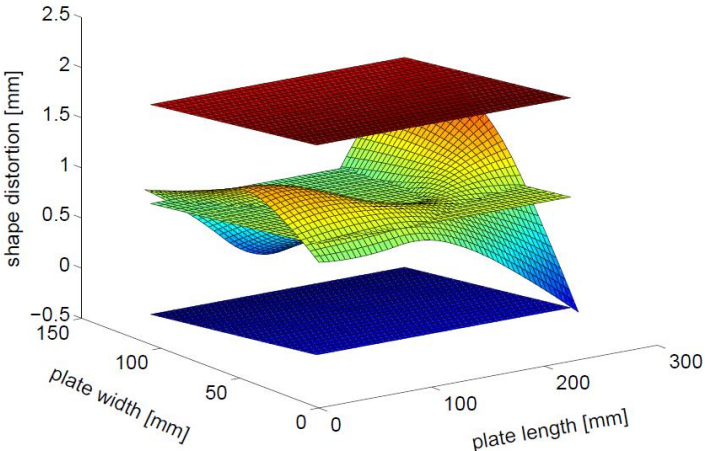
Figure 70 - 1-FSW-1 distortion measurement from MATLAB®.
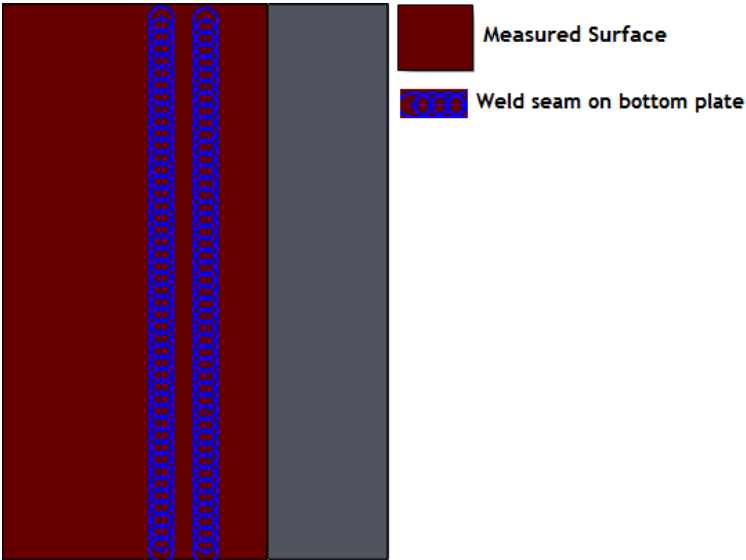
Figure 71 - Scheme with analyzed surface for distortions.

3.7.2. Microhardness Measurements

Microhardness measurements were made in a Struers Duramin microhardness test machine, presented in figure 72, and performed by a master thesis student from the Metallurgic department of FEUP.

Microhardness tests were performed in order to obtain the hardness profile of the weld affected zone, but also to see if the mixing of the adhesive during the welding affects the hardness of the specimens. The hardness profiles can help on the interpretations of the weld microstructures and mechanical properties.

The tests were conducted in the middle thickness of the specimens, with indentations every 0.5 mm, along the weld zone and into the base material of the upper and lower plates, and also vertical lines were tested, of the NZ (nugget zone) and HAZ (heat affected zone) on the advancing and retreating side. The tests are named Low Force Vickers Micro indentation hardness due to the using 300 gf load in each indentation (HV0.3). All tests were made following the standard NP EN ISO 6507-1 2011.

The lines of the profiles are represented in figure 73.
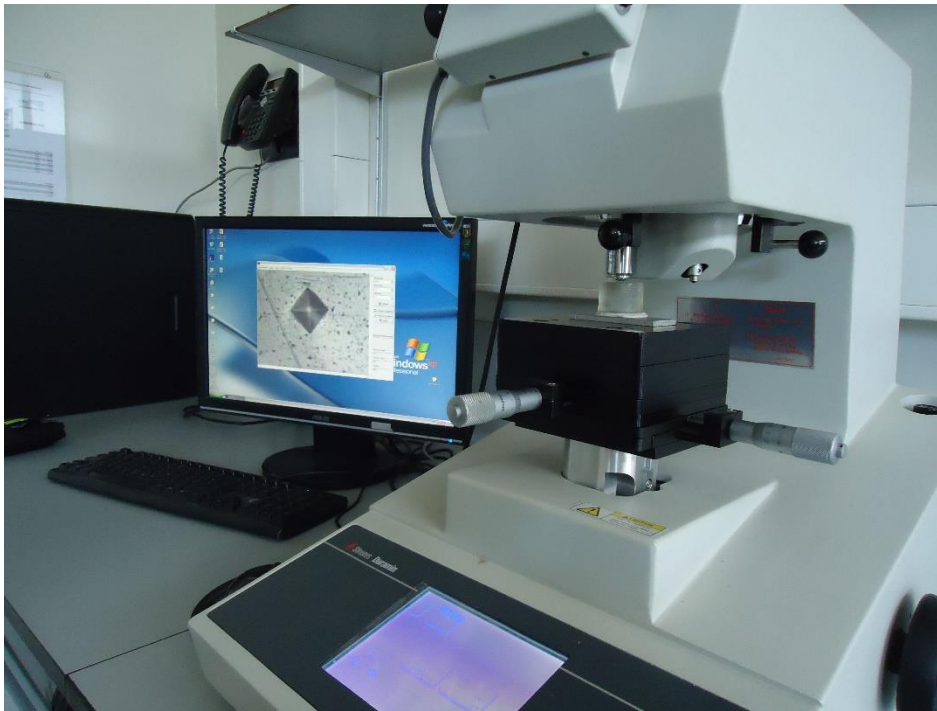
Figure 72 – Struers Duramin microhardness test machine.
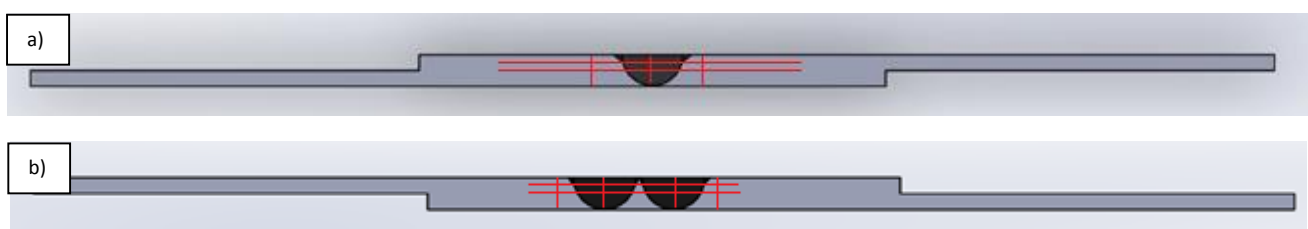
Figure 73 – Lines of the profiles tested to obtain the hardness with a) 1 welding pass; b) 2 welding passes.

3.7.3. Micrographs

The microstructure of the welded joints was analyzed using a Leica DM4000 M. At machine. Figure 74 presents, with a 5x zoom, the macrostructure of the front view in a hybrid joint where the two plates can be seen starting to mix with each other and the hook defect that is a characteristic associated to the advancing side of welding.
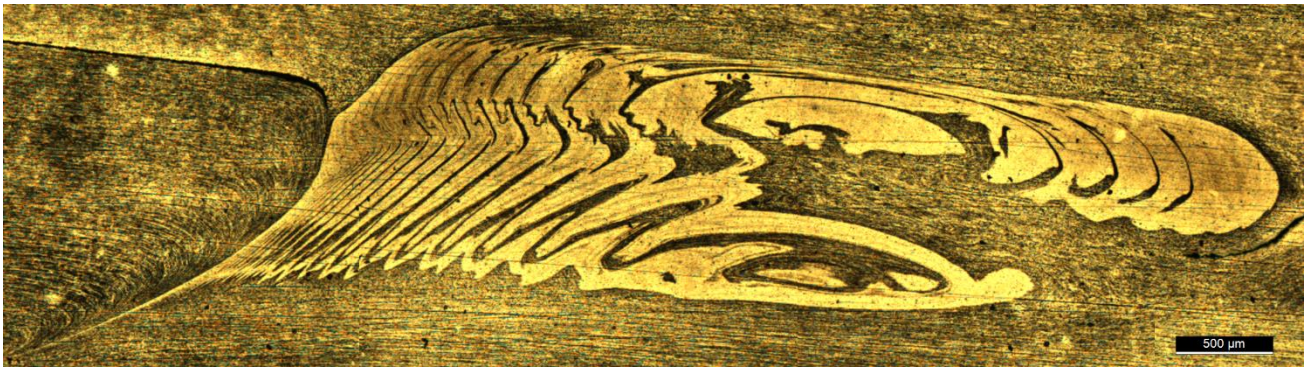
Figure 74 – Macrostructure at TMAZ-NZ of a hybrid joint.

Aluminum alloys always contain impurities, mostly iron and silicon [41]. Microstructures in HAZ was observed along with the hook defect formed on all joints. The hook was measured in order to see the length of this common defect in the advancing side of FSW.

Chapter 4 – Experimental Results and Discussion

Along this chapter it will be presented the results from the experimental work and further discussion.

4.1. Analysis of Temperature on the Upper Plate during FSW

In figure 75 it is possible to observe that the maximum temperature achieved on the upper surface of the upper plate was 250 ºC, however the limits of the thermal camera were reached and it was clear that much higher temperatures were achieved during the welding of the two 1-Hyb-4A joints. These joints had a continuous layer of non-cured adhesive and were made with 450 kgf of downward force. The distance displayed in the horizontal axis only serves to see how the heat is dispersed along the plate. Both 1-Hyb-4A joints showed very similar results and, as expected, the temperature is higher before reaching its maximum value than after this peak due to the fact that the tool had just passed through this zone, thermally affecting it.
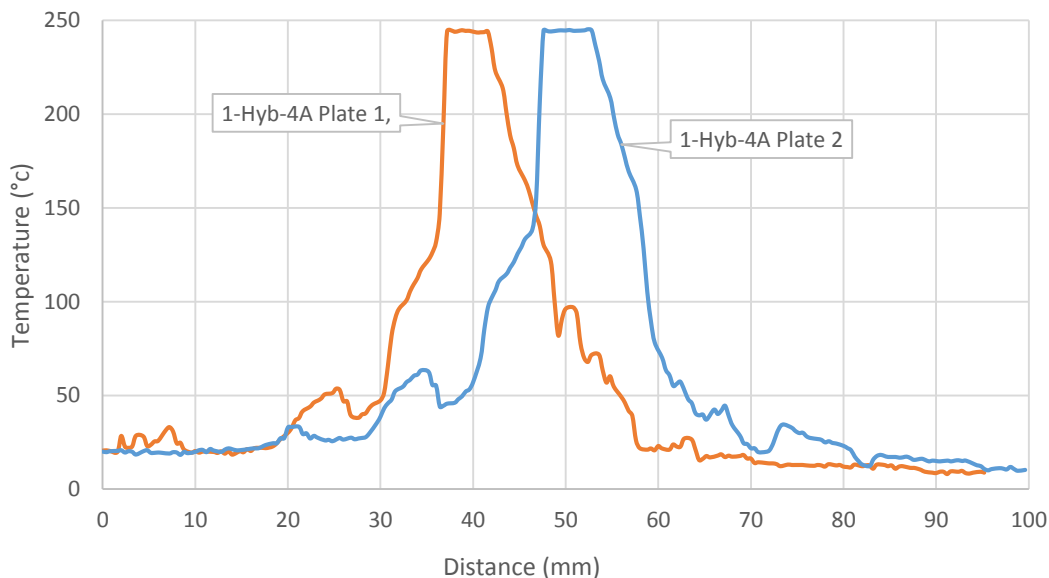
Figure 75 – Temperature during FSW in 1-Hyb-4A specimen.

Figure 76 displays the results for the specimen 2-FSW-2 during the two passes of welding. The temperature achieved was above 250 ºC on the first welding pass and a peak of 239 ºC for the second welding pass. This difference is against what happens with a thermocouple analysis, where a higher temperature was registered in the second welding pass due to the thermal effect caused by the first welding pass. However this variance of results between the two tests is justified by the fact that the thermal camera is reading the values from the surface of the upper plate while the thermocouples were in the adhesive (between the plates), in other words, the thermal inertia of the adhesive and the dissipation of heat by convection in the upper aluminum plate are responsible for this variance.

Comparing the results with the hybrid specimen, it is possible to see that the welded only joint (2-FSW-2) achieved lower temperature values, which may be explained by the fact that the adhesive has less conductivity than the aluminum and worked as a thermic insulation, not allowing the heat to conduct to the back plate, leading to a higher peak of temperature in the upper plate.
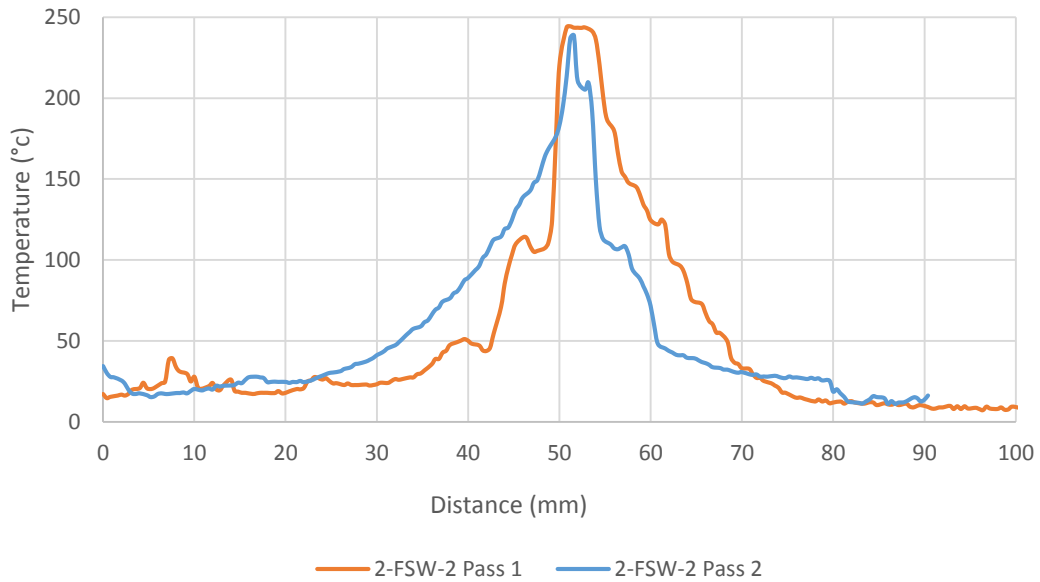
Figure 76 - Temperature during FSW in 2-FSW-2 specimen.

4.2. Single Lap Shear Tests

Along this section will be presented the results and the discussion from the static and fatigue tests on the manufactured joints on this project.

4.2.1. Results of Single Lap Shear Test

4.2.1.1. Single Lap Shear Test for Welded Only Joints

Figure 77 shows the load-displacement curve for welded joints only with one pass. The details of the tensile results are in table 16.
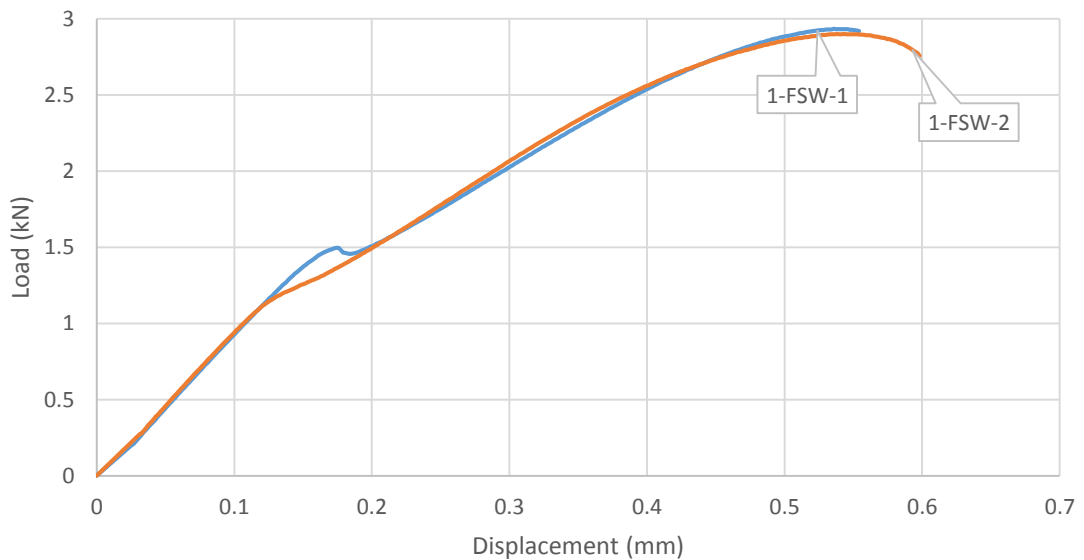
Figure 77 – Single lap shear test on SLJ specimen 1-FSW-1 and 1-FSW-2.

Table 16 – Single lap shear test results for 1-FSW-1 and 1-FSW-2.

	Spec-01	Spec-02	Spec-03	Average	Max	Min	+	-	Joint
Max Load (N)	2943.8	2962.8	2904.8	**2937.2**	2962.8	2904.8	25.67	32.35	1-FSW-1
Max Displ (mm)	0.548	0.531	0.552	**0.544**	0.552	0.531	0.0083	0.0125	
Max Load (N)	2932.4	2849.0	2928.5	**2903.3**	2932.4	2849.0	29.08	54.29	1-FSW-2
Max Displ (mm)	0.549	0.538	0.548	**0.545**	0.549	0.538	0.0041	0.0072	

Figure 78 shows the load-displacement curve for welded only joints with two passes of welding. The details of the tensile results are presented in table 17.
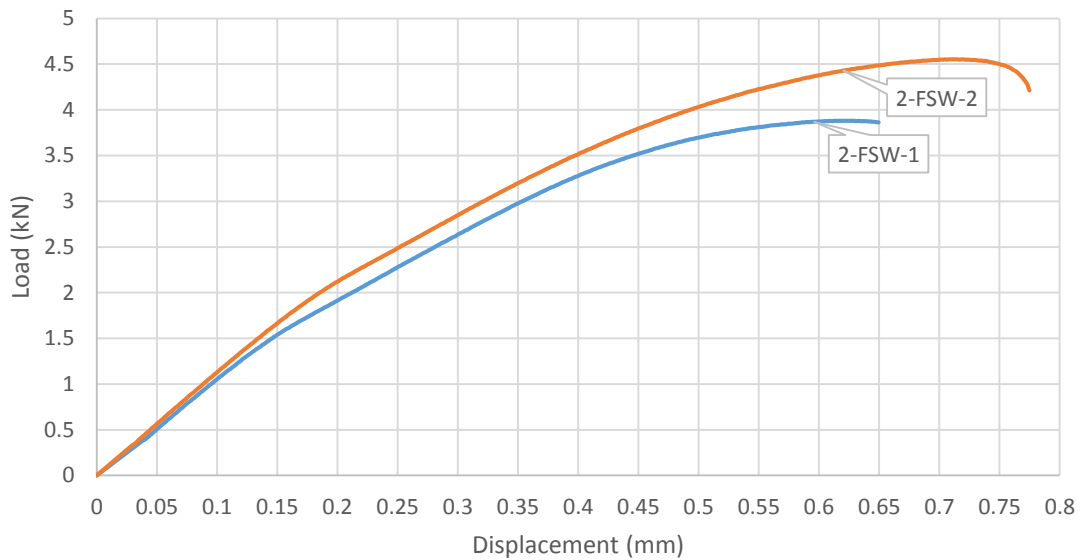
Figure 78 - Single lap shear test on SLJ specimens 2-FSW-1 and 2-FSW-2.

Table 17 – Single lap shear test results for 2-FSW-1 and 2-FSW-2.

	Spec-01	Spec-02	Spec-03	Average	Max	Min	+	-	Joint
Max Load (N)	3815.5	4140.6	3710.5	**3888.9**	4140.6	3710.5	251.73	178.39	**2-FSW-1**
Max Displ (mm)	0.611	0.670	0.604	**0.628**	0.670	0.604	0.04	0.0242	
Max Load (N)	4638.7	4389.5	4647.3	**4558.5**	4647.3	4389.5	88.78	169.02	**2-FSW-2**
Max Displ (mm)	0.726	0.694	0.720	**0.713**	0.726	0.694	0.0124	0.0189	

Since FSW requires some space for the tool to go through during welding, it was necessary to manufacture plates with 230x100 mm and then cut them in 20 mm wide specimens. The cutting process was performed at Tecnogial®, but it was noticed that the cutting method used was not the most suited for this geometry of joints and as such some joints were damaged during the cutting process. Another batch of the best welded joints was tested, asked specifically to be cut with a miller, and as expected there was a clear improvement of the maximum load and displacement of the new joints as may be seen in figure 79. The results of the new welded joints are presented in table 18.
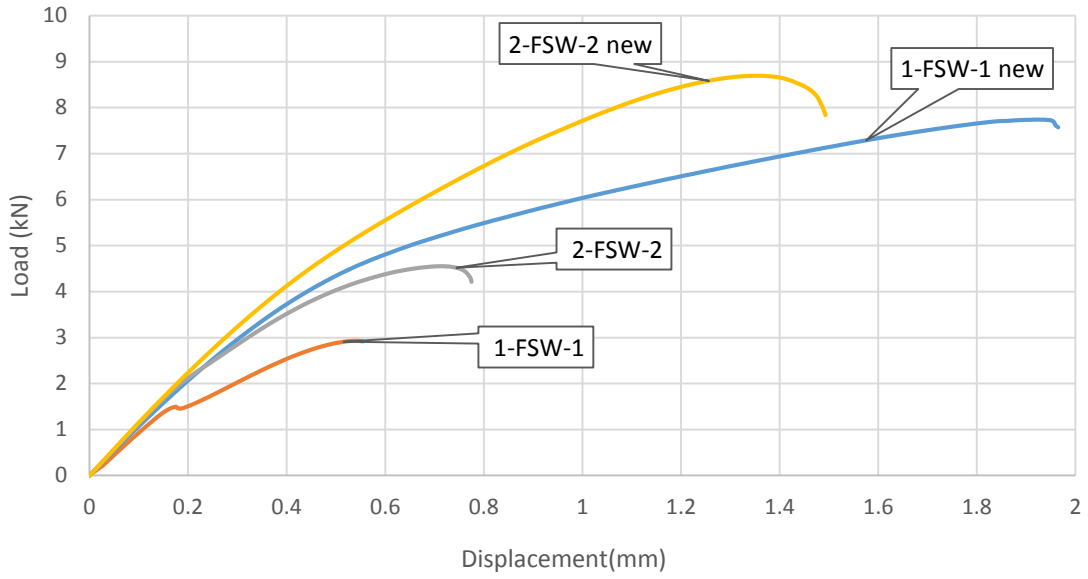
Figure 79 - Single lap shear test on SLJ specimens 1-FSW-1 and 2-FSW-2.

Table 18 - Single lap shear test results for the new 1-FSW-1 and 2-FSW-2.

	Spec-01	Spec-02	Spec-03	Average	Max	Min	+	-	Joint
Max Load (N)	7746.9	7761.2	-	**7754.0**	7761.2	7746.9	7.15	7.15	**1-FSW-1**
Max Displ (mm)	1.958	1.847	-	**1.902**	1.958	1.847	0.0555	0.0555	
Max Load (N)	8430.3	9116.1	-	**8773.2**	9116.1	8430.3	342.91	342.91	**2-FSW-2**
Max Displ (mm)	1.318	1.493	-	**1.406**	1.493	1.318	0.0875	0.0875	

4.2.1.2. Single Lap Shear Test for Adhesive Joints

Figure 80 represents the load-displacement curve of the adhesive SLJ with a sandblasting surface treatment (AD-SB) and with an anodization treatment (AD-A). The details of the tensile results are in table 19.
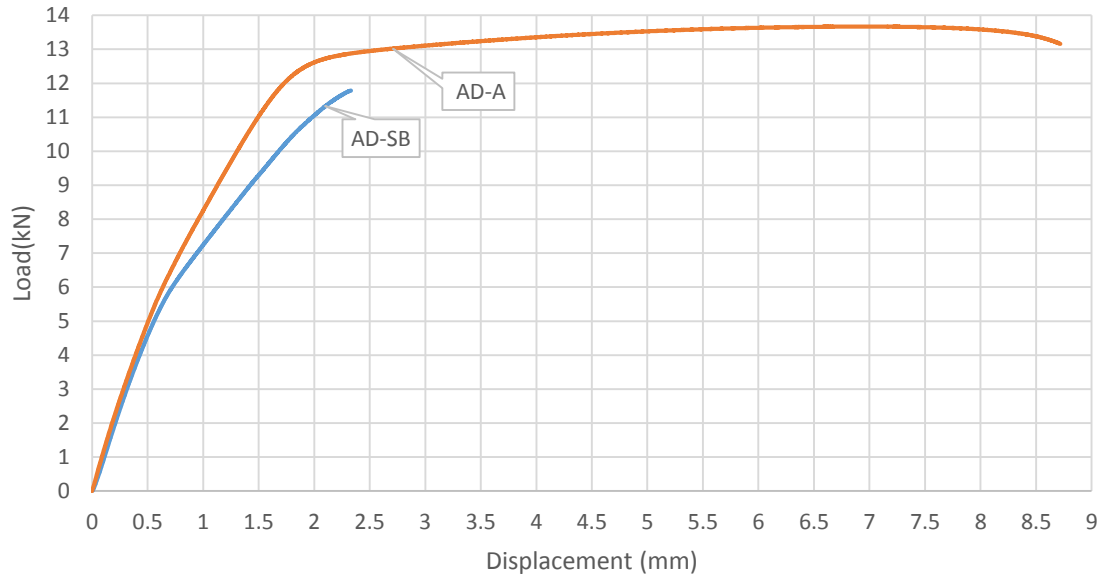
Figure 80 – Single lap shear test on SLJ specimen AD-SB and AD-A.

Table 19 – Single lap shear test results for AD-SB and AD-A.

	Spec-01	Spec-02	Spec-03	Average	Max	Min	+	-	Joint
Max Load (N)	11881.7	11958.5	12121.5	**11987.2**	12121.5	11881.7	134.26	105.55	AD-SB
Max Displ (mm)	2.322	2.368	2.710	**2.467**	2.710	2.322	0.2433	0.1449	
Max Load (N)	13692.2	13678.0	13643.5	**13671.2**	13692.2	13643.5	20.97	27.74	AD-A
Max Displ (mm)	6.920	7.133	6.603	**6.885**	7.133	6.603	0.2472	0.2819	

4.2.1.3. Single Lap Shear Test for Hybrid Joints

The hybrid joints' load-displacement curves were obtained using 3 specimens for each joint. The welding parameters and curing circumstances are in table 15.

Figure 81 presents the load-displacement curve of the hybrid joints with one pass and with FSW performed within 30 minutes after adhesive laying. The joints 1-Hyb-1SB and 1-Hyb-2SB were manufactured with channels of adhesive, and 1-Hyb-3SB and 1-Hyb-4SB have the same, respectively, welding parameters but with a continuous layer of adhesive. The results of the 4 joints are displayed in table 20 and table 21.
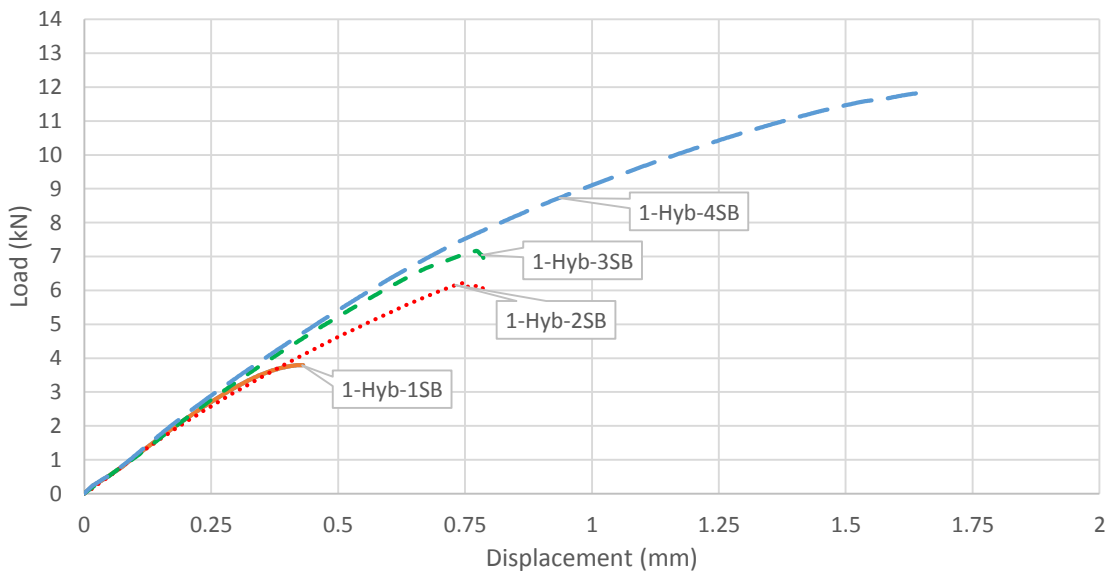
Figure 81 – Single lap shear test on SLJ specimen 1-Hyb-1SB, 1-Hyb-2SB, 1-Hyb-3SB and 1-Hyb-4SB.

Table 20 - Single lap shear results for 1-Hyb-1SB and 1-Hyb-2SB.

	Spec-01	Spec-02	Spec-03	Average	Max	Min	+	-	Joint
Max Load (N)	3507.7	3972.4	3971.2	**3817.1**	3972.4	3507.7	155.28	309.39	1-Hyb-1SB
Max Displ (mm)	0.411	0.431	0.444	**0.429**	0.444	0.411	0.0150	0.0175	
Max Load (N)	6617.8	8639.9	6502.9	**7253.5**	8639.9	6502.9	1386.35	750.61	1-Hyb-2SB
Max Displ (mm)	0.782	1.357	0.740	**0.959**	1.357	0.740	0.3974	0.2195	

Table 21 - Single lap shear results for 1-Hyb-3 and 1-Hyb-4.

	Spec-01	Spec-02	Spec-03	Average	Max	Min	+	-	Joint
Max Load (N)	7664.0	7511.1	6645.0	**7273.3**	7664.0	6645.0	390.64	628.36	**1-Hyb-3SB**
Max Displ (mm)	0.820	0.822	0.755	**0.799**	0.822	0.755	0.0237	0.0440	
Max Load (N)	11451.9	12202.1	12134.0	**11929.3**	12202.1	11451.9	272.79	477.41	**1-Hyb-4SB**
Max Displ (mm)	1.623	1.802	1.722	**1.716**	1.802	1.623	0.086	0.092	

Figure 82 presents the hybrid joints load-displacement curve with one pass and with welding performed more than 8 hours after bonding (fully cured). The joints 1-Hyb-5SB and 1-Hyb-6SB are with channels of adhesive and 1-Hyb-7SB with a continuous layer of adhesive along the overlap. The results of the 3 joints are displayed in table 22 and table 23.
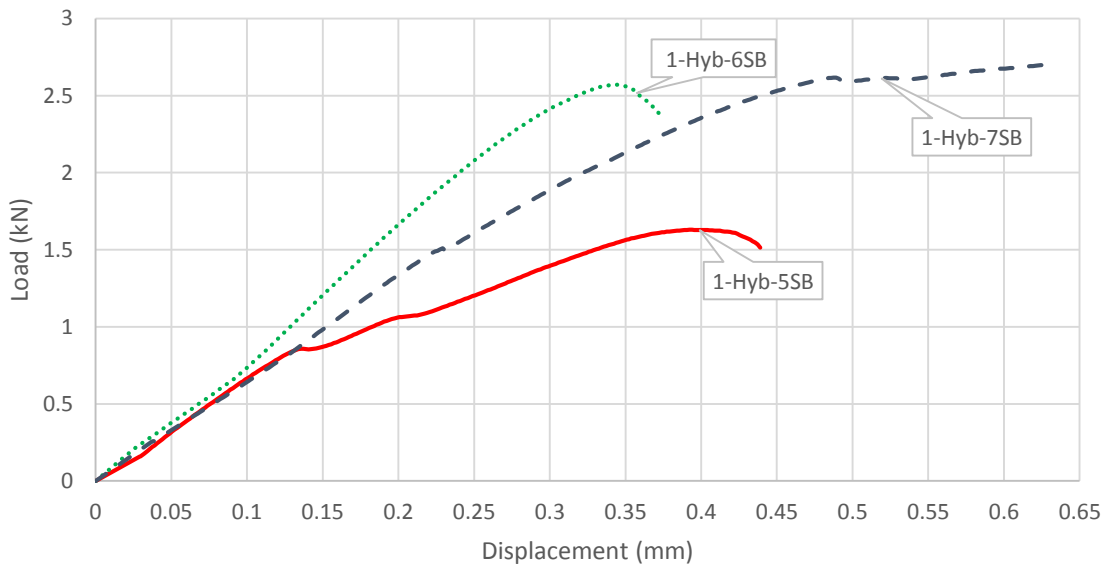
Figure 82 - Single lap shear of SLJ specimens 1-Hyb-5SB, 1-Hyb-6SB and 1-Hyb-7SB.

Table 22 - Single lap shear results for 1-Hyb-5SB and 1-Hyb-6SB.

	Spec-01	Spec-02	Spec-03	Average	Max	Min	+	-	Joint
Max Load (N)	1729.2	1549.8	-	**1639.5**	1729.2	1549.8	89.67	89.67	**1-Hyb-5SB**
Max Displ (mm)	0.422	0.385	-	**0.403**	0.422	0.385	0.0184	0.0184	
Max Load (N)	2110.0	3023.5	4062.6	**3065.4**	4062.6	2110.02	997.23	955.33	**1-Hyb-6SB**
Max Displ (mm)	0.331	0.336	0.812	**0.493**	0.812	0.331	0.3187	0.1616	

Table 23 - Single lap shear results for 1-Hyb-7SB.

	Spec-01	Spec-02	Spec-03	Average	Max	Min	+	-	Joint
Max Load (N)	2839.9	2507.8	3538.5	**2962.1**	3538.5	2507.8	576.41	454.22	**1-Hyb-7SB**
Max Displ (mm)	0.622	0.481	1.584	**0.896**	1.584	0.481	0.6885	0.4151	

The hybrid joint 1-Hyb-5SB had only 2 specimens to test due to the fact that when these specimens were clamped on the tensile test machine, the joint broke due to torsion originated from the slack between the 2 grips. This was probably due to the specimens cutting operation and since the results were very poor, it was decided to not perform more tests on this configuration.

Figure 83 shows the load-displacement curve for the joints with two welding passes, with FSW right after bonding and with/without channels of adhesive. The results of the single lap shear tests are presented in table 24 and table 25. For the specimen 2-Hyb-4SB, due the irregularity of the results, it was chosen to show only the curve that had better displacement and loading until failure.

Also, in figure 83 the 2-Hyb-4A joints' curve is presented, which were manufactured using the same process parameters as 2-Hyb-4SB but with anodized surfaces before bonding.
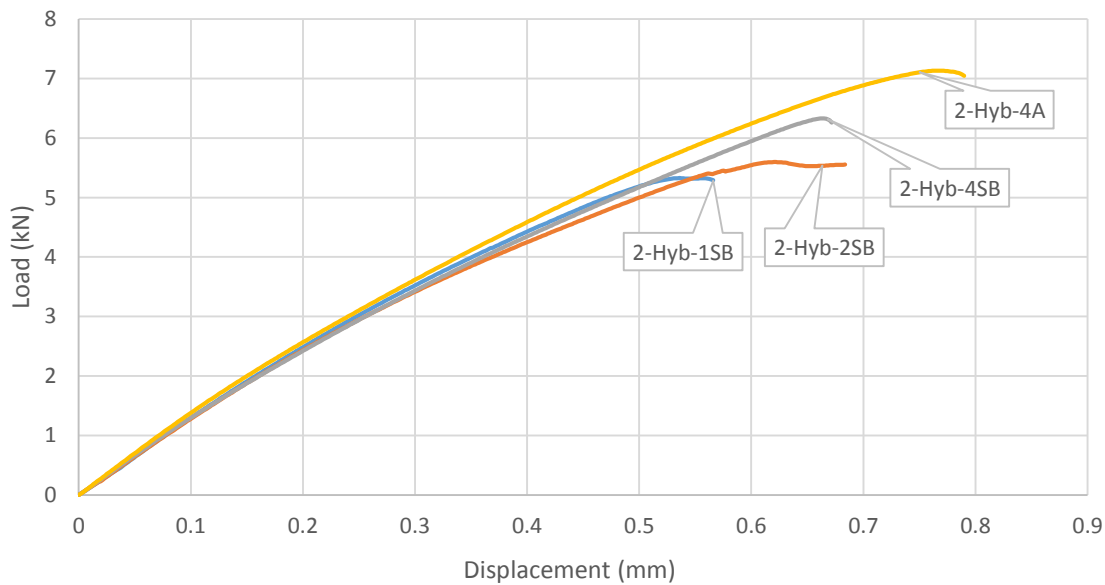
Figure 83 – Single lap shear test on SLJ specimens 2-Hyb-1SB, 2-Hyb-2SB, 2-Hyb-4SB and 2-Hyb-4A.

Table 24 – Single lap shear test results for 2-Hyb-1SB and 2-Hyb-2SB.

	Spec-01	Spec-02	Spec-03	Average	Max	Min	+	-	Joint
Max Load (N)	7301.0	5060.6	5639.8	**6000.5**	7301.0	5060.6	1300.52	939.90	**2-Hyb-1SB**
Max Displ (mm)	0.779	0.504	0.612	**0.632**	0.779	0.504	0.1474	0.1273	
Max Load (N)	6303.9	5400.5	6078.8	**5927.7**	6303.9	5400.5	376.17	527.24	**2-Hyb-2SB**
Max Displ (mm)	0.696	0.569	0.685	**0.650**	0.696	0.569	0.0460	0.0809	

Table 25- Single lap shear test results for 2-Hyb-4 with sandblasting and anodization treatment.

	Spec-01	Spec-02	Spec-03	Average	Max	Min	+	-	Joint
Max Load (N)	2734.1	2189.6	6330.0	**3751.2**	6330.0	2189.6	2578.73	1561.66	2-Hyb-4SB
Max Displ (mm)	0.272	0.479	0.658	**0.470**	0.658	0.272	0.1888	0.1978	
Max Load (N)	8667.5	7093.1	6759.0	**7506.5**	8667.5	6759.0	1160.96	747.50	2-Hyb-4A
Max Displ (mm)	1.001	0.775	0.750	**0.842**	1.002	0.750	0.1594	0.0921	

Figure 84 shows the load-displacement curve for a double welding pass joint with FSW done more than 8h after bonding (fully cured) and with channels for the adhesive. The results of the single lap shear test are in table 26.
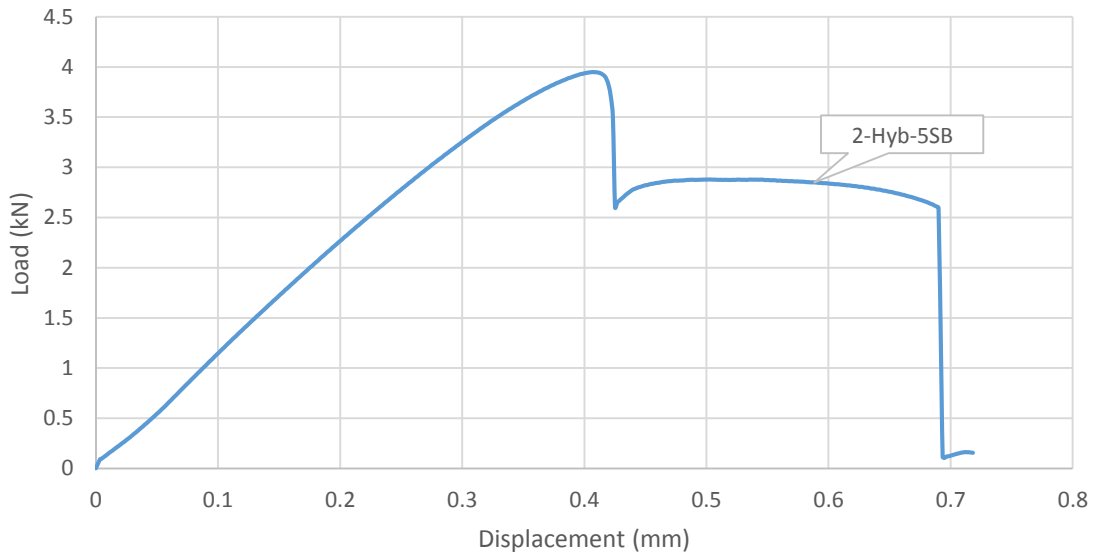
Figure 84 - Single lap shear test on SLJ specimen 2-Hyb-5SB.

Table 26 - Single lap shear test results for 2-Hyb-5SB.

	Spec-01	Spec-02	Spec-03	Average	Max	Min	+	-	Joint
Max Load (N)	3949.5	2316.9	-	**3133.2**	3949.5	2316.9	816.32	816.32	2-Hyb-5SB
Max Displ (mm)	0.407	0.253	-	**0.330**	0.407	0.253	0.0768	0.0768	

Only two 2-Hyb-5SB specimens were tested, also due to the lack of adhesion of the adhesive and when clamping some specimens were broken.

Once found out that the best tensile curve was from specimen 1-Hyb-4SB, single lap joints were manufactured using the same procedure but with anodization as surface treatment, leading to the specimen 1-Hyb-4A. Anodization was also performed to the specimen 2-Hyb-4A in order to find out if better results can be achieved with 2 welding passes.

The load-displacement curve for the single lap shear tests on the anodized hybrid joints are in figure 85 and the results are in table 27.
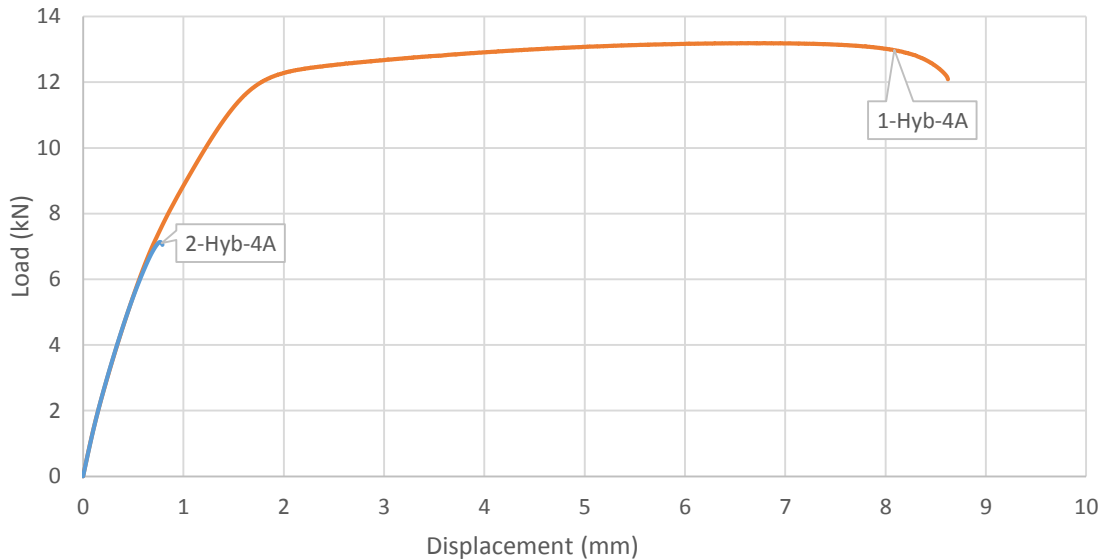
Figure 85 - Single lap shear test on SLJ specimens 1-Hyb-4A and 2-Hyb-4A.

Table 27 – Single lap shear test results for 1-Hyb-4A and 2-Hyb-4A.

	Spec-01	Spec-02	Spec-03	Average	Max	Min	+	-	Joint
Max Load (N)	13197.3	13185.4	-	**13191.3**	13197.3	13185.4	5.95	5.95	**1-Hyb-4A**
Max Displ (mm)	6.66	6.70	-	**6.68**	6.71	6.66	0.025	0.025	
Max Load (N)	8667.5	7093.1	6759.0	**7506.5**	8667.5	6759.0	1160.96	747.51	**2-Hyb-4A**
Max Displ (mm)	1.002	0.775	0.750	**0.842**	1.002	0.750	0.1594	0.0921	

Single lap shear tests were performed in 4 specimens, however the results of 2 specimens were not consistent and as such, were excluded.

4.2.2. Discussion of Single Lap Shear Test Results

4.2.2.1. *Single Lap Shear Test for Welded Only Joints*

Regarding the SLJ shear tests some observations can be made. Comparing welded only joints with one welding pass, the results for displacement and maximum load are similar to each other, see figure 86. However, the joints with two welding passes showed not only higher strength and EA but also different values between themselves, being the only variation also the tool down force, between 320-400 kgf for 2-FSW-1 to 400-450 kgf for 2-FSW-2. The best results were found in the 2-FSW-2 joint that presented a higher maximum load and displacement until failure.
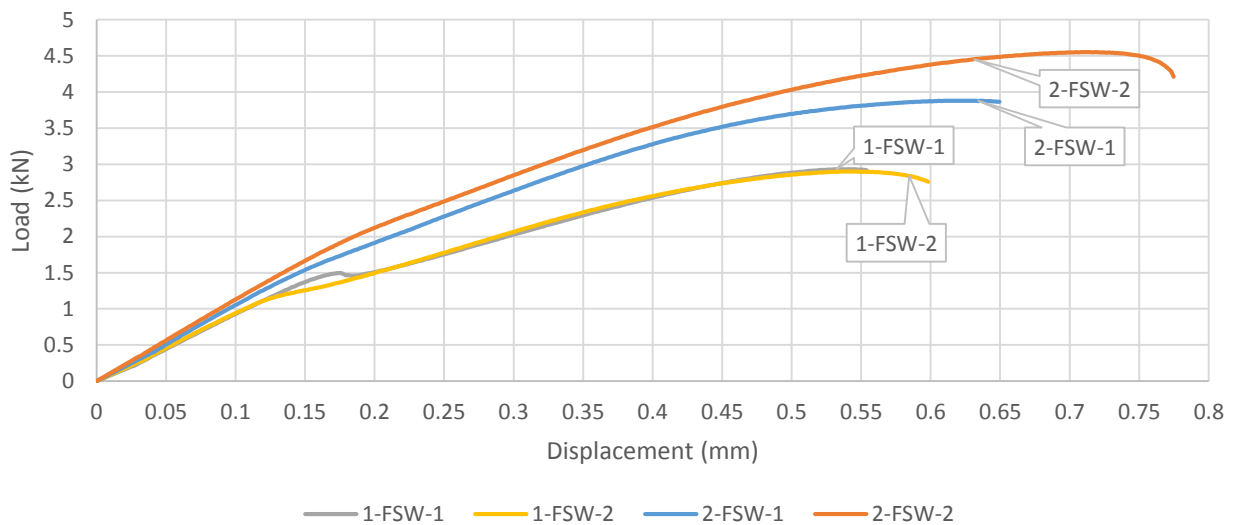
Figure 86 - Single lap shear test on SLJ specimens 1-FSW-1, 1-FSW2, 2-FSW-1 and 2-FSW-2.

These were the expected results, also shown in [42, 43], the joints that had the hook defect suppressed (joints with two welding passes) had better displacement and maximum load than the joints with only one welding pass. The solution to avoid the hook defect was the control of the tool rotation direction during the process as figure 87 shows. When using two passes, the advancing side was directed towards the middle of the joint, in both of the passes, and with this method the retreating side holds most of the loads during the single lap shear test, consequentially leading to better results.
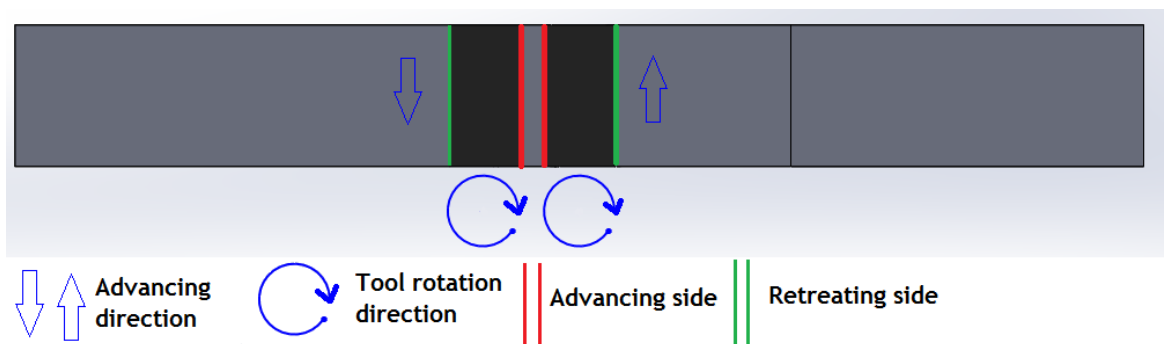
Figure 87 - Scheme with illustration of the advancing and retreating side of the weld seam.

Besides the results of the single lap shear tests, figure 88 shows that the failure in the welded joints with two passes was on the retreating side as expected [42, 44]. All the FSW joints happen to have the failure, when subjected to the single lap shear test, in the heat affected zone (HAZ) due to the microstructure transition (fine recrystallized grain in NZ and larger grains in HAZ).
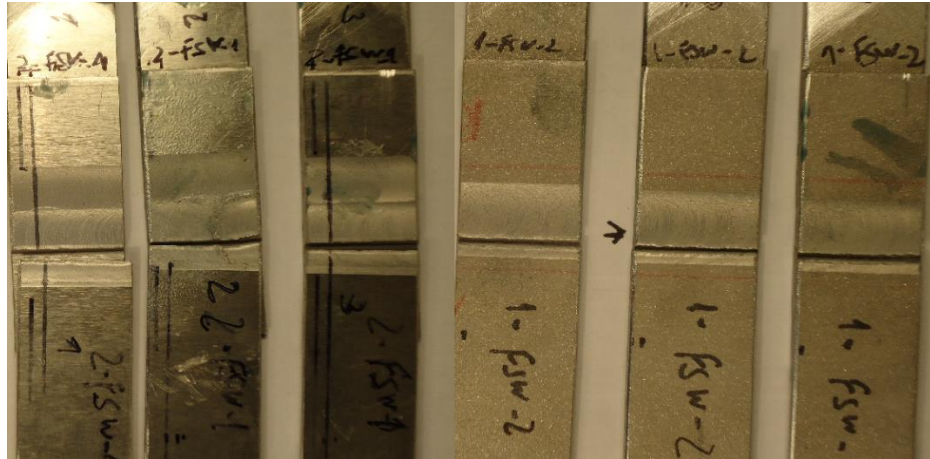
Figure 88 – Failure on SLJ specimens 2-FSW-1 (three specimens on the left) and 1-FSW-2(three specimens on the right).

Another conclusion is that with higher down force of the tool in the joints with two welding passes leads to better results. The joint 2-FSW-2 showed considerably better strength and displacement at rupture when comparing with the second best results of the welded joints (2-FSW-1), with a 17.2 % improvement on the maximum load and 13.5 % on the maximum displacement.

As mentioned before, the specimens cutting method was not the most suited and different results were obtained when testing the welded only joints, as presented in figure 89.

It was found out that in 1-FSW-1 had the higher EA since it had more displacement at rupture. The joint 2-FSW-2 is more rigid, leading to a higher maximum load. Analyzing these new results, it can be concluded that suppressing the hook defect did not have the outcome that was expected since both joints 1-FSW-1 (one welding pass) and 2-FSW-2 (two welding passes) had very similar results even with the suppressing of the hook effect on the two welding passes joint.
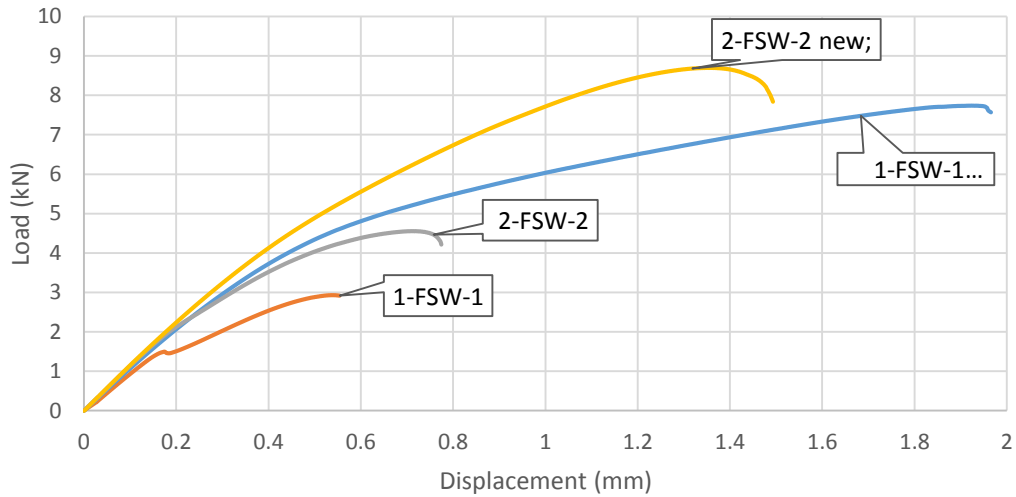
Figure 89 - Single lap shear test on SLJ specimens 1-FSW-1 and 2-FSW-2.

4.2.2.2. Single Lap Shear Test for Adhesive Joints

As previously mention in section 4.2.1.2, the adhesive specimens are distinguished, between themselves, by the surface treatment employed before bonding. The load-displacement curves of both adhesive joints are presented in figure 90 and there is a severe improvement of the maximum load and final displacement in the specimen AD-A, which is the one with anodized surfaces. The joint AD-SB is the one that was submitted to sandblasting and degreasing as surface treatment before bonding.
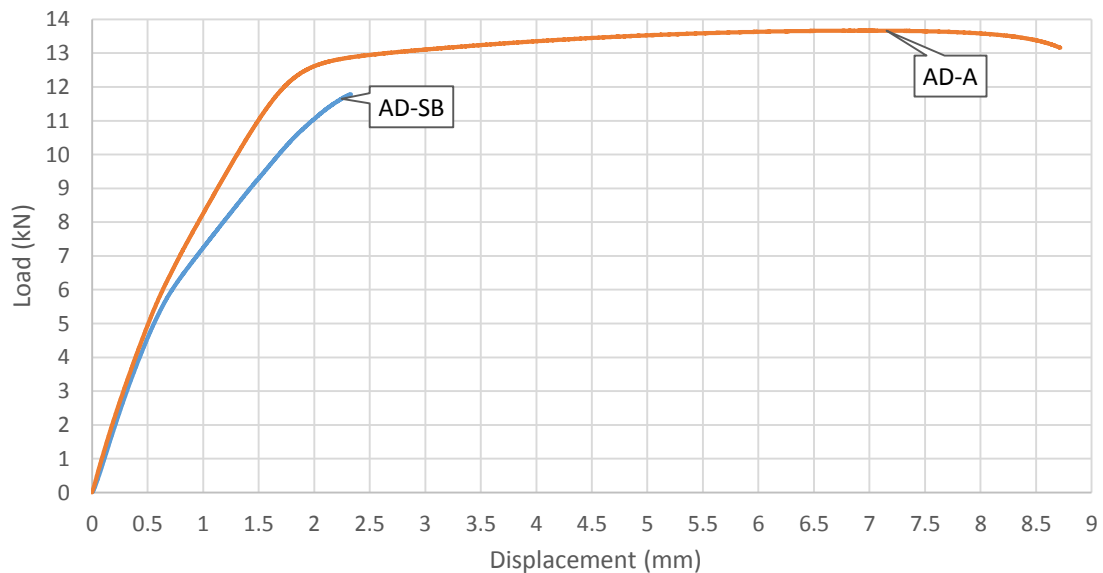
Figure 90 – Single lap shear test on the SLJ specimen AD-SB and AD-A.

The improvement of the anodized joint is of about 14 % of maximum loading, and when this value of loading is achieved there is an improvement of 179 % of the displacement. This difference between both specimens is due to the lack of adhesion that was found on the AD-SB joint, as is presented in figure 91, where adhesion failure was verified. On the contrary, figure 92 shows the joint AD-A with a cohesive failure in the adherent, where the bonded area was stronger than the aluminum itself.
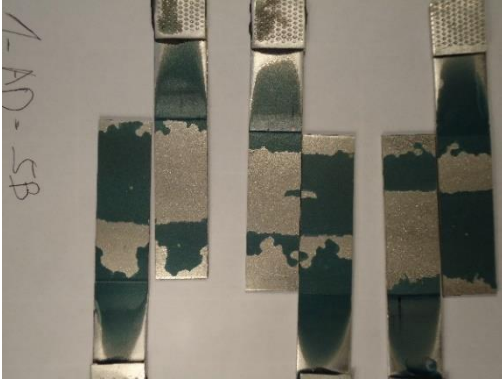
Figure 91 - Failure on SLJ specimen AD-SB.   Figure 92 - Failure on SLJ specimen AD-A.

The conclusion from these results is that anodization as surface treatment to bond aluminum is the most suitable treatment when compared to sandblasting treatment. These results are due to the effect that anodizing has on the surface to be bonded, where a layer of oxides is created, consequently improving the free energy of the bonded surface and the adhesion of the adhesive to the aluminum. So it is expected that by applying an anodization treatment to the hybrid joints, better results will be obtained.

4.2.2.3. Single Lap Shear Test for *Hybrid Joints*

Regarding the results of hybrid joints, the specimens with one welding pass and with FSW done right after the application of the adhesive will be discussed first. The specific parameters for each of these joints are listed in table 15 and the results of the single lap shear tests are presented in figure 93. As it is possible to see, the best results were obtained on the joints that used a continuous layer of adhesive (1-Hyb-3SB and 1-Hyb-4SB) instead of the ones that used channels of adhesive (1-Hyb-1SB and 1-Hyb-2SB). Between these two joints with better mechanical properties, the maximum load and displacement are presented in 1-Hyb-4SB. The joint 1-Hyb-4SB only had higher down force of the tool during FSW when compared with 1-Hyb-3SB that had 400 kgf instead of 450 kgf. Although 1-Hyb-4A is by far the best load-displacement curve, with higher maximum load and displacement. This superiority of the specimen 1-Hyb-4A is due to the surface treatment that allowed the adhesive to have a good adhesion, supporting higher loads and absorbing more energy.
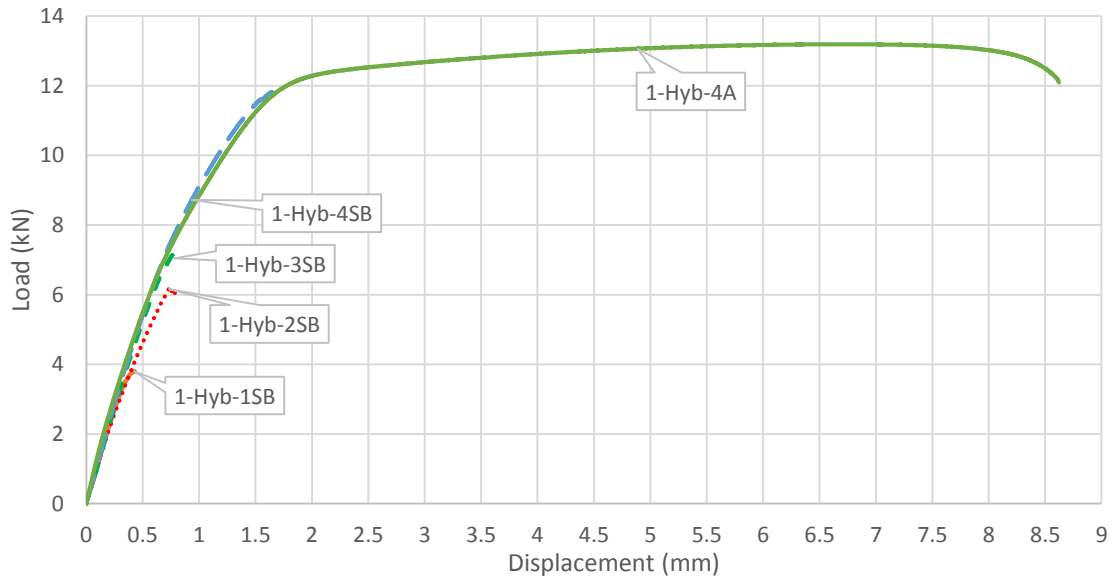
Figure 93 - Single lap shear test on the SLJ specimen 1-Hyb-1SB, 1-Hyb-2SB, 1-Hyb-3SB, 1-Hyb-4SB and 1-Hyb-4A.

The failure mode of each specimen is demonstrated in figure 94, where it is possible to realize that all specimens had adhesive failure, except 1-Hyb-4A (anodized) that had adherent failure. It is important to notice that 1-Hyb-1SB and 1-Hyb-2SB both had creation of bubbles during the manufacture and that that reduced the resistance of the joints. The failure mode of these two joints are shown in figure 94 a) and b).
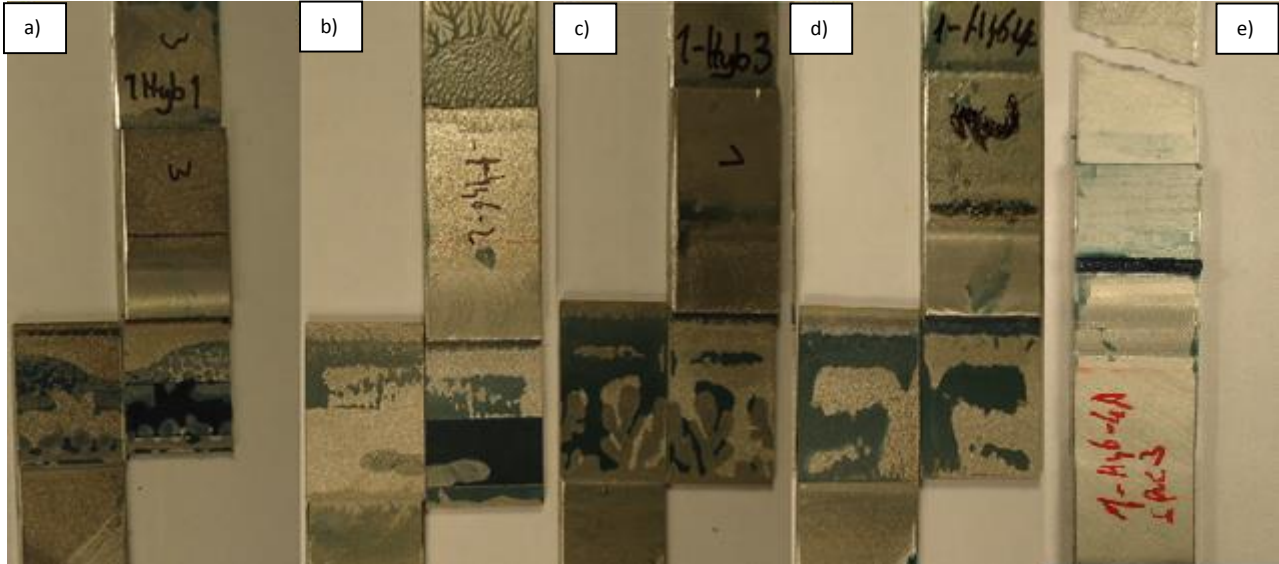
Figure 94- Failure on SLJ specimen: a) 1-Hyb-1SB; b) 1-Hyb-2SB; c) 1-Hyb-3SB; d) 1-Hyb-4SB; e) 1-Hyb-4A.

The joint with sandblasting treatment that showed the best results in the single lap shear tests (1-Hyb-4SB) also showed adhesive failure due to the insufficient adhesion between adhesive and aluminum.

Still in the group of one welding pass joints, there are the joints that were welded after the adhesive was fully cured (>8h). In conjunction with those joints, the results of the joint (2-Hyb-5SB) will be also presented in figure 95, using the same curing process but with two welding passes.
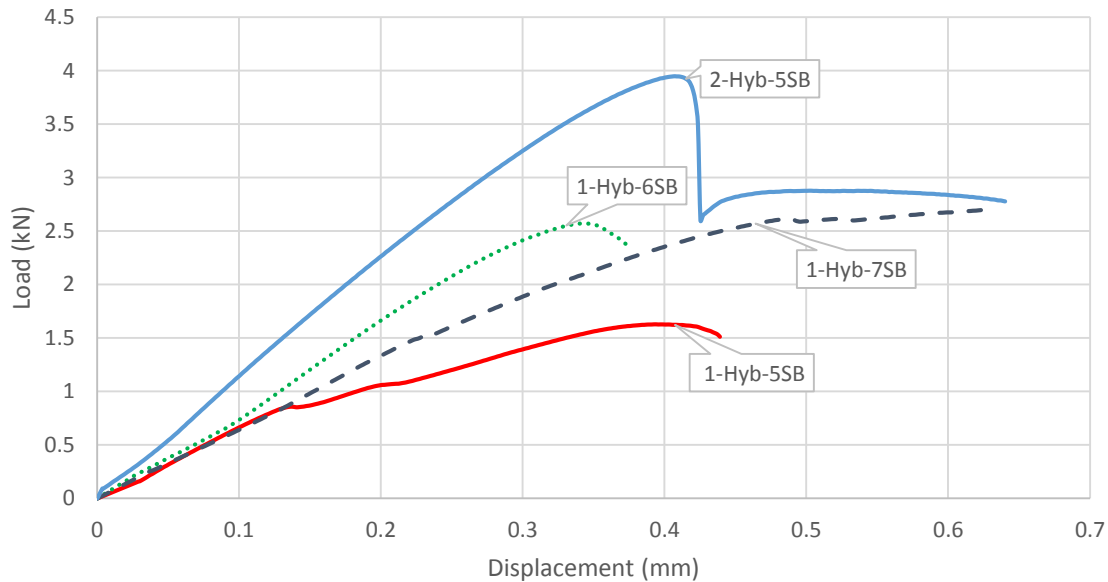
Figure 95 – Single lap shear test on the SLJ specimen 1-Hyb-5SB, 1-Hyb-6SB, 1-Hyb-7SB and 2-Hyb-5SB.

It is clear that the joint with two welding passes (2-Hyb-5SB) has the better results regarding the maximum load and displacement, even with use of channels of adhesive. The use of two welding passes improved the hardness and resistance of the joint. The reason of the results being so poor in this type of joint is due to the damage to the fully cured adhesive caused during the FSW. This damage provoked by the FSW results in the welding holding most of the load during tests. However, just like on the welded only joints, the joint 1-Hyb-7SB achieved the same displacement but with lower strength than the joint 2-Hyb-5SB. Still on the double welding pass joint (2-Hyb-5SB), it is clear that there is drop of load after 0.4 mm of displacement that is justified by failure of the adhesive and after that, the holding until failure was supported by the weld. Comparing the joints with one welding pass, the best result is the one that uses a continuous layer of adhesive (1-Hyb-7SB), which despite the similar maximum load of the specimen 1-Hyb-6SB, achieved an improvement of 82 % of displacement until failure. Unfortunately 1-Hyb-7SB is the joint that used 400 kgf of pin force, and with the 450 kgf of the joint 1-Hyb-8SB, better results could be achieved, however the joint 1-Hyb-8SB was one of the joints that were damage during the FSW process.

The failure mode was also adhesive in all the specimens as shown in figure 96.
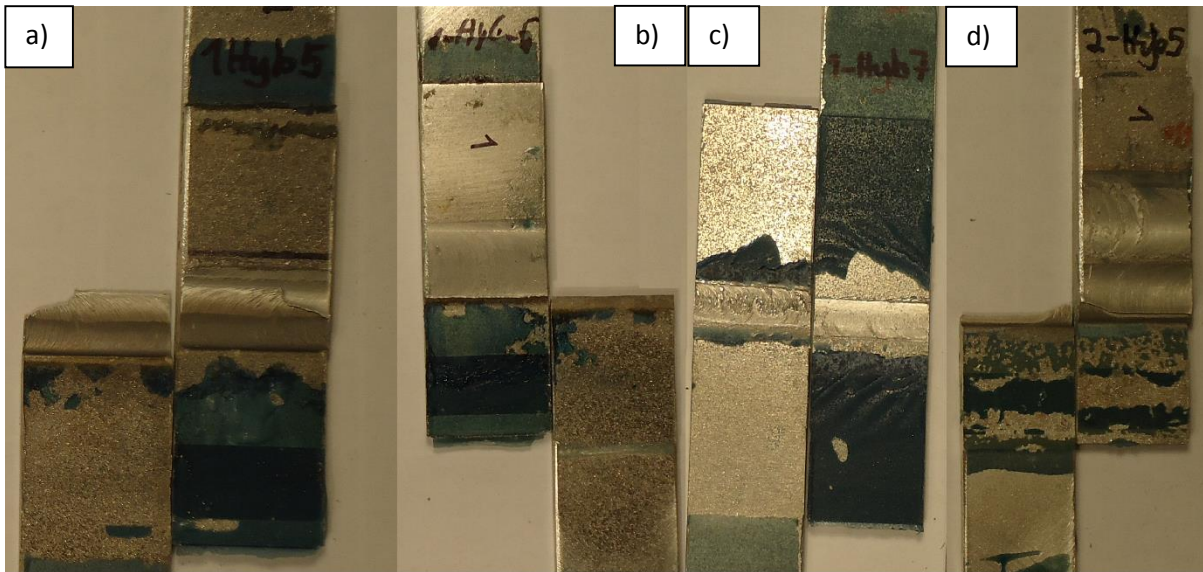
Figure 96 – Failure on SLJ specimen: a) 1-Hyb-5SB; b) 1-Hyb-6SB; c) 1-Hyb-7SB; d) 2-Hyb-5SB.

The results of the single lap shear tests in the joints with two welding passes and FSW right after bonding are displayed in figure 97. The joints with channels of adhesive showed very similar results, despite the fact that 2-Hyb-1SB uses 400-320 kgf instead of the 450-400 kgf of down force of the tool that 2-Hyb-2SB uses. Figure 97 also presents the results of 2-Hyb-4SB and 2-Hyb-4A joints that have a continuous layer of adhesive.
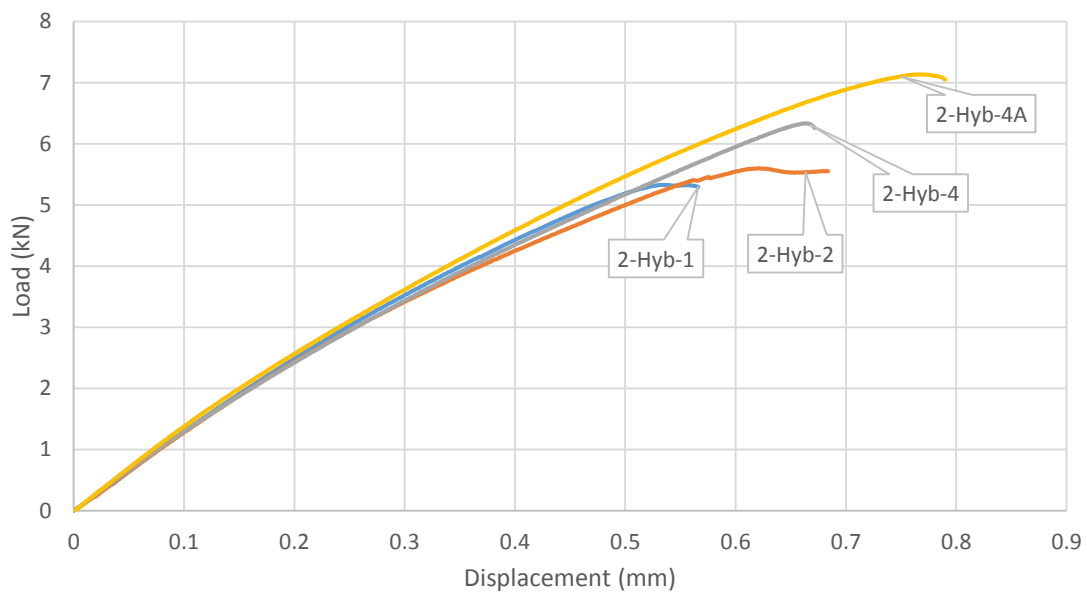
Figure 97 – Single lap shear test on SLJ specimen 2-Hyb-1SB, 2-Hyb-2SB, 2-Hyb-4SB and 2-Hyb-4A.

The load/displacement curve with higher values was achieved by the joint 2-Hyb-4SB, although may be verified that the specimens 2-Hyb-1SB and 2-Hyb-2SB (joints with channels of adhesive) have a very similar load/displacement curve. The individual load displacement curve of the joints with channels of adhesive with higher values of maximum load and EA was achieved by the specimen 2-Hyb-2SB that indicates again that higher tool force leads to better results.

Also, once again, the joint that received anodization treatment and a continuous layer of adhesive (2-Hyb-4A) showed a higher maximum load and displacement when compared with the joints with two weld passes.

The failure mode shows, once again, that all the joints had adhesion failure as is shown in figure 98. Even the specimen 2-Hyb-4A, with anodization treatment, shows adhesive failure but still has better resistance than the others joints.
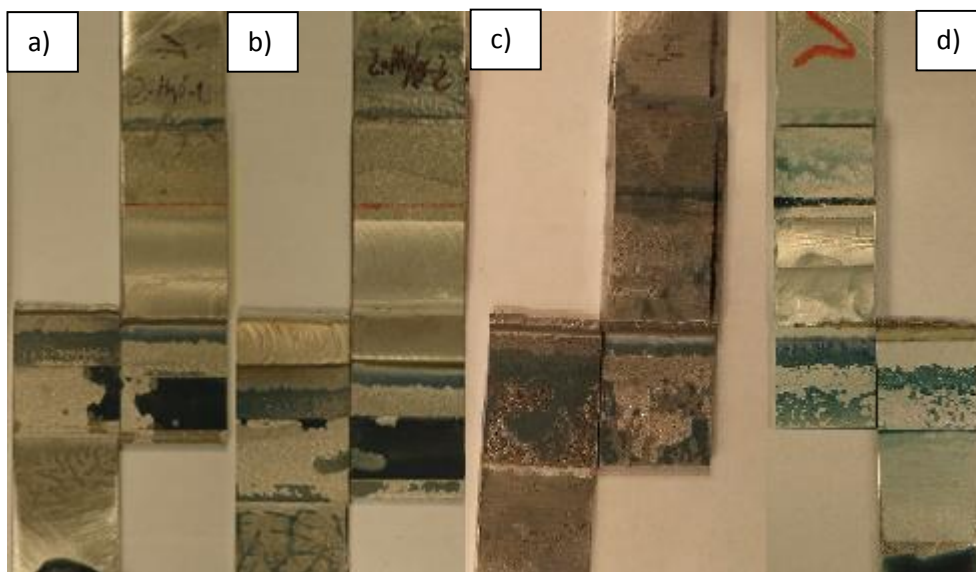
Figure 98 - Failure on SLJ specimen: a) 2-Hyb-1SB; b) 2-Hyb-2SB; c) 2-Hyb-4SB; d) 2-Hyb-4A.

4.2.2.4. *Summary of single lap shear tests*

This section will summarize the comparison of the best results for the single lap shear tests performed on hybrid, welded and bonded joints for each group of parameters.
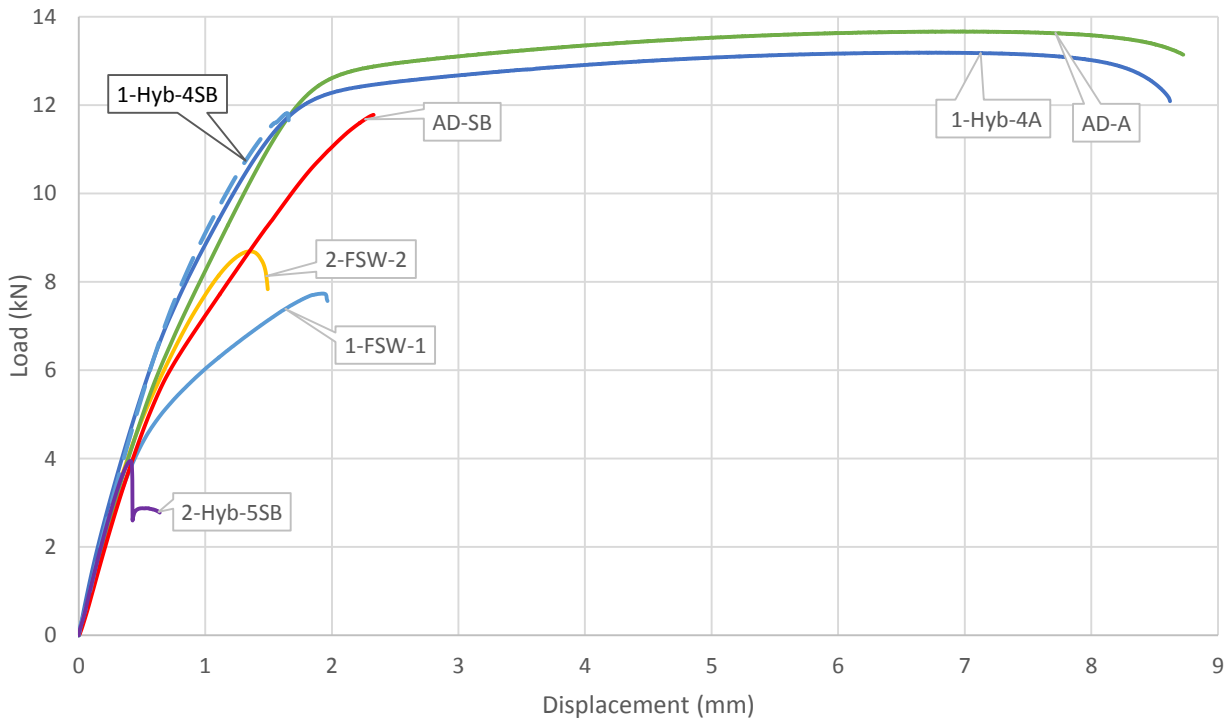
Figure 99 - Single lap shear tests of the specimens with best results (with and without anodization).

Presented in figure 99 are the joints with higher strengths and EA's from single lap shear tests:

- 1-FSW-1 – FSW only with 400 kgf;
- 2-FSW-2 – FSW only, two passes of welding with 400-450 kgf,;
- 1-Hyb-4SB – FSW right after bonding (<30min), one pass of welding with 450 kgf, continuous layer of adhesive;
- 2-Hyb-1SB – FSW right after bonding (<30 min), two welding passes with 320-400 kgf, channels of adhesive;
- 2-Hyb-5SB – FSW after >8h of curing, two welding passes 320-400 kgf, channels of adhesive;
- AS-SB – Adhesive joint with sandblasting as surface treatment;
- AD-A – Adhesive joint with anodization as surface treatment;
- 1-Hyb-4A – FSW right after bonding (<30min), one pass of welding with 450 kgf, continuous layer of adhesive and anodization as surface treatment.

From all the joints that used sandblasting as surface treatment, when comparing the load versus displacement curve, it is obvious that the adhesive joint (without FSW) is the one that had better results. The adhesive joint achieved similar maximum load when compared with the hybrid joint 1-Hyb-4SB but with an improvement of 44 % of the displacement, meaning that the adhesive joint allows more energy absorption. Table 28 presents the other comparisons that are important to mention.

Table 28 - Load displacement improvement of the best specimens of each group of parameters.

Specimens	Load improvement	Displacement improvement
AD-SB vs 2-FSW-2	37 %	75 %
1-Hyb-4SB vs 2-FSW-2	36 %	22 %
2-Hyb-1SB vs 2-Hyb-5SB	52 %	55 %

After all these comparisons it is clear that the adhesive joint is better than all hybrid or welded joints only but it is important to retain that an extensive overlap was used in order to allow FSW.

Regarding the joints that received anodization as surface treatment, the results are clearly above all the other joints that had sandblasting as surface treatment. Comparing 1-Hyb-4A and AD-A specimens, the results are very similar, having a slightly higher value for the maximum load on the joint AD-A. Also, it can be seen in figure 99 that the tensile curves for these two specimens are very similar elastic and plastic deformation due to the fact that is the adherent that is being tested, since the joint itself is stronger than the aluminum.

Comparing the joint AD-A with the adhesive joint with sandblasting as surface treatment (AD-SB) there is an improvement of 14 % of the maximum load and a 145 % improvement of the displacement when the maximum load is achieved. The maximum load gap is relevant, but the important characteristic is the 145 % improvement of the displacement, showing the higher capacity of the AD-A specimen to absorb energy.

These results for the joints 1-Hyb-4A and AD-A are not completely decisive since the failure happened on the adherent instead of the joint. But at least for this configuration it is possible to see the superiority of the anodized joints.

4.3. Single Lap Fatigue Tests

4.3.1. Results for Single Lap Fatigue test

4.3.1.1. Fatigue Test for Welded Only Joints

As mention in section 3.6.2, S-N curves were plotted for welded only joints 1-FSW-1 and 2-FSW-2, for the hybrid 1-Hyb-4A joint and the adhesive joint AD-A.

Since the amount of available specimens was limited, it was only possible to take some points of the S-N curve of the best welded joints for one and two welding passes. The S-N curve is represented in figure 100.
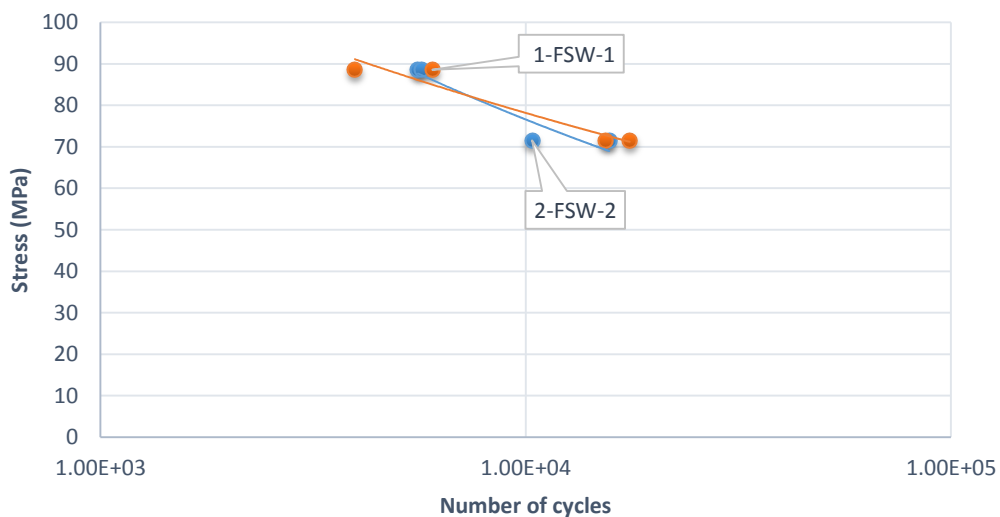
Figure 100 - S-N curve at R = 0.1 of specimens 1-FSW-1 and 2-FSW-2.

4.3.1.2. Fatigue Test for Adhesive Joints

As mention in section 3.6.2, it was decided to perform fatigue tests in the anodized adhesive joints and the resulting S-N curve is presented in figure 101.
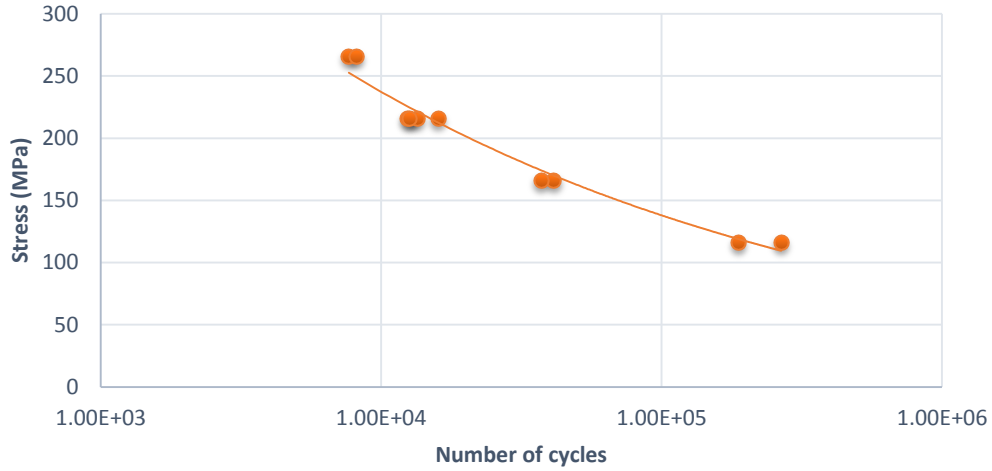
Figure 101 – S-N curve at R = 0.1 of specimen AB-A.

4.3.1.1. *Fatigue test for Hybrid Joints*

After quasi-static tests, there was an interest to submit the best hybrid joint to a fatigue test, since it is expected to lead to better results, 1–Hyb-4A was the chosen one. Some plates were anodized and the process parameters employed in joint 1-Hyb-4SB (hybrid joint with higher strength and EA) were used to manufacture such new joints. Fatigue test results for 1-Hyb-4A are presented in figure 102. Due to the low number of specimens of 1-Hyb-4 with sandblasting as surface treatment, it was decided not to test these joints to the fatigue.
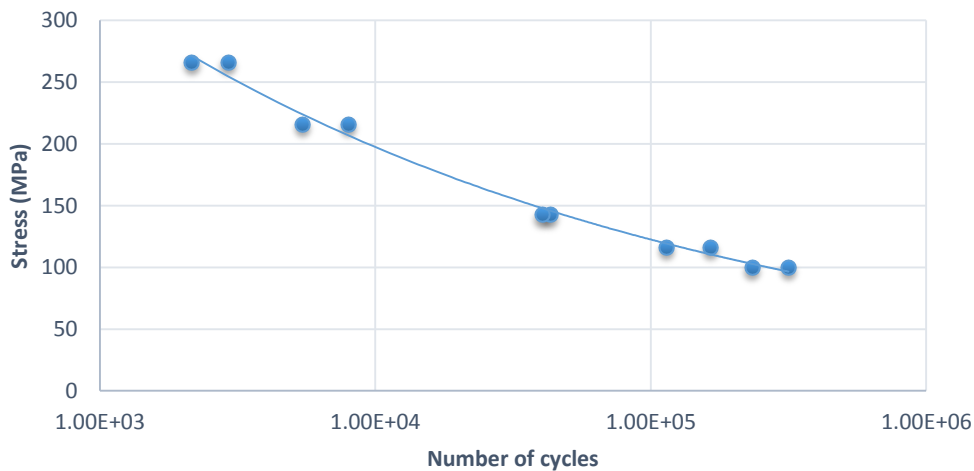
Figure 102 – S-N curve at R = 0.1 of specimen 1-Hyb-4A.

4.3.2. Discussion Single Lap Fatigue Tests Results

Concerning the results of the fatigue tests, the S-N curves of all the joints tested to fatigue are represented in figure 103. Unfortunately it was not possible to take more points of the weld only joints, but there are still conclusions to extract. The specific results of the number of cycles and stress are presented in table 30. The mean of the S-N curves were obtained by fitting a linear regression Eq.(3), assuming σ as the independent variable. Table 29 presents the values m and K_0 for all the S-N curves
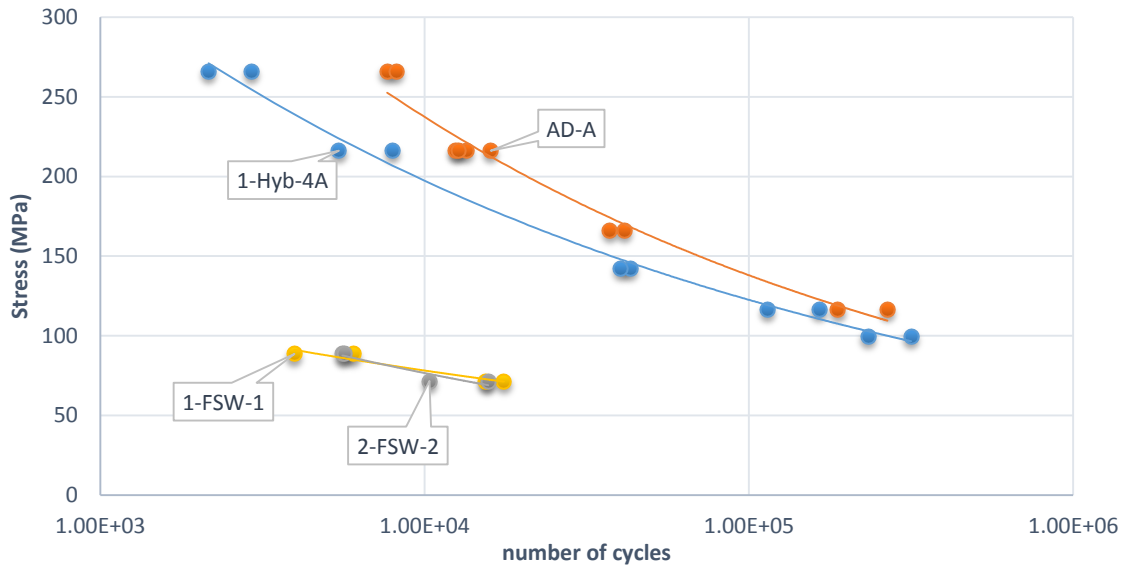
Figure 103 – S-N curves at R = 0.1 of specimens 1-FSW-1, 2-FSW-2, 1-Hyb-4A and AD-A.

Table 29 - m and K_0 values for all S-N curves.

Condition	m	K_0	Fatigue Strength at 1 x 10^5 cycles (MPa)
AD-A	4.237	1.141×10^{14}	68
1-FSW-1	6.024	2.483×10^{15}	32
2-FSW-2	4.310	1.309×10^{12}	22
1-Hyb-4A	4.831	1.225×10^{15}	66

$$N_r \sigma^m = K_0 \ (3)$$

Eq. (3) does not take into account the "infinite" life specimens.

Table 30 - Fatigue test results for specimens AD-A, 1-Hyb-4A, 1-FSW-1 and 2-FSW-2.

Specimen	Number of cycles	Stress (MPa)	Failure
AD-A	7667	266	Substrate
	8157		
	13447	216	
	12433		
	12681		
	41305	166	
	37227		
	267556	116	
	187976		
1-Hyb-4A	2157	266	Weld(advancing side)
	2922		
	5437	216	
	7969		
	43026	143	Weld(retreating side)
	40255		
	164633	116	
	113991		
	316128	100	
	233421		
1-FSW-1	5578	89	Weld (advancing side)
	5679		
	15710	72	
	10348		
2-FSW-2	3962	89	Weld
	6034		
	17558	72	
	15426		

Analyzing figure 103 and table 29, the conclusion is that the best S-N curve is achieved using adhesive only, although the best hybrid joint 1-Hyb-4A also has similar behavior and results. This difference between these two joints is in agreement with the type of failure that happens in each joint. On the hybrid joint the failure happens in the weld and on the adhesive joint it happens on the adherent (see figure 105).

Concerning the welded joints, both of them are clearly weaker than the hybrid/adhesive joints, and the results between them are very similar as was also found on the single lap shear tests.

One particularity is the fact that for the joints 1-Hyb-4A, when tested under fatigue with higher values of stress, it leads to a failure at the advancing side as expected due to the hook defect, however from the micrographic analysis it is possible to see that this joint has no observable hook defect but since it was one of first joints manufactured it might be a sporadic situation. For lower stresses, the retreating side is the one that fails and that might be justified by the fact that when the joint is heavily loaded the hook defect cannot be suppressed by the adhesive, but when lower stresses are applied, the adhesive can hold the load imposed on the joint and does not break through the advancing side. Also the retreating side, as can be seen in figure 104 , allows the adhesive to fully mix with the aluminum and even create a seam of

adhesive along the weld's retreating side on the surface of the upper plate, and that might be the reason for the failure happening at the retreating side when loaded with lower loads.

Another characteristic observed was that with higher loading force in the fatigue tests, the lower is the bending provoked on the joints before the failure, which is expected since at lower loads the joints are tested for more time, allowing the aluminum to deform and bend.
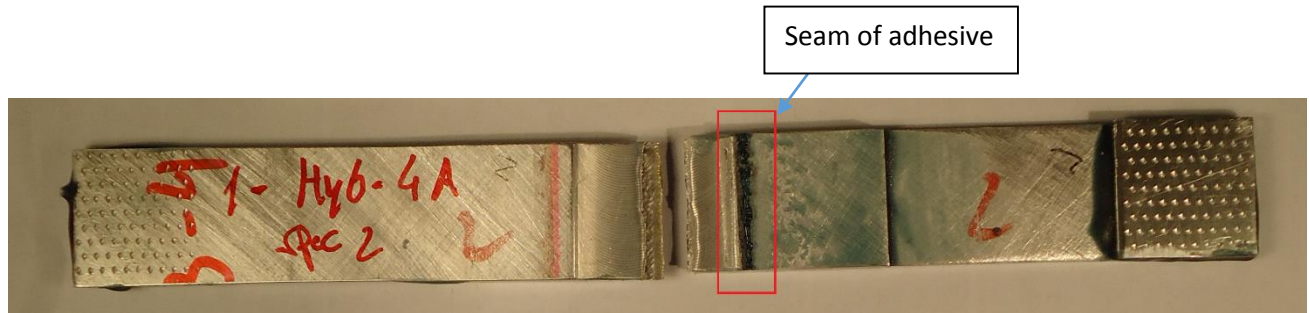
Figure 104 - Specimen 1-Hyb-4A failure after tested to fatigue.
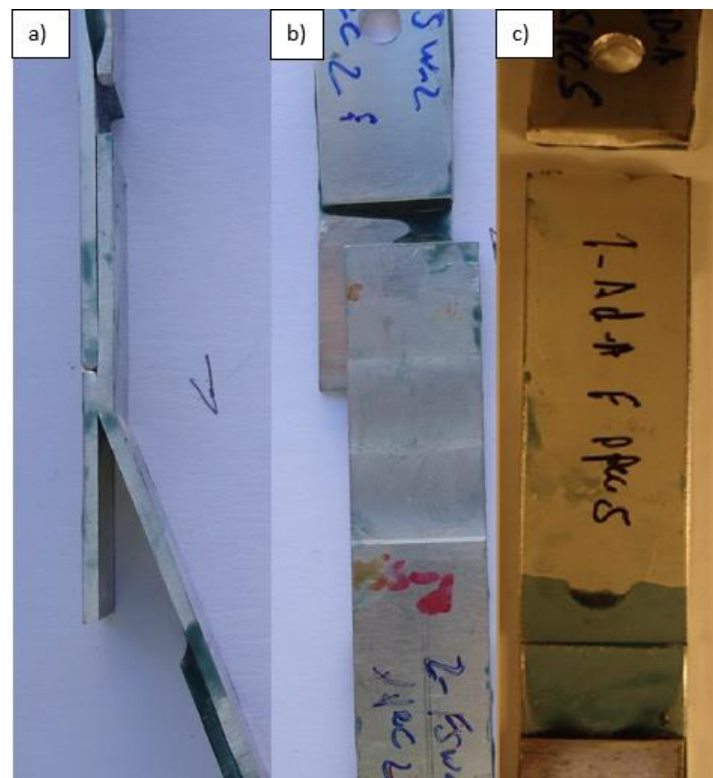
Figure 105 - Failure mode for SLJ specimens when tested to fatigue: a) 1-FSW-1; b) 2-FSW-2; c) AD-A.

In figure 105 it is possible to see the failure mode in the other three joints tested for fatigue. The joint 1-FSW-1 failed at the advancing side as expected in the heat affected zone, the joint 2-FSW-2 had a normal failure at the retreating side due to the configuration imposed (both advancing sides turn to the middle of the joint) and AD-A presented a failure at the extremity of the joint due to the concentration of loads on this zone during the fatigue tests.

4.4. Other Analyses on Welded and Hybrid Joints

4.4.1. Distortions Measurements

The distortions results of the SLJ's that were employed to FSW are represented in figure 106. The objective of this type of this analysis is determining which distortions FSW provokes in the SLJ with and without adhesive. This kind of analysis is important in order to determine the tolerance in distortions that, for example, the aerospace industry requires [45].
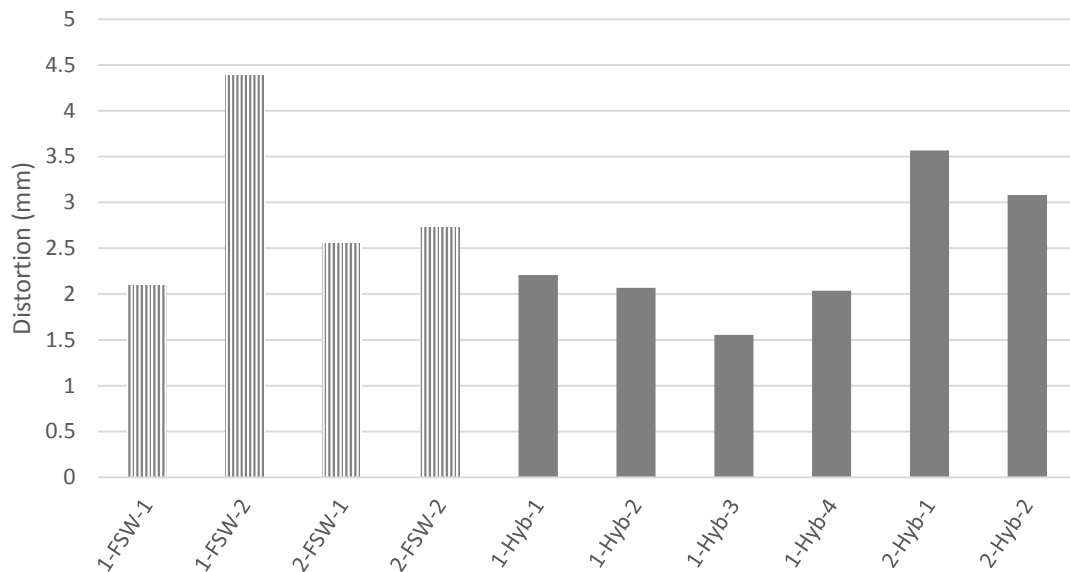
Figure 106 - Distortion measurements.

From the results of the distortion measurements, the welded only joints show an increase of distortion with the increasing of the vertical load force of the pin, for example, 1-FSW-1 to 1-FSW-2 where the gap of values is more accentuated when compared with the double pass joints. This conclusion is justified by the higher heat provoked by the tool during the FSW when it is performed with higher values of downward force of the tool. All the single pass hybrid joints had shown similar values of distortions. Regarding the hybrid joints manufactured with channels of adhesive, the distortions are maintained or reduced with the increase of the downward force of the tool. On the contrary, when there is a continuous layer of adhesive the behavior is similar to the single pass welded joints, where there is an increase of distortions with the increase of vertical force of the pin.

The lowest value achieved was by the specimen 1-Hyb-3SB that used an uncured continuous layer of adhesive when the FSW was done, which might be justified by the fact that the adhesive worked as a "damper" for the vertical force. Another reason for these low values of distortions is the fact that adhesive is less thermally conductive than aluminum, limiting the heat input in the bottom plate where was these values were measured.

Concerning the double pass specimens, it was verified that the hybrid joints with channels of adhesive showed higher values of distortions when compared to the double pass FSW only, possibly because the channels of the adhesive worked as isolation of the heat produced during the welding process, leading to higher heat and consequently higher distortion on the bottom plate.

4.4.2. Micro and Macrostructure

Along this chapter the results for the micro and macrostructure analysis will be discussed and presented.

Figure 107 shows the microstructure of the NZ in a) and HAZ in b), where the NZ presents more concentration of intermetallic phases/2nd phase particles when compared to HAZ. This happens due to the fact that the pin of the FSW tool, when it is working, cuts/breaks these particles, as can be seen in figure 107. The particles in the nugget zone are smaller than the ones that are in the HAZ.
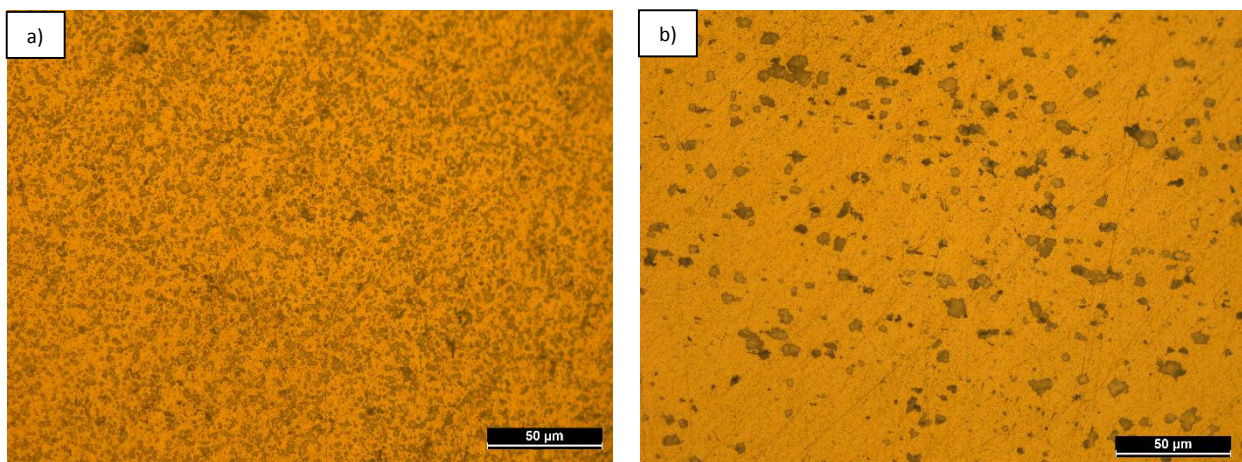
Figure 107 - Microstructure of specimen 1-Hyb-4SB with: a) NZ; b) HAZ.

The length of hook defect was also checked and it was found out that the higher value is on the hybrid specimen 1-Hyb-3SB, presented in figure 108 b), however figure 108 a) shows that the specimen 1-Hyb-4SB has no observable hook defect. This absence or probably small of the hook defect might be the reason that 1-Hyb-4SB joint had the best tensile curves. Another pattern is that with more downward force of the tool, the hook effect is less significant and that was also according with the tensile results, in which for the same manufacture process, the joints with less force of the tool are weaker.

Table 31 - Length of the hook defect.

Specimen	Length of the hook defect (µm)
1-FSW-1	1292.7
1-FSW-2	508.3
2-FSW-1 1st pass	630.8
2-FSW-1 2nd pass	673.1
2-FSW-2 1st pass	935.8
2-FSW-2 2nd pass	914.6
1-Hyb-3SB	1176.4
1-Hyb-4SB	-
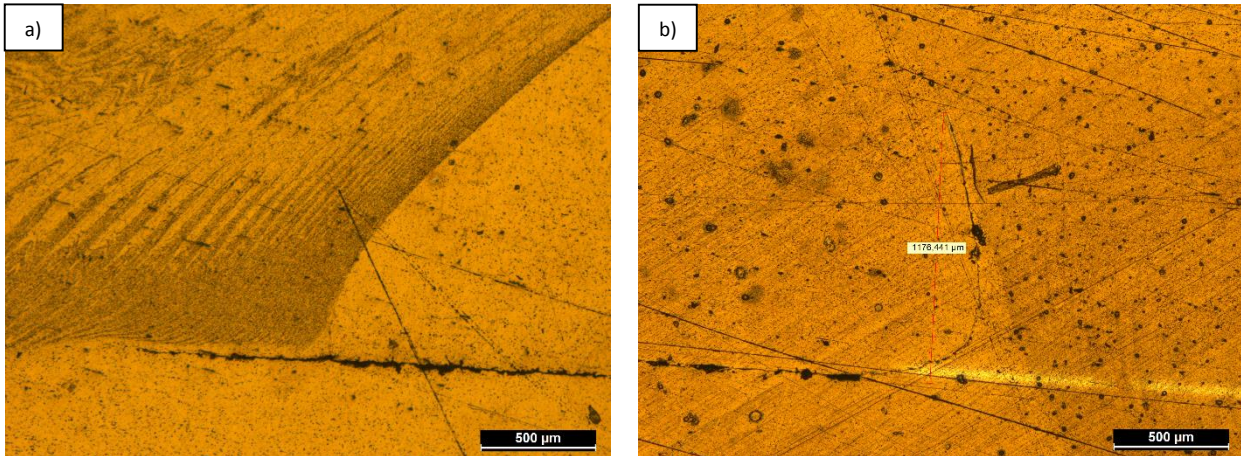
Figure 108 - Macrostructure of specimen: a) 1-Hyb-4SB; b) 1-Hyb-3SB.

Despite the fact that 1-Hyb-4SB does not have the hook defect, it has shown to have the defect known as cold lap defect, presented in figure 109, that is a bad mixing and fusing of material and normally appears on the retreating side of the FSW.
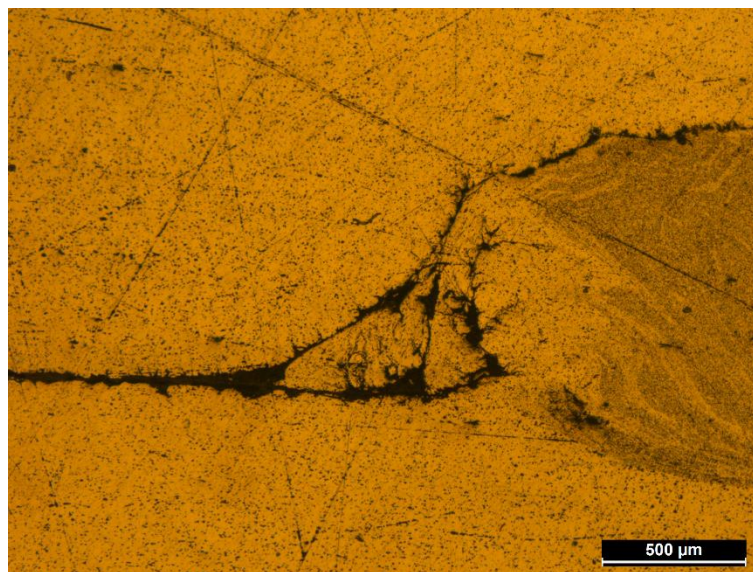
Figure 109 - Cold lap defect on specimen 1-Hyb-4SB.

4.4.3. Microhardness Profiles

The microhardness tests were performed on hybrid and welded only joints since the adhesive has no influence in the hardness of the material. The results for the welded joints are presented from figure 110 to figure 113.

From the analysis of figure 110 where the microhardness profile of the welded only joints with one pass is presented, it may be verified that the average hardness in the nugget zone (NZ) is significantly lower than the base material, but in the upper plates it can be seen that near the frontier of the pin diameter (TMAZ), at the advancing side, the lowest value of hardness is found for each joint, 55 HV 0.3 for 1-FSW-1 and 46 HV 0.3 for 1-FSW-2. The 1-FSW-2 specimen got the lower hardness profile in both, upper and lower plates, since it was the one that had more downward force of the tool during the welding process. Also, the upper plate, in both specimens, is most affected by the welding, leading to lower results of hardness. In [36], it is mentioned that the variation of microhardness values in the welded area and base material is due to the difference of the microstructures of both zones.
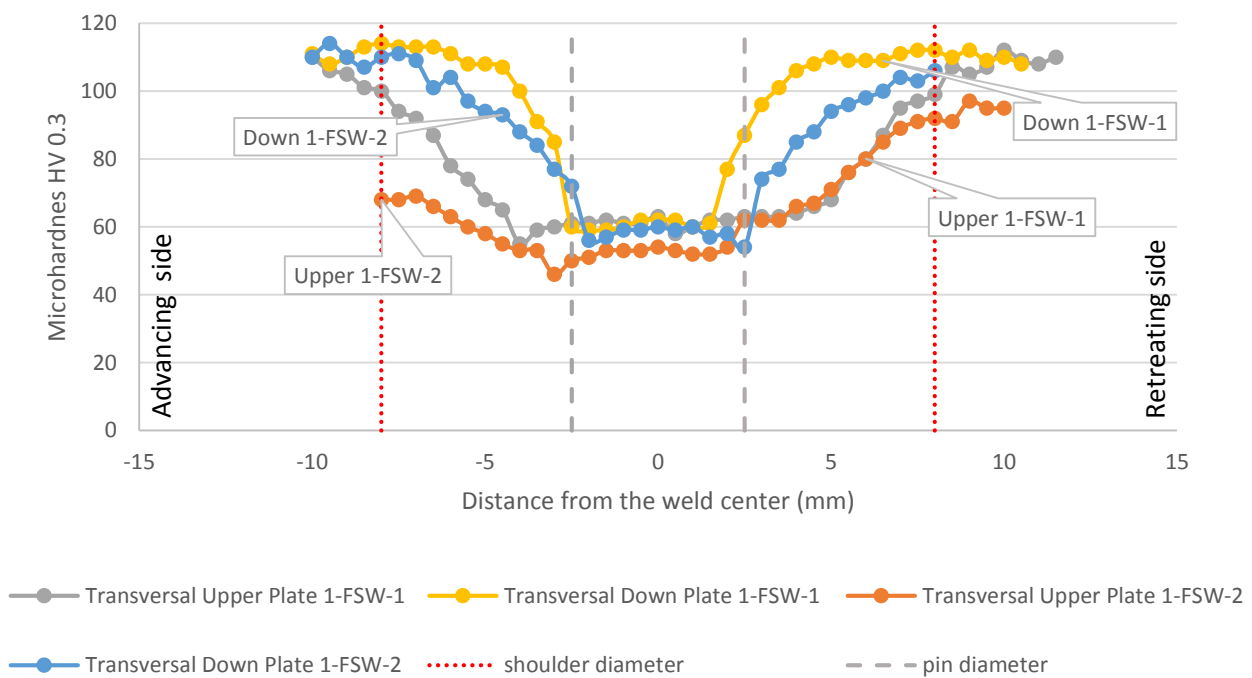
Figure 110 – Microhardness profile of specimens 1-FSW-1 and 1-FSW-2 (Transversal).

From the analysis of figure 111, where the vertical profiles of microhardness are presented, the lower values of hardness are found in the NZ's as expected and 1-FSW-2 is slightly softer than 1-FSW-1. Also the bottom plate that is presented from 2-4 mm shows higher values of hardness in both joints.
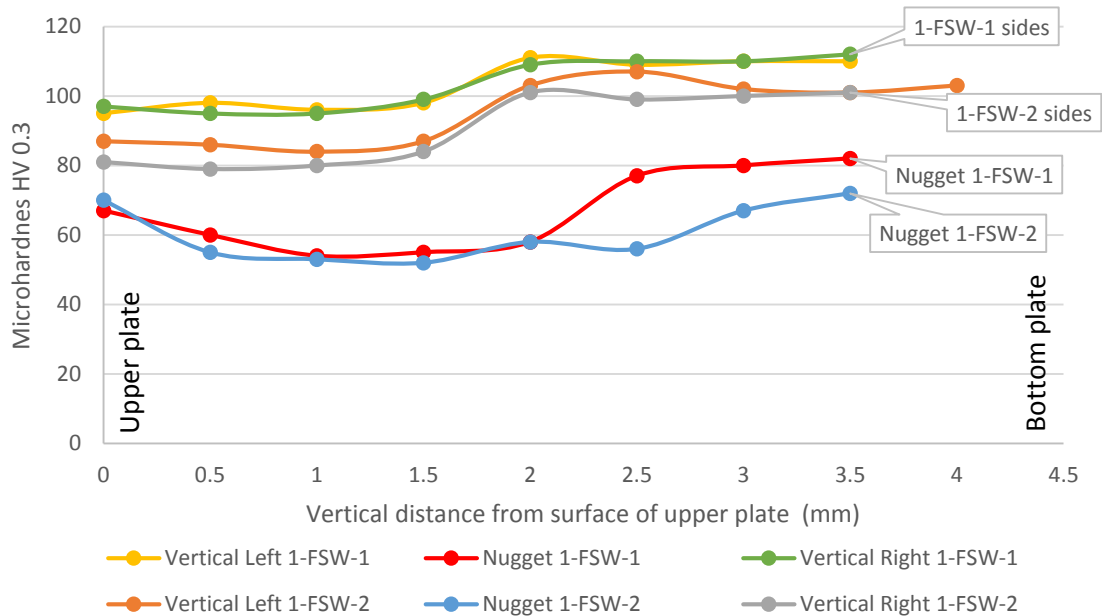
Figure 111 – Microhardness profile of specimens 1-FSW-1 and 1-FSW-2 (Vertical).

Analyzing figure 112, where the transversal profile of microhardness on the specimens 2-FSW-1 and 2-FSW-2 is represented, it is clear that once again the NZ holds the most of the lower hardness values. In each joint, the lower plates got the higher values of hardness and the joint 2-FSW-2 is generally more affected and with a lower hardness profile, which is a consequence of the higher down force of the tool during FSW. The value of 52 HV 0.3 was the lowest hardness found, present in both specimens and still inside of the extrusion zone.
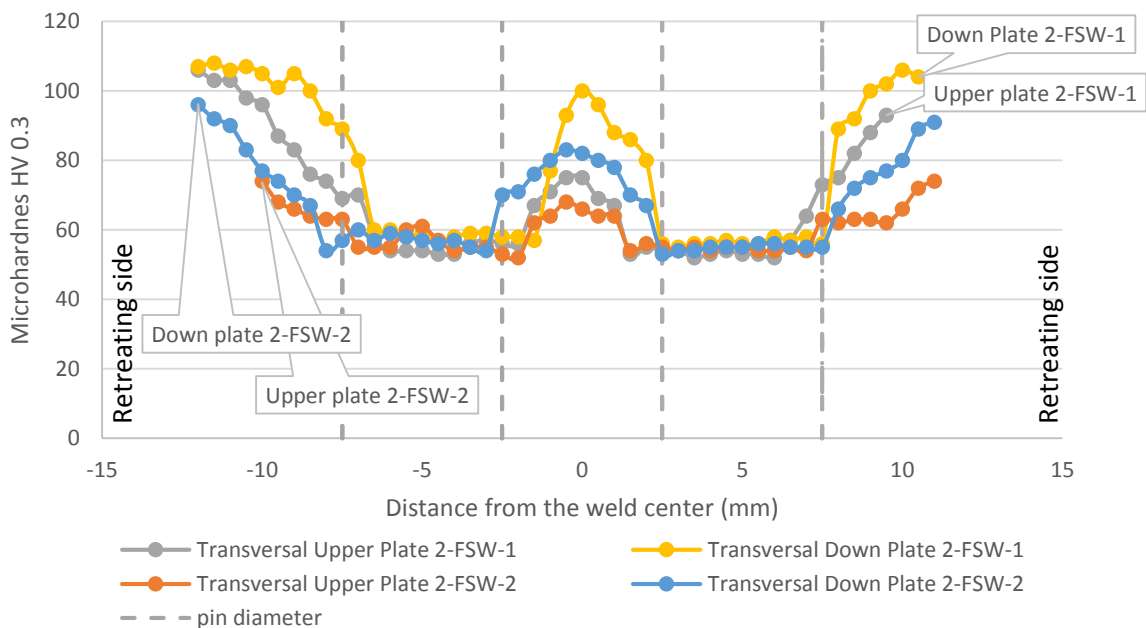
Figure 112 – Microhardness profile of specimens 2-FSW-1 and 2-FSW-2 (Transversal).

99

Figure 113 a) shows the microhardness vertical profile of the nuggets in both specimens 2-FSW-1 and 2-FSW-2 and b) the sides of the joints. The NZ's are harder in the specimens 2-FSW-1 due to the lower downward force of the toll during welding. The same difference of hardness happens inside the results of the same joint, where the first welding pass with higher down force of the tool leads to a lower hardness profile. Also, in figure 113 b) a peak of lower hardness can be spotted, that might indicate a defect and also the contact with TMAZ since the maximum length allowed for the microhardness test machine was 30 mm and the vertical line tested might be too close to the TMAZ, leading to lower hardness values.
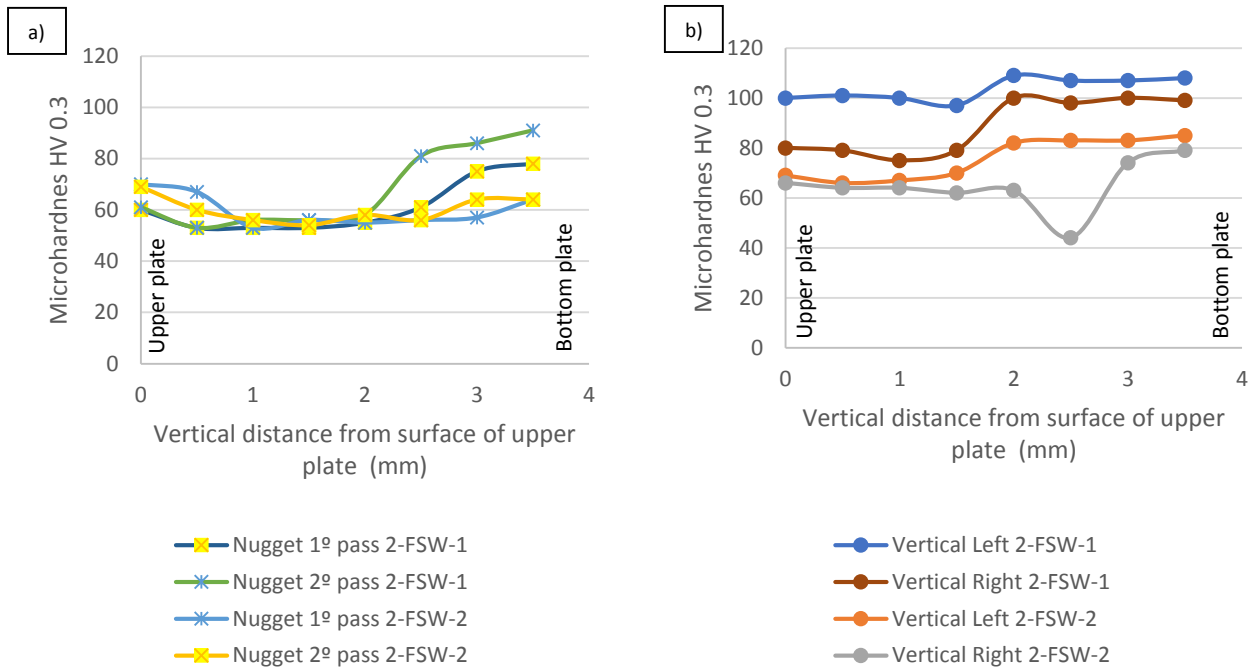
Figure 113 – Microhardness profile on specimens 2-FSW-1 and 2-FSW-2 (Vertical) with: a) Nuggets; b) Sides.

The results for the hybrid joints are presented in figure 114 and figure 115. The hardness profile of the hybrid joints is similar to the results of the only welded joints and that indicates that the mix of adhesive does not influence the hardness of the material/weld. The lowest value found was 53 HV 0.3 on the 1-Hyb-3 specimens. The NZ is where the hardness profile is lower and both hybrid joints' profiles have shown to have very similar results.
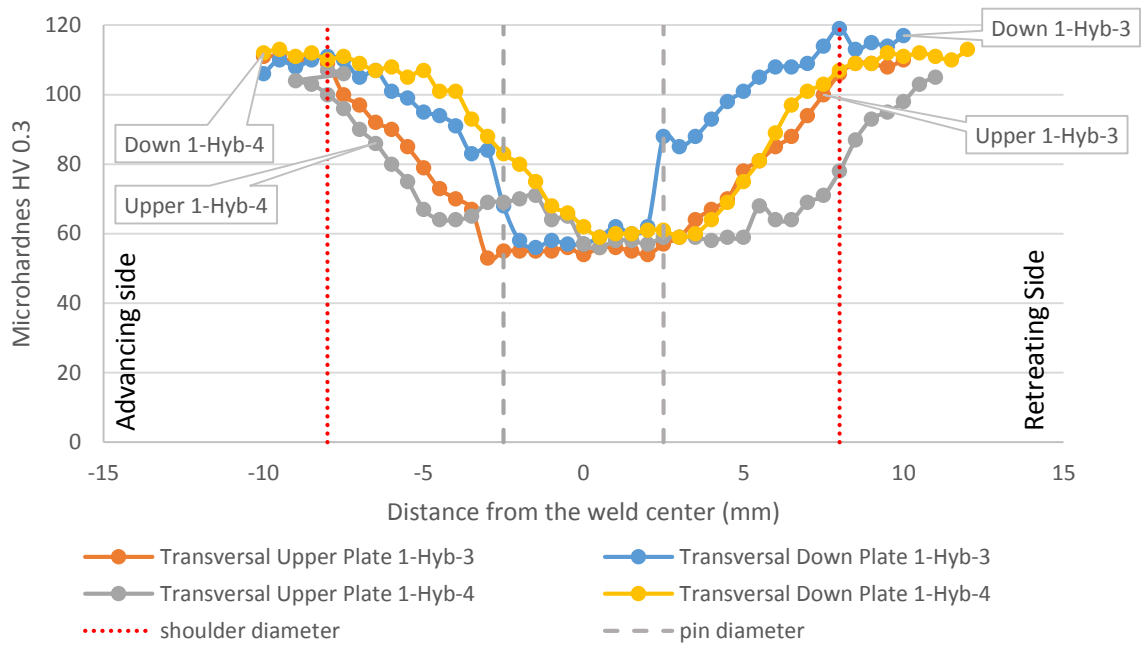
Figure 114 – Microhardness profile of specimens 1-Hyb—3SB and 1-Hyb-4SB (Transversal).
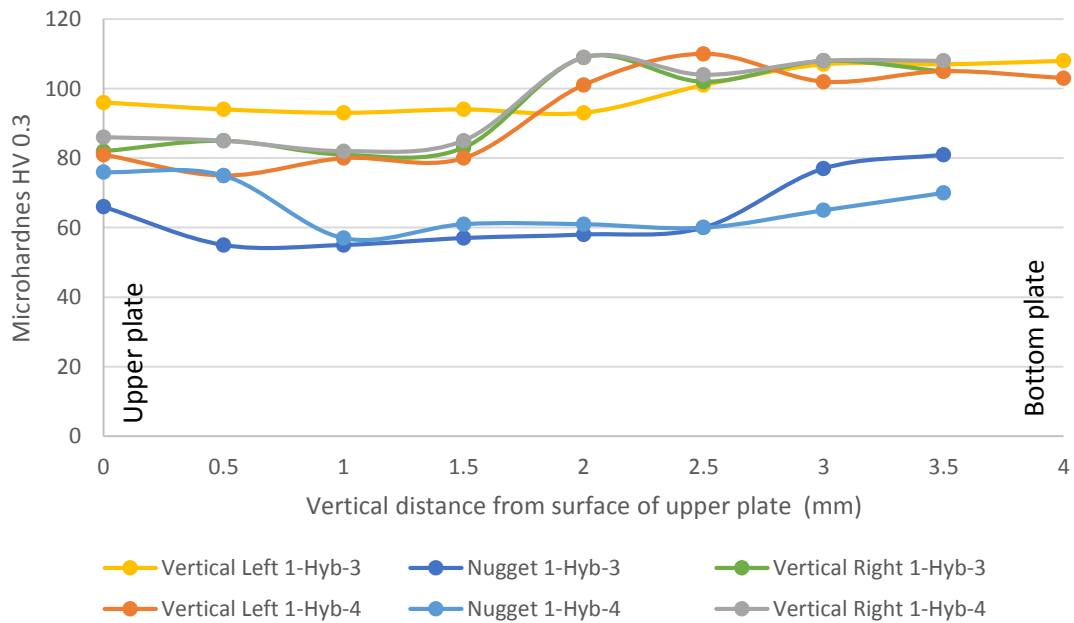
Figure 115 - Microhardness profile of specimens 1-Hyb-3SB and 1-Hyb-4SB (Vertical).

All the specimens showed an increase of hardness along the HAZ towards the base material. The minimum hardness values are coincident with the limits of the pin in all joints. The lowest hardness value is usually presented at the advancing side of the welding. During the welding the loss of T6 condition is expected, leading to lower values of mechanical properties reflected in the drop of hardness.

In [41], it is stated that for AA's such as 6082, the main strengthening precipitate is β″-Mg5Si6. This precipitate is stable for temperatures lower than 200°C and responsible for the hardening. Since in FSW temperatures over 200-250 ℃ are expected, it leads to the dissolution of the precipitate β″ during the welding process [46], resulting in absence of it in the HAZ and NZ. The NZ is the most affected area due to the deformation of the material by the pin, formation of coarse precipitates and loss of hardening precipitates. However due to the recrystallization, some hardness is recovered. The reason for the TMAZ to typically have the lowest hardness values is high plastic deformation suffered in this zone that leads to an incomplete or even absence of recrystallization.

For future work, it should be considered to remake the T6 treatment on the joints, since it would probably recover some of the hardness that is lost during the welding.

Chapter 5 - Concluding Remarks and Future Work

5.1. Conclusion

Along this thesis welded, adhesive and hybrid joints were manufactured and tested under tensile and fatigue tests. Also some analysis were made, such as distortions measurements, microhardness profiles, micrographs, temperature during FSW and mechanical characterization of the adhesive.

In order to understand if the mix of adhesives during the FSW process affected the resistance of the hybrid joints, besides joints with a continuous layer of adhesive, specimens with channels of adhesive were also manufactured to prevent the mixing of the adhesive with the flow of aluminum created in the FSW. A continuous layer of adhesive has proven to be the most effective configuration, achieving better static results.

A group of FSW parameters was also varied where specimens with one and two welding passes were manufactured as well as the downward force. The best hybrid configuration, regarding the strength of the lap joint, was achieved by one welding pass with 450 kgf of downward force, 1000 rpm of rotation speed of the welding tool, 200 mm/min of crosshead speed in combination with the continuous 0.2 mm thick layer of adhesive that was applied right before the FSW is performed. Concerning the tool used, it had a 2.8 mm of pin length, 16 mm of shoulder diameter and 5 mm of pin diameter. Other parameters regarding the welding were the 5 seconds of dwell time, 0.1 mm/min of plunge speed and 0° of tilt angle in tool during the process.

Regarding the joints with sandblasted surfaces and submitted to tensile tests, the adhesive joints achieved higher maximum load until failure when compared to both FSW (with one or two welding passes), moreover it had a 37 % and 75 % improvement in the maximum load and displacement, respectively, than the best welded only joint. The best hybrid SLJ showed similar results in strength to the adhesive joint but with a lower displacement at failure. Since recrystallization occurs during FSW, combined with defects such as the hook defect, a lower energy absorption is verified and consequently lower displacement until failure.

The sandblasting treatment has shown to be unsatisfactory and leads to adhesive failures and poor results under tensile and fatigue tests. In order to overcome this difficulty, PAA was applied as surface treatment, leading to better results under the mentioned tests. The type of failure that occurred in the anodized plates showed that the overlap length was over dimensioned for this configuration, resulting in failure of the adherents instead of the joint itself.

The tensile tests were made in order to know the static mechanical properties of hybrid joints and compare with AB and FSW only joints. It was found out that the hybrid joints that obtained better strength and EA during tensile tests were the ones that had adhesive applied right before FSW, being the weld process done while the adhesive is in a non-cured state.

Regarding the joints with anodization as surface treatment, the adhesive joint showed better mechanical properties in the tensile tests, however the hybrid specimen once again were able to achieve similar maximum load of the adhesive joint in Onethe tensile tests, but this time was also able to have similar displacement until failure, resulting also in failure of the substrate. Note that the anodized joints had shown severe improvements over the sandblasted joints with the same manufacture procedure.

Concerning the fatigue tests, the anodized adhesive joint showed a better S-N curve, holding more cycles in general than the best hybrid joint (1-Hyb-4 with anodization), however the results do not have a high gap between them. The FSW joints only show a very small number of cycles, when a similar stress of the hybrid and adhesive joint is applied. Between the welded joints only, the results are similar under the tensile and fatigue tests. The failure mechanism of the adhesive anodized joint showed that the full length of the joint should be augmented in order to reduce the concentration of tensions at the failure zone during the fatigue test.

From the results of the microhardness analysis, it was found out that the adhesive does not influence the hardness of the material. The hardness profile at the NZ is always significantly lower than the base material hardness. Most of the joints had the lowest value of hardness positioned in the frontier of the pin diameter, at the TMAZ. All the specimens showed an increase of hardness in the HAZ towards the base material.

From the analysis of the micro and macrostructures of the joints it was verified that the joints with only one welding pass had the higher values of hook length. The hybrid joint that has proven itself stronger and resistant under tensile and fatigue tests (1-Hyb-4) showed no observable hook defect but on the other hand, it had a defect on the retreating side known as cold lap defect. With higher down force of the tool the length of the hook is decreased. The joint that showed the largest hook defect was 1-Hyb-3SB that also had the lowest point of hardness in the advancing side.

The distortion analysis, that were made to understand the influence of the process for this property, showed higher values of distortions in an FSW only joint, with one pass of 450 kgf of downward force. The lower value of distortion was achieved by a hybrid joint with a continuous layer of adhesive and one welding pass with 400 kgf of downward force.

5.2. Future Work

Since friction stir weldbonding is a very recent technique there are still a lot of improvements that can and should be considered. The geometry of the single lap joints was over dimensioned, regarding the overlap length used that did not allow a cohesive failure at the adhesive joints when subjected to the tensile and fatigue tests. A reduction of the overlap length from 60 mm to 30 mm might be a good solution since it still allows the application of FSW on the joint, however the best solution would be an optimization study in order to obtain the correct value of the overlap length.

Another point to take into consideration is the full length of the joint that should be extended due to the stress concentration, during the fatigue test, in the zone right after the grips. A joint with more length would reduce the effect of stresses concentration and would result in more coherent results.

In order to obtain more reliable results for the shear stress and shear modulus, aluminum specimens should be manufactured for TAST. However, in order to avoid elastic deformations the specimens should be redesign. Another alternative should be the application of a surface treatment or the use of primaries in order to augment the adhesion to the adherents.

Since it was not possible to manufacture T-joints due to the lack of time and some technical problems, some tests should be done in order to find out what is the contribution of this hybrid process is and what is the best group of parameters that should be employed.

Regarding the hardness results, the T6 treatment of the joints should be remade after welding since some of the hardness could be recovered.

Finally, all the further joints should be done using anodization as it is the surface treatment with which the best possible results are obtained.

Appendices

A1– Surface preparation Phosphoric Acid Anodization/Sandblasting

Manufacturing adhesive joints requires a surface treatment that is applied to the work pieces before bonding. Depending on the substrate material and the adhesive used, the type of surface treatment varies and some are more suited than others. This process is done in order to guarantee the maximum adherence of the adhesive to the work piece, in order to make joints with good properties and with failures on the adhesive (cohesive failure) instead of failure at the interface (adhesive failure).

During this dissertation two types of surface treatments were implemented: sandblasting and anodization of the aluminum.

Initially all the specimens were "sandblasted" and then degreased with acetone in order to create roughness and clean the surface to be bonded, respectively. The process is simple and fast, just requires to previously cleaning of the surfaces and then perform sandblasting on the plates desired to joint.

PAA treatment basically creates an oxide layer at the surface of the substrate, leading to better adherence. To perform this process it was initially necessary to prepare the aluminum to be anodized, using sandpaper to create roughness and then submerge the aluminum in acetone by using a household ultrasonic cleaner to fully clean the surface to be bonded. After this the PAA was done following the standard D3933, where a solution of 12 % acid phosphoric and 88 % of distilled water (% of mass) was prepared. Once the substrates are submerge in the solution, it is necessary to create a closed circuit that will allow current to travel through the substrates, and for this purpose a power supply was used while a voltage of 16 V was maintained on the circuit. Figure 116 and figure 117 show the circuit used and the power supply, respectively.

Cathode

Figure 116 - Circuit to make PAA treatment.
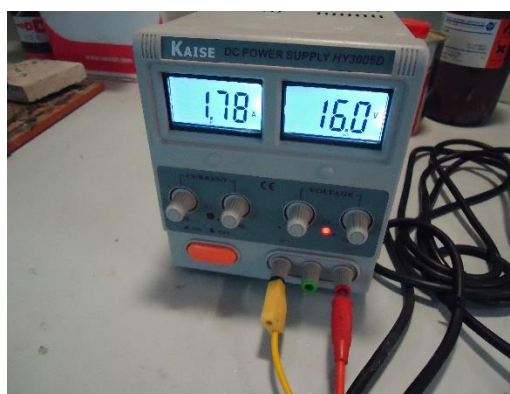
Figure 117 - Power supply while anodization occurs.

The specimens are submerged for 25 minutes and then are removed from the solution, followed by acetone cleaning, once again using an ultrasonic cleaner. During the PAA process it is not always possible to maintain the voltage at 16 V and that might be for two reasons: bad

solution that was already used or badly mixed the acid and water, or the contact area was too big for the power supply not allowing 16 V to be maintain.

In order to maintain the treatment intact, it is necessary avoid contact between the anodized surface and any exterior dust/air or anything that can contaminate it. For this purpose it is wrapped in aluminum foil until the moment that the adhesive is going to be applied. The followed standard states that it is recommended to bond the substrates in the following 3 days after the treatment.

References

1. Kallee, S., Nicholas, E., and Thomas, W., *Friction Stir Welding- Invention, Innovations and Applications.* Kei Kinzoku Yosetsu(Journal of Light Metal Welding and Construction), 2005. **43**(11): p. 34-35.
2. Kusuda, Y., *Honda develops robotized FSW technology to weld steel and aluminum and applied it to a mass-production vehicle.* Industrial Robot: An International Journal, 2013. **40**(3): p. 208-212.
3. Krasnowski, K., Hamilton, C., and Dymek, S., *Influence of the tool shape and weld configuration on microstructure and mechanical properties of the Al 6082 alloy FSW joints.* Archives of Civil and Mechanical Engineering, 2015. **15**(1): p. 133-141.
4. Mishra, R.S. and Ma, Z., *Friction stir welding and processing.* Materials Science and Engineering: R: Reports, 2005. **50**(1): p. 1-78.
5. Nandan, R., DebRoy, T., and Bhadeshia, H., *Recent advances in friction-stir welding–process, weldment structure and properties.* Progress in Materials Science, 2008. **53**(6): p. 980-1023.
6. Rai, R., De, A., Bhadeshia, H., and DebRoy, T., *Review: friction stir welding tools.* Science and technology of welding and joining, 2011. **16**(4): p. 325-342.
7. Inaniwa, S., Kurabe, Y., Miyashita, Y., and Hori, H. *Application of friction stir welding for several plastic materials*. in *Proceedings of the 1st International Joint Symposium on Joining and Welding: Osaka, Japan, 6-8 November 2013*. 2014. Woodhead Publishing.
8. Steel, R., Packer, S., Fleck, R., Sanderson, S., and Tucker, C. *Advances in FSW and new applications*. in *Proceedings of the 1st International Joint Symposium on Joining and Welding: Osaka, Japan, 6-8 November 2013*. 2014. Woodhead Publishing.
9. Steel, R.J., Nelson, T.W., Sorensen, C.D., and Packer, S.M. *Friction stir welding of steel T-joint configurations*. in *Proceedings of the international offshore and polar engineering conference*. 2005.
10. Richter-Trummer, V., Suzano, E., Beltrão, M., Roos, A., dos Santos, J., and de Castro, P., *Influence of the FSW clamping force on the final distortion and residual stress field.* Materials Science and Engineering: A, 2012. **538**: p. 81-88.
11. Yazdanian, S. and Chen, Z. *Effect of friction stir lap welding conditions on joint strength of aluminium alloy 6060*. in *IOP Conference Series: Materials Science and Engineering*. 2009. IOP Publishing.
12. Keivani, R., Bagheri, B., Sharifi, F., Ketabchi, M., and Abbasi, M., *Effects of pin angle and preheating on temperature distribution during friction stir welding operation.* Transactions of Nonferrous Metals Society of China, 2013. **23**(9): p. 2708-2713.
13. Besharati-Givi, M.-K. and Asadi, P., *Advances in friction-stir welding and processing*. 2014: Elsevier.
14. Larsson, R., *Welding assembly for friction stir welding*. 2001, Google Patents.
15. Ebnesajjad, S. and Landrock, A.H., *Adhesives technology handbook*. 2014: William Andrew.
16. da Silva, L.F., *Slides teorica 1 - Processos avançados de Produção.*
17. He, X., *A review of finite element analysis of adhesively bonded joints.* International Journal of Adhesion and Adhesives, 2011. **31**(4): p. 248-264.
18. *GERGONNE - The Adhesive Solution*. 2012 2015- 08-20]; Available from: http://adhesifs.gergonne.fr/en/marches/automobile-transports-1.html.
19. Banea, M.D., da Silva, L.F., Campilho, R.D., and Sato, C., *Smart adhesive joints: an overview of recent developments.* The Journal of Adhesion, 2014. **90**(1): p. 16-40.
20. da Silva, L.F., Pirondi, A., and Öchsner, A., *Hybrid adhesive joints*. Vol. 6. 2011: Springer Science & Business Media.
21. Liu, L. and Ren, D., *A novel weld-bonding hybrid process for joining Mg alloy and Al alloy.* Materials & Design, 2011. **32**(7): p. 3730-3735.
22. Santos, I., Zhang, W., Goncalves, V., Bay, N., and Martins, P., *Weld bonding of stainless steel.* International Journal of Machine Tools and Manufacture, 2004. **44**(14): p. 1431-1439.
23. Darwish, S., *Weldbonding strengthens and balances the stresses in spot-welded dissimilar thickness joints.* Journal of materials processing technology, 2003. **134**(3): p. 352-362.

24.   Darwish, S., *Analysis of weld-bonded dissimilar materials.* International journal of adhesion and adhesives, 2004. **24**(4): p. 347-354.

25.   Campilho, R., Pinto, A., Banea, M.D., and da Silva, L.F., *Optimization study of hybrid spot-welded/bonded single-lap joints.* International Journal of Adhesion and Adhesives, 2012. **37**: p. 86-95.

26.   Gomez, S., Onoro, J., and Pecharroman, J., *A simple mechanical model of a structural hybrid adhesive/riveted single lap joint.* International journal of adhesion and adhesives, 2007. **27**(4): p. 263-267.

27.   Sadowski, T., Kneć, M., and Golewski, P., *Experimental investigations and numerical modelling of steel adhesive joints reinforced by rivets.* International Journal of Adhesion and Adhesives, 2010. **30**(5): p. 338-346.

28.   Sadowski, T., Golewski, P., and Zarzeka-Raczkowska, E., *Damage and failure processes of hybrid joints: adhesive bonded aluminium plates reinforced by rivets.* Computational Materials Science, 2011. **50**(4): p. 1256-1262.

29.   Sadowski, T. and Zarzeka-Raczkowska, E., *Hybrid Adhesive Bonded and Riveted Joints–Influence of Rivet Geometrical Layout on Strength of Joints/Połączenia Hybrydowe Klejowo-Nitowe-Wpływ Geometrii Rozmieszczenia Nitów Na Wytrzymałość Połączeń.* Archives of Metallurgy and Materials, 2012. **57**(4): p. 1127-1135.

30.   Esmaeili, F., Zehsaz, M., Chakherlou, T., and Barzegar, S., *Fatigue life estimation of double lap simple bolted and hybrid (bolted/bonded) joints using several multiaxial fatigue criteria.* Materials & Design, 2015. **67**: p. 583-595.

31.   Kelly, G., *Load transfer in hybrid (bonded/bolted) composite single-lap joints.* Composite structures, 2005. **69**(1): p. 35-43.

32.   Sun, C., Bhawesh, K., Wang, P., and Sterkenburg, R., *Development of Improved Hybrid Joints for Composite Structures.* Composite Structures, 2005. **35**: p. 1-20.

33.   Wang, H. and Liu, L., *Analysis of the influence of adhesives in laser weld bonded joints.* International Journal of Adhesion and Adhesives, 2014. **52**: p. 77-81.

34.   Liu, L., Ren, D., and Li, Y., *Static mechanics analyses of different laser weld bonding structures in joining AZ61 Mg alloy.* International Journal of Adhesion and Adhesives, 2011. **31**(7): p. 660-665.

35.   Chowdhury, S., Chen, D., Bhole, S., Cao, X., and Wanjara, P., *Lap shear strength and fatigue behavior of friction stir spot welded dissimilar magnesium-to-aluminum joints with adhesive.* Materials Science and Engineering: A, 2013. **562**: p. 53-60.

36.   Harris, D. and Norman, A. *Properties of friction stir welded joints: a review of the literature*. in *EUROSTIR, Progress report presented at the 6th PSG Meeting*. 2003.

37.   Cavaliere, P., Squillace, A., and Panella, F., *Effect of welding parameters on mechanical and microstructural properties of AA6082 joints produced by friction stir welding.* Journal of materials processing technology, 2008. **200**(1): p. 364-372.

38.   Steuwer, A., Peel, M., and Withers, P., *Dissimilar friction stir welds in AA5083–AA6082: the effect of process parameters on residual stress.* Materials Science and Engineering: A, 2006. **441**(1): p. 187-196.

39.   De Moura, M., Daniaud, R., and Magalhães, A., *Simulation of mechanical behaviour of composite bonded joints containing strip defects.* International journal of adhesion and adhesives, 2006. **26**(6): p. 464-473.

40.   da Silva, L.F., Dillard, D.A., Blackman, B., and Adams, R.D., *Testing adhesive joints: best practices*. 2012: John Wiley & Sons.

41.   Moreira, P.M.G.P., *Lightweight Stiffened Panels: Mechanical Characterization of Emerging Fabrication Technologies*, in *Mechanical Department* 2008, PhD Thesis, Faculdade de Engenharia da Universidade do Porto

42.   Fersini, D. and Pirondi, A., *Analysis and modelling of fatigue failure of friction stir welded aluminum alloy single-lap joints.* Engineering Fracture Mechanics, 2008. **75**(3): p. 790-803.

43.   Ren, S.R., Ma, Z.Y., and Chen, L.Q., *Effect of welding parameters on tensile properties and fracture behavior of friction stir welded Al–Mg–Si alloy.* Scripta Materialia, 2007. **56**(1): p. 69-72.

44.   Commin, L., Dumont, M., Masse, J.E., and Barrallier, L., *Friction stir welding of AZ31 magnesium alloy rolled sheets: Influence of processing parameters.* Acta Materialia, 2009. **57**(2): p. 326-334.

45.   Guan, Q., *A survey of development in welding stress and distortion controlling in aerospace manufacturing engineering in China.* WELDING IN THE WORLD-LONDON-, 1999. **43**: p. 64-74.

46.   Svensson, L.-E., Karlsson, L., Larsson, H., Karlsson, B., Fazzini, M., and Karlsson, J., *Microstructure and mechanical properties of friction stir welded aluminium alloys with special reference to AA 5083 and AA 6082.* Science and Technology of Welding and Joining, 2000. **5**(5): p. 285-296.